Geothermal Energy

REVIEW

Open Access

Assessment of deep geothermal research and development in the Upper Rhine Graben

Matthis Frey[1*], Kristian Bär[2], Ingrid Stober[3], John Reinecker[2], Jeroen van der Vaart[1] and Ingo Sass[1,4]

*Correspondence:
frey@geo.tu-darmstadt.de

[1] Institute of Applied Geosciences, Department of Geothermal Science and Technology, Technical University of Darmstadt, Schnittspahnstraße 9, 64287 Darmstadt, Germany
[2] GeoThermal Engineering GmbH, An Der Raumfabrik 33C, 76227 Karlsruhe, Germany
[3] Institute of Earth and Environmental Sciences, University of Freiburg, Albertstr. 23b, D-79104 Freiburg, Germany
[4] GFZ German Research Centre for Geosciences, Section 4.8: Geoenergy, Telegrafenberg, 14473 Potsdam, Germany

Abstract

Deep geothermal energy represents a key element of future renewable energy production due to its base load capability and the almost inexhaustible resource base. Especially with regard to heat supply, this technology offers a huge potential for carbon saving. One of the main targets of geothermal projects in Central Europe is the Upper Rhine Graben, which exhibits elevated subsurface temperatures and reservoirs with favorable hydraulic properties. Several decades of intensive research in the region resulted in a comprehensive understanding of the geological situation. This review study summarizes the findings relevant to deep geothermal projects and thus provides a useful working and decision-making basis for stakeholders. A total of nine geological units have been identified that are suitable for deep geothermal exploitation, comprising the crystalline basement, various sandstone formations and Mesozoic carbonates. An extensive lithostratigraphic, structural, geochemical, hydraulic and petrophysical characterization is given for each of these potential reservoirs. This paper furthermore provides an overview of the available data and geological as well as temperature models.

Keywords: Upper Rhine Graben, Geothermal energy, Renewable energies, Reservoir characterization, Open data

Introduction

The Upper Rhine Graben (URG) is a major target for deep geothermal exploration in Central Europe due to the highly elevated geothermal gradient of locally more than 100 K/km (e.g., Soultz-sous-Forêts) (Schellschmidt and Clauser 1996; Pribnow and Schellschmidt 2000; Agemar et al. 2012; Baillieux et al. 2013) and the abundance of large fault zone providing potential fluid pathways (Bächler et al. 2003; Guillou-Frottier et al. 2013; Duwiquet et al. 2021). According to Kock and Kaltschmitt (2012), the technical potential for deep geothermal utilization in the URG sums up to 186 TWh/a, which is approximately 5% of the annual primary energy demand of Germany (AG Energiebilanzen 2021). A number of suitable reservoir horizons have been identified and characterized in the course of numerous research projects over the last decades and the hydro- as well as petrothermal potentials have been determined in local or regional studies (Commission of the European Communities 1979; Hurter and Schellschmidt

2003; Kohl et al. 2005; Agemar et al. 2022; Sass et al. 2011; Arndt 2012; GeORG Projektteam 2013; Stober and Bucher 2015; Bär et al. 2016; Aretz et al. 2016).

Exploration in the URG started with the first discoveries of oil-bearing sandstones at Merkwiller-Pechelbronn (Böcker 2015; Reinhold et al. 2016). In the twentieth century, large-scale hydrocarbon exploration was conducted, reaching its peak between the 1950s and 1980s. By 1989, more than 440 exploration wells and 550 production wells had been drilled and a dense network of 2D reflection seismic profiles with a total length of more than 5000 km had been shot (Durst 1991; Jodocy and Stober 2008). This extensive data basis allows detailed investigations on the structural setting, lithological properties, stratigraphy as well as petrophysical, chemical and thermal properties of the Cenozoic horizons. Conventional exploration data (seismic and well data) resolving the Mesozoic, Permo-Carboniferous and crystalline basement structures, on the other hand, remained sparse, resulting in high model uncertainties with respect to these horizons (Frey et al. 2021b).

The exploration for deep geothermal resources in the URG came into focus during the energy crisis in the 1970s. First geothermal wells drilled are Bühl 1 (1979), Cronenbourg GCR-1 (1980) and Bruchsal GB-BR1 and GB-BR2 (1983/84) with more or less success (Bertleff et al. 1988; Pauwels et al. 1993; Meixner et al. 2014). In the late 1980s, the European EGS (Enhanced Geothermal Systems) project was launched in Soultz-sous-Forêts (France, central URG) with the aim of extracting heat from fractured granitic rock as a new power source (Gérard and Kappelmeyer 1987; Dezayes et al. 2005a). Between 1987 and 2004, a total of 5 research wells (GPK1-4 and EPS1) with a maximum depth of partly more than 5000 m were drilled to obtain a comprehensive understanding of the hydrothermal circulation in deep geothermal reservoirs (Dezayes et al. 2005b; Genter et al. 2010). Several hydraulic, chemical stimulations and long-term circulation tests were carried out to increase and monitor the permeability of the fracture network between the wells (Evans et al. 2005; Portier et al. 2009; Schill et al. 2017). To date, Soultz is still one of the most important model sites for EGS systems worldwide and provides an extremely valuable reference for the design of such projects (Genter et al. 2010). After the Renewable Energy Sources Act came into force in 2000, the development of the geothermal sector was further accelerated, leading to the realization of several additional projects in the last two decades (Baumgärtner et al. 2013; Baujard et al. 2017; Reinecker et al. 2019). At present, there are six active deep geothermal heat and/or power plants in the URG. Additionally, thermal waters for balneological purposes are extracted at numerous locations, especially along the main border faults, but as well in the graben center (e.g., Baden-Baden, Bad Krozingen, Bad Bellingen, Freiburg, Weinheim). Nevertheless, the technical potential is currently exploited only to a very small extent (Paschen et al. 2003; Kock and Kaltschmitt 2012), which can be attributed to various reasons. The complex geology and tectonic activity pose considerable risks during the drilling operation and reservoir development. But difficulties with the legal framework (e.g., mining law) or lack of public acceptance represent also serious problems.

In this review, a detailed geological description of the main horizons and tectonic structures suitable for deep geothermal exploitation in the URG region is presented. They have been identified based on the expected reservoir temperature and the hydraulic permeability of the formation or fault zone. In addition, this study summarized all

available data regarding the relevant hydrogeological, hydraulic, hydrochemical and petrophysical properties of each reservoir unit. Subsequently, a review of the structural setting, the stress field, natural seismicity, available temperature data, the geothermal projects and the existing 3D models in the URG is provided herein. This article is intended to serve as a comprehensive information basis and decision support. However, for each site additional specific exploration measures may be required, as the geological conditions in the URG are due to its complex tectonic setting laterally highly variable. Additionally, the conditions at surface and societal challenges (e.g., infrastructure, public acceptance) play a key role and may pose significant risks to the projects, but are only briefly discussed here.

Geological setting

The URG is the central part of the European Cenozoic Rift System (ECRIS), which consists of several interlinked tectonic rifts, extending from the Mediterranean to the North Sea (Fig. 1) (Illies and Fuchs 1974; Prodehl et al. 1992, 1995; Ziegler 1992, 1994; Ziegler and Dèzes 2005; Dèzes et al. 2004; McCann 2008). The main strike direction of the approximately 300 km long and 30 to 40 km wide URG is NNE–SSW in the southern and central part and roughly N–S in the northern part. The structure is bounded to the north by the Rhenish Massif, the Hesse Depression and the Vogelsberg, to the south by the Swiss Jura Mountains and at the graben shoulders by the Black Forest, the Vosges, the Odenwald and the Palatinate. Well-founded concepts about the paleogeographic

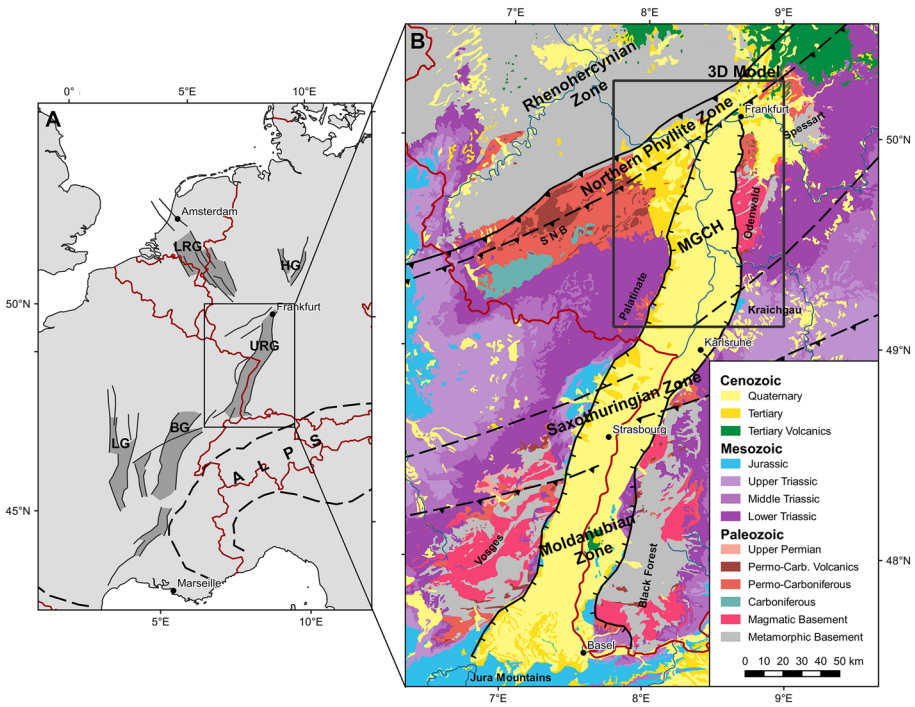

Fig. 1 **A** Simplified map of the European Cenozoic Rift System (adapted from Ziegler and Dèzes 2005), dark grey areas represent rift-related sediment basins. *BG* Bresse Graben, *HG* Hessian grabens, *LG* Limagne Graben, *LRG* Lower Rhine Graben, *MGCH* Mid-German Crystalline High, *SNB* Saar-Nahe Basin, *URG* Upper Rhine Graben. **B** Geological map of the URG including the main stratigraphic units (adapted from BGR 2016)

and tectonic development as well as the lithology, structure, facies, stratigraphy, diagenesis and metamorphism of the individual horizons were established inter alia by Andres and Schad (1959), Straub (1962), Sauer (1962), Rothe and Sauer (1967), Illies and Mueller (1970), Villemin et al. (1986), Villemin and Coletta (1990), Sissingh (1998), Michon and Merle (2000), Gaupp and Nickel (2001), Behrmann et al. (2003), Behrmann et al. (2005), Reinhold et al. (2016) and Perner (2018). In the following, an overview about the Phanerozoic evolution of the URG region is given. A summary of the lithostratigraphic sequence in the URG is shown in Fig. 2.

Variscan orogeny

The basement in the URG region represents primarily the structure of the Variscan fold belt that was first defined by Suess (1926) and Kossmat (1927). Comprehensive descriptions and discussions of the Variscan Orogeny are, for example, given in Behr et al. (1984), Franke (1989), Dallmeyer et al. (1995), Oncken (1997), Franke (2000), Matte (2003), Kroner et al. (2008) and Zeh and Gerdes (2010).

Prior to the continental collision between the Silurian and Lower Devonian, the vast Rheic Ocean, located to the south of Laurussia, was subducted northwards (Nance et al. 2010). This led to a drift of the Armorican Terrane Assemblage, consisting of several microplates including Franconia, Saxothuringia and Moldanubia, towards Laurussia (Crowley et al. 2000). These terranes disintegrated from the northern margin of Gondwana during the Cambrian and Ordovician (Kemnitz et al. 2002) and typically consist of Neoproterozoic crust, overlain by a Neoproterozoic to Lower Carboniferous passive margin sequence and intruded by subduction-related magmatic complexes.

Back-arc extension resulted in the opening of the Rhenohercynian Basin during the Lower Devonian (Fig. 3) (Stets and Schäfer 2011; Franke et al. 2017). At first, mainly siliciclastic and carbonate shelf sediments were deposited, but with increasing extension during the middle Devonian also oceanic crust was formed in the deeper parts of the basin (Franke 1995b; Belka and Narkiewicz 2008). According to Zeh and Gerdes (2010), the subduction direction of the Rheic Ocean changed to the south in the Upper Devonian resulting in a new magmatic arc, known as the Mid-German Crystalline High (MGCH) (Reischmann and Anthes 1996; Anthes and Reischmann 2001). The prior island arc between the Rheic Ocean and the Rhenohercynian Basin was then partially underplated beneath the MGCH (Oncken 1997; Oncken et al. 1999). Further to the south, the Saxothuringian Basin was subducted underneath Moldanubia, which resulted in widespread magmatic activity, e.g., indicated by granitic intrusions in the Black Forest and Vosges (Okrusch et al. 1995; Skrzypek et al. 2014).

The final closure of the oceanic basins took place in the Lower Carboniferous and was followed by the collision of Laurussia with the Armorican Terrane Assemblage and Gondwana in Visean and Namurian times (Eckelmann et al. 2014). As a result, the individual microplates were juxtaposed and the sedimentary sequences of the marine basins and continental margins were partly thrust onto the crystalline basement (Behr and Heinrichs 1987; Hegner et al. 2001; Kroner et al. 2008; McCann et al. 2008). The degree of metamorphism varies significantly across the fold belt (Oncken et al. 1995; Okrusch 1995). While the Rhenohercynian Zone and Saxothuringian Basin show only a low-grade overprint, the MGCH shows typical medium- to high-grade regional

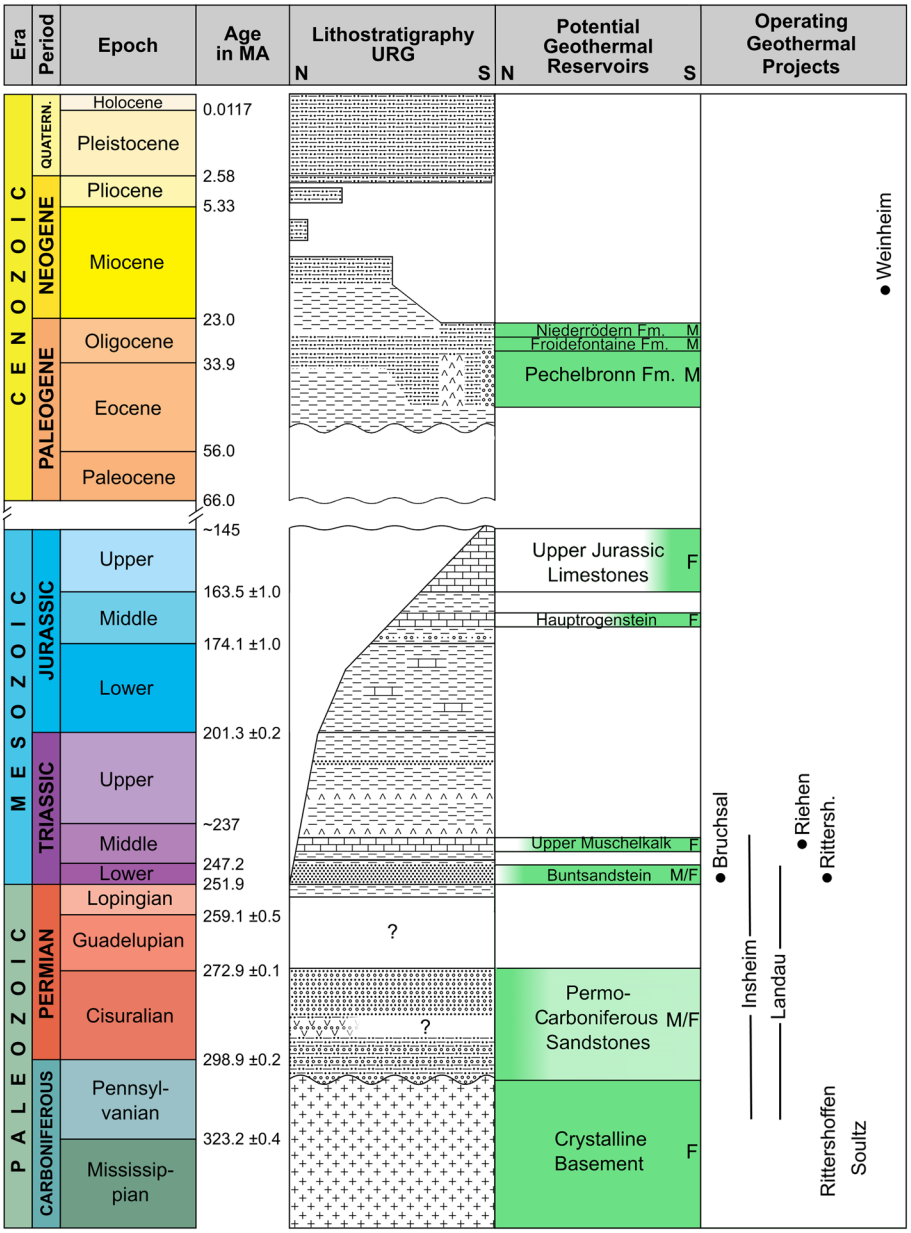

Fig. 2 Lithostratigraphic sequence in the Upper Rhine Graben with the potential geothermal reservoir units (modified after GeORG Projektteam (2013) and Deutsche Stratigraphische Kommission (2016)). It is indicated whether the fluid flow in the reservoir horizon is dominated by fractures (F) or matrix (M). For a detailed visualization of the Tertiary succession, see also Fig. 9. The regional importance of each horizon is indicated by the color gradient

metamorphic conditions. In contrast, the metamorphism was temperature-dominated in the Moldanubian Zone, indicated by partial melting.

Permo-Carboniferous and Mesozoic sediment basins

At the end of the Variscan Orogeny in the Upper Carboniferous, a rapid collapse of the orogen occurred and several NE–SW striking intramontane molasse basins (Figs. 3 and 4a), such as the Saar-Nahe Basin, the Hessian Depression, the Vosges-Kraichgau Basin

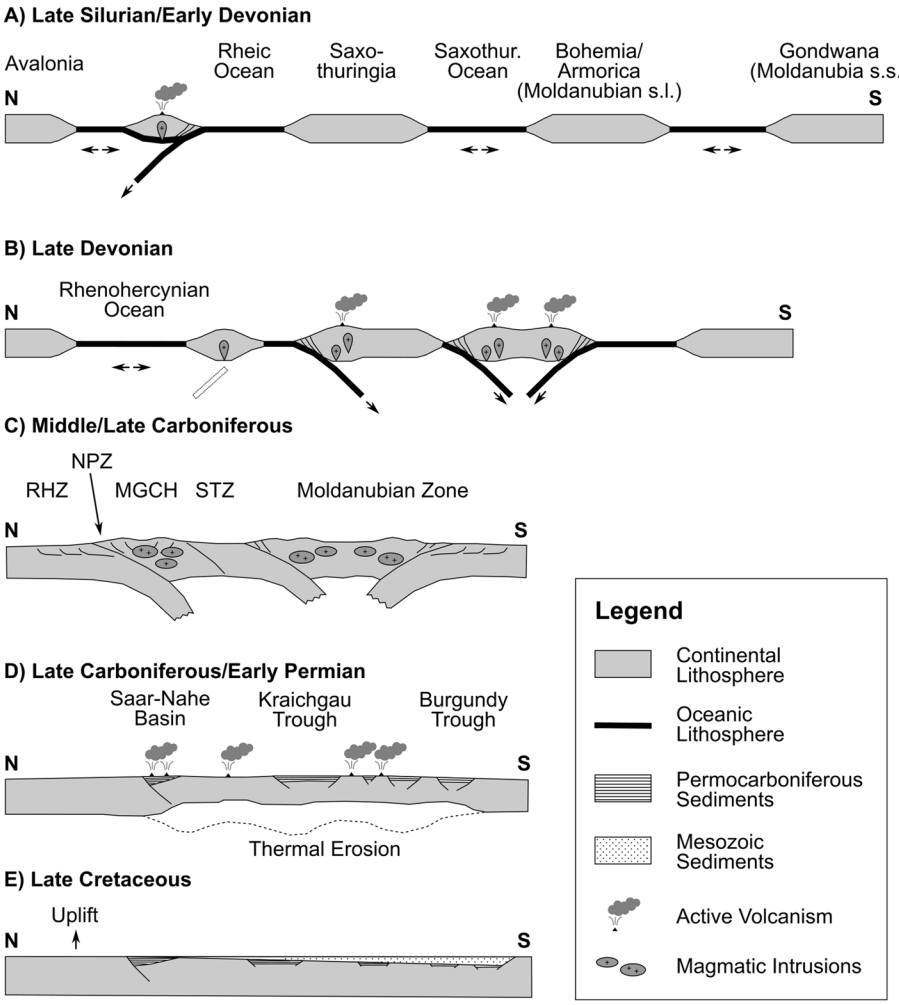

Fig. 3 Plate tectonic evolution of the lithosphere in the Upper Rhine Graben region from the Upper Silurian until Upper Carboniferous (adapted from Franke (2000) and Zeh and Gerdes (2010)). *MGCH* Mid-German Crystalline High, *NPZ* Northern Phyllite Zone, *RHZ* Rhenohercynian Zone, *STZ* Saxothuringian Zone

and the Burgundy Basin, formed along pre-existing Variscan fault zones (Henk 1993; Weber 1995b; Stollhofen 1998; Schumacher 2002; Schäfer 2011). The erosion of the surrounding mountain ranges produced large quantities of clastic sediments that were deposited in these isolated basins, reaching a maximum thickness of up to 10 km in the Saar-Nahe Basin (Henk 1992). The Permo-Carboniferous succession is in the lower part dominated by fluvial–lacustrine conglomerates, sandstones and claystones. Later, the sedimentation was increasingly controlled by aeolian transport, indicating an arid environment (Schäfer 1989; Schäfer and Korsch 1998; Stollhofen 1998; Aretz et al. 2016). Furthermore, rifting in the Lower Permian was accompanied by widespread mantle-driven volcanic activity mostly between 300 and 290 Ma, which shows a mafic to felsic composition (von Seckendorff et al. 2004; von Seckendorff 2012). In the Upper Permian (Fig. 4b), no evaporite cycles were deposited in the URG area, but the Zechstein is characterized by marginal facies deposits with a high proportion of fine-clastic sediments (Hug and Vero 2008).

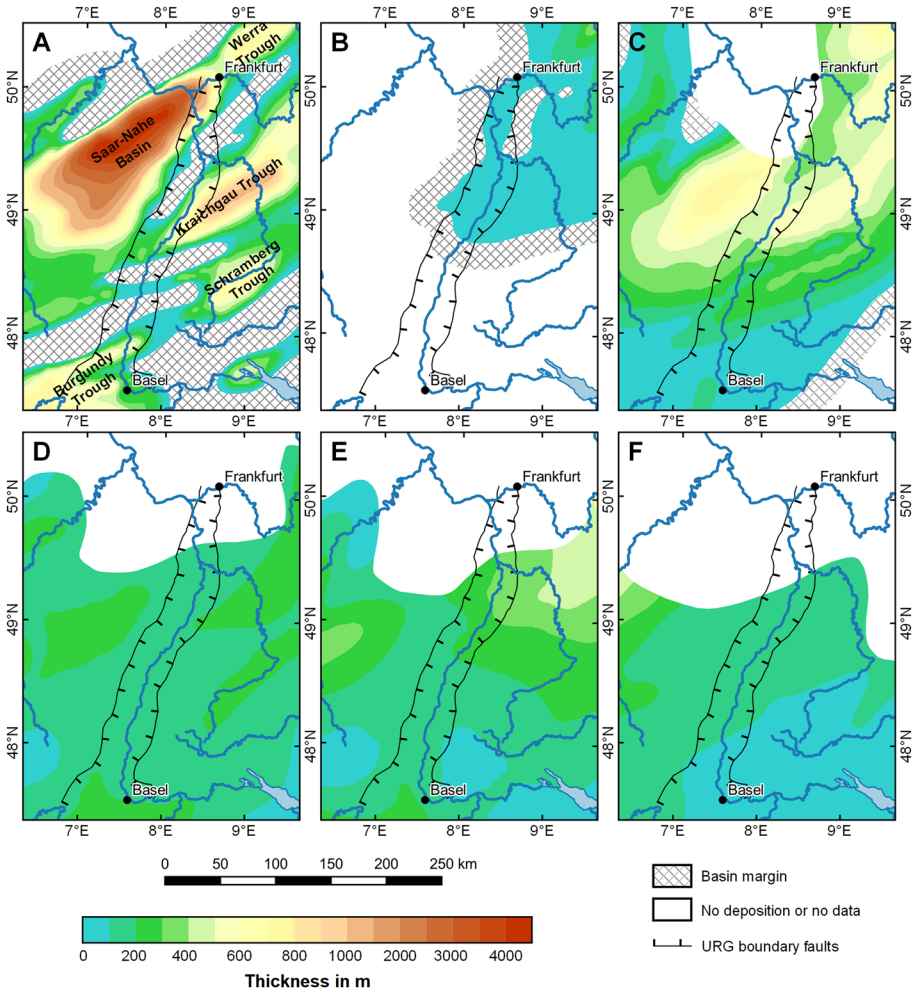

Fig. 4 Paleogeographic situation in the URG region (modified after Boigk and Schöneich 1974). Reconstructed sediment thickness after deposition for **A** the Permo-Carboniferous, **B** the Upper Permian (Zechstein), **C** the Lower Triassic (Buntsandstein), **D** the Middle Triassic (Muschelkalk), **E** the Upper Triassic (Keuper) and **F** the Lower Jurassic (Lias)

The subsequent Triassic is divided into the three independent lithostratigraphic groups Buntsandstein, Muschelkalk and Keuper in the Germanic Basin (Boigk and Schöneich 1974; Schröder 1982; Aigner and Bachmann 1992; Feist-Burkhardt et al. 2008). After the regression of the Zechstein Sea at the end of the Permian, continental facies were again predominantly deposited (Scholze et al. 2017). In comparison to the Permo-Carboniferous, sedimentation of the Buntsandstein (Fig. 4c) was no longer limited to the isolated Variscan sub-basins (Backhaus 1974; Feist-Burkhardt et al. 2008; Lepper et al. 2014), but the highest thickness was still reached in the Saar-Nahe Basin and the Kraichgau Depression (Boigk and Schöneich 1974).

During the Middle Triassic a wide-ranging transgression occurred (Fig. 4d), leading to the development of the Germanic Basin into a marginal sea of the Tethys Ocean (Szulc 2000; Götz and Gast 2010; McKie 2017). Deep and shallow marine areas were spatially separated by the Variscan orogen, with seaways existing along tectonic depressions. The intramontane basins and especially the Burgundy Trough still represented major

depocenters during this time, but sedimentation occurred on a broad scale in the whole Germanic Basin (Boigk and Schöneich 1974). During the deposition of the Muschelkalk, several transgression and regression cycles took place, which are documented as alternating deposits of evaporites including halite, shallow-marine carbonates and deep-water carbonates (Schwarz 1975; Hagdorn 1999; Götz 2004). The Keuper sequence (Fig. 4e) shows an alternation of clastic sediments with evaporites, indicating a frequent change between continental and shallow marine conditions (Vecsei and Duringer 2003; Barnasch 2010; Franz et al. 2018). Similarly, cycles of arid and humid climate conditions are documented in the succession. Large delta regions are typical for this period, which have a predominant sediment transport in southwestern directions.

In the Lower Jurassic (Fig. 4f), southern Germany became part of the epicontinental shelf by a renewed transgression of the Peri-Tethys (Pienkowski et al. 2008; Barth et al. 2018). Under these conditions, mainly black shales and clays were deposited. In the Middle Jurassic, an alternating deposition of sandstone, clays and especially oolithic limestones is recorded in the URG. Deposits from the Upper Jurassic are preserved in the URG only up to the Oxfordian. During the Cretaceous, large uplift movements occurred along the Rhenish Massif, which led to considerable erosion of the Mesozoic and partly the Paleozoic sediments in the northern URG (Pflug 1982). For this reason, the stratigraphic horizons below the Tertiary sediments become steadily older from south to north.

Cenozoic graben formation

The URG formed as a result of the changing lithospheric stress field in the foreland of the Alpine Orogeny and can therefore be classified as a passive rift. It is likely that pre-existing NNE–SSW striking Variscan, Permo-Carboniferous and Mesozoic discontinuities, shear or fault zones, were reactivated (Edel et al. 2007; Grimmer et al. 2017). The plate tectonic relationships and the deformation of the Alpine foreland on a lithosphere scale are presented, e.g., in Ziegler et al. (1995), Sissingh (1998), Dèzes et al. (2004), Cloetingh et al. (2005) and Ziegler and Dèzes (2005).

The Cenozoic changes in the Central European stress regime led to an extension of the lithosphere parallel to the orogenic belt and to an uplift of the mantle in the URG region. During the development of the URG, the regional stress field was repeatedly redirected (Buchner 1981; Schumacher 2002; Behrmann et al. 2003; Dèzes et al. 2004) (Fig. 5), resulting in reactivation of faults and changes of the fault movement direction. This led to variable subsidence and uplift rates and to local displacements of the deposition centers. Two main phases of graben development are generally distinguished (Illies 1978; Hüttner 1991; Schwarz 2006), an initial mostly extensional phase from Eocene to Lower Miocene and a later transtensional to transpressional phase from Miocene to Quaternary. A detailed paleogeographic reconstruction of the URG from Eocene to Pliocene is given in Berger et al. (2005).

The formation of the URG was initiated by an acceleration of the northward directed compressional movement of the Alpine Orogen that resulted in an E–W oriented crustal extension of the foreland in the Middle to Upper Eocene (Villemin et al. 1986; Ziegler et al. 1995; Dèzes et al. 2004). During this period, lacustrine clays and siltstones were deposited in locally confined basins, accompanied by a period of

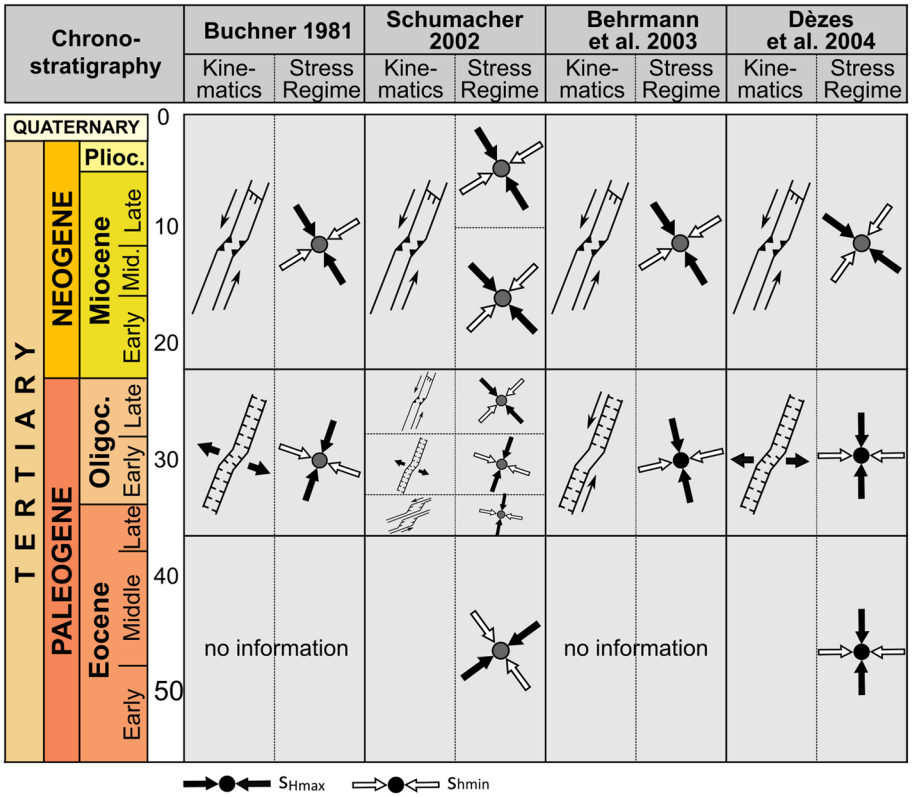

Fig. 5 Different models of the Cenozoic evolution of the URG (compiled by Schwarz et al. 2006)

increased volcanic activity at the graben shoulders (Lippolt et al. 1974; Illies 1977). By the Upper Eocene (Priabonium), two depositional centers had formed in the southern URG, the Mulhouse and Strasbourg Basins, whose extent reflected the location of the Permo-Carboniferous molasse basins of the Variscan Orogen (Pflug 1982).

In the Lower Oligocene (Rupelian), the strongest rifting phase occurred, which covered the entire graben and led to the deposition of the thick Pechelbronn and Froidefontaine Formations (Gaupp and Nickel 2001; Derer et al. 2003; Grimm 2005). For this period, a main direction of the deformation between WSW–ENE and WNW–ESE was determined (Fig. 5). With increasing subsidence, two and locally three marine transgressions with connections to the North German Basin and the South German Molasse Basin took place (Meier and Eisbacher 1991; Berger et al. 2005; Rousse et al. 2012). During the Upper Oligocene (Chattian), the extension came to a halt in the southern URG, and the depositional center was successively shifted northwards (Illies and Fuchs 1974).

The further development of the URG is influenced by an anti-clockwise rotation of S_{Hmax} that resulted in a reactivation of the faults in a sinistral strike–slip sense, with S_{hmin} oriented in SW–NE direction (Buchmann and Connolly 2007). This was caused by an abrupt decrease in the convergence between Europe and Africa during the Lower Miocene (Rosenbaum et al. 2002). The southern URG was affected by strong uplift, which is documented by a pronounced erosional unconformity and a hiatus from the Lower Miocene to Pliocene. Between 18 and 15 Ma, volcanic activity

reached its peak at the Kaiserstuhl (Wagner 1976). Conversely, the northern URG was characterized by high subsidence rates, which led to continuous sedimentation until the Quaternary.

Structural geology, recent stress field and seismicity

Structural geology

The complex and multiphase Cenozoic graben evolution resulted in a cross-sectional asymmetry with either the Eastern Main Boundary Fault (EMBF) or the Western Main Boundary Fault (WMBF) being more prominent. Graben formation-related subsidence shifted gradually from south to north (Illies 1978; Derer et al. 2005; Grimm 2005; Hinsken et al. 2007) resulting also in an asymmetry along strike of the graben structure (Fig. 6). Oblique normal faulting dominates the structural inventory within the Tertiary sedimentary infill of the URG, directly linked to the graben evolution. The graben main border faults as well as major faults parallel to the graben strike have a considerable share of sinistral strike–slip component not directly visible in seismic sections. 3D seismics are needed to restore and interpret the detailed structural inventory and fault kinetics on regional to local scale (e.g., Reinhold et al. 2016).

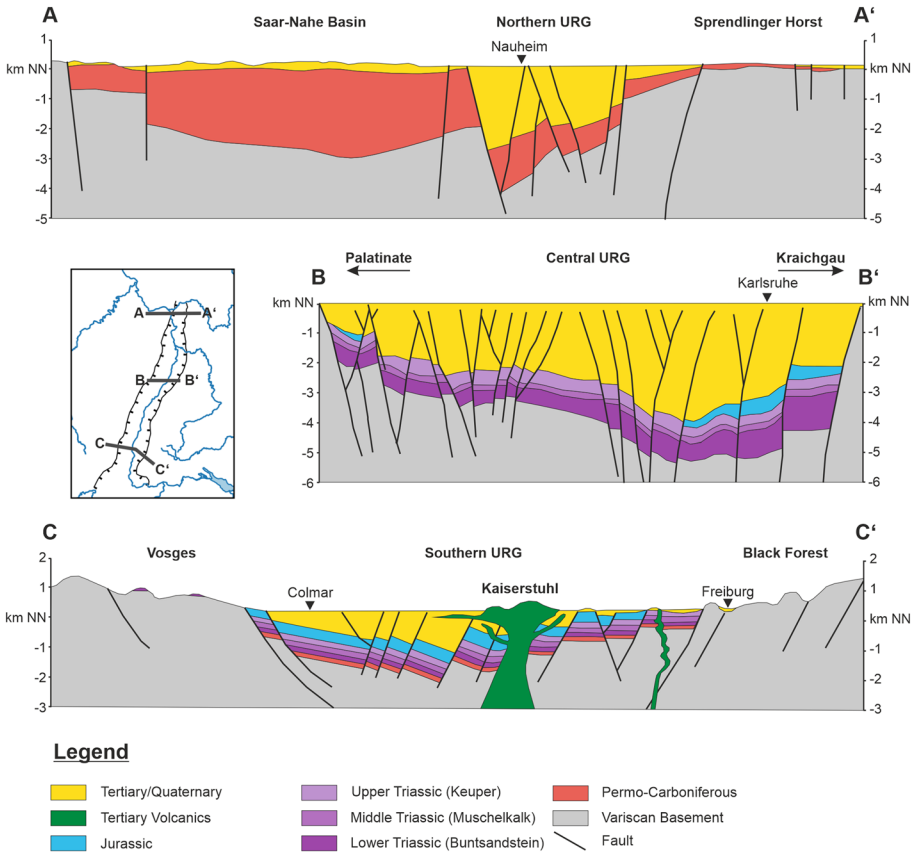

Fig. 6 Three geological cross sections through the northern (AA'), central (BB') and southern URG (CC') (modified after Arndt 2012; GeORG Projektteam 2013; LGRB 2022)

Prior to the URG development, the Variscan basement as well as the Permo-Mesozoic sedimentary cover have been faulted by NW–SE and NNE–SSW striking faults (e.g., Grimmer et al. 2017) of which some have been reactivated during Tertiary evolution. Mapping of faults within the Variscan crystalline basement using 2D or 3D seismics is often not possible with confidence as seismic reflectors are missing. Instead faults clearly visible in Permo-Mesozoic successions may be traced down into the crystalline basement wherever possible. However, faults within the crystalline basement and the overlaying Permo-Mesozoic succession form the main targets for deep geothermal exploration. All major projects in the URG so far target larger scale fault structures in this succession (Dezayes et al. 2005a; Teza et al. 2008; Baumgärtner et al. 2013; Duringer et al. 2019).

Fault zones with a vertical displacement of several 100 m to over 1000 m can promote or inhibit fluid transport through the rock depending on their internal structure, activity and orientation in the regional stress field (Barton et al. 1995; Caine et al. 1996; Evans et al. 1997; Gudmundsson et al. 2001; Meixner et al. 2014). The fault core, consisting mostly of fault gouges, fault breccias, clay smear and mineralizations, represents a potential barrier to fluid transport in inactive fault zones (Morrow et al. 1984). In active fault zones, however, flow paths can be formed or kept open in this unit by constantly re-breaking fractures, i.e., by earthquakes, that have been cemented in the meantime by upwelling thermal waters, thus increasing permeability (Stober and Bucher 2015; Agemar et al. 2017; Guillou-Frottier et al. 2020). Increased permeability is to be expected in the highly fractured damage zones (Caine et al. 1996; Faulkner et al. 2010) adjacent to both sides of the fault core. Permeability here is mainly dependent on fracture density, mean fracture lengths, degree of cross-linking of fractures and the mean fracture (fault) orientation within the respective local stress field (Jafari and Babadagli 2011). Fractures mechanically tend to be open when perpendicular to σ3 (mode I: opening, dilation) or with a high ratio of shear stress in the fracture plane to normal stress acting on the fracture plane. With the analytical modeling of slip (T_s) and dilation tendency (T_d) of fault zones, the spatial distribution of potentially 'open' or hydraulically conducting areas can be visualized (Morris et al. 1996; Ferrill and Morris 2003). However, due to mineralization along fractures and the complex geometry of the fault zone, the permeability structure within and along the fault zone is in detail more complex and may vary significantly laterally and with depth as well as between different geological units (Sausse and Genter 2005; Ledésert et al. 2010; Dezayes et al. 2010; Meller and Ledésert 2017). Open conduits may localize hydraulic flow along fractures and where fractures (or faults) are intersecting.

Present-day stress field

Knowledge on in situ stress is important to understand subsurface fluid flow controlled by fracture systems and to prevent wellbore stability problems. Information on the in situ stress state in the URG are mainly derived from earthquake focal mechanisms (FMS) and borehole data such as borehole breakouts (BO), drilling induced tensile fractures (DITF) and leak-off tests (LOT) (see Heidbach et al. (2016) for a detailed description on stress indicators and Reiter et al. (2016) for a detailed description of the WSM database in Germany and adjacent areas). Furthermore, an overview of the orientation

and magnitudes of the regional stress field is provided by the 3D numerical modeling of Ahlers et al. (2021).

Published stress studies at Soultz (Rummel and Baumgärtner 1991; Cuenot et al. 2006; Cornet et al. 2007; Dorbath et al. 2010), Bruchsal (Meixner et al. 2014), Rittershoffen (Azzola et al. 2019) and Basel (Valley and Evans 2009, 2019) have analyzed BO and DITF occurrence in detail and have proposed vertical stress profiles incorporating density logs for calculating vertical stress (i.e., overburden) as well as LOT and formation integrity tests (FIT) for minimum horizontal stress (S_h) magnitude estimation. Magnitude of maximum horizontal stress (S_H) has been estimated using the hypothesis of a frictional limit of optimally oriented faults (Zoback et al. 2003). Formation pressures are found to be hydrostatic with static water table close to ground surface.

The stress regime in the URG is derived by regional FMS studies (Ahorner 1983; Bonjer et al. 1984; Plenefisch and Bonjer 1997; Cuenot et al. 2006; Ritter et al. 2009; Homuth et al. 2014) and varies between strike–slip and normal faulting. Indications for thrust faulting are sparse and most probably reflect local inversion tectonics (e.g., Illies and Greiner 1979). Figure 7 displays the orientation of S_H as documented in the WSM database and recently published studies. In addition, unpublished stress reports from drilling projects throughout the URG reveal essentially the same, roughly N–S to NW–SE oriented S_H orientation. Local perturbations of the stress field result mainly from mechanically weak and active fault zones including URG border faults. Valley (2007), for example, reported a strong localized rotation of the maximum horizontal stress component linked to the occurrence of a large-scale permeable fault at Soultz-sous-Forêts. Perturbation may be significant over short distances and should be kept in mind when defining potential target zones and planning drilling projects.

Natural seismicity

Seismicity, whether natural or induced, poses a significant risk to deep geothermal projects. For this reason, a detailed study of historic events is essential to assess the seismic hazard. A detailed discussion of the induced seismicity related to geothermal projects is given in chapter 7. The tectonically active URG is marked by increased seismicity compared to adjacent regions in Central Europe (e.g., Grünthal et al. 2018), but in contrast to other continental rift valley systems, such as the East African Rift, events in access of magnitude of 3 are rare. In the European seismic hazard map of Giardini et al. (2014), the hazard to the URG is indicated as moderate with a 10% probability of exceeding a peak ground acceleration of 0.2 g in a 50-year interval.

The strongest historically documented event is the 1356 Basel earthquake with an estimated local magnitude of 6.7 to 7.1 (Fäh et al. 2009) which caused severe destruction to the city. Meghraoui et al. (2001) determined a mean recurrence interval of 1500 to 2500 years for seismic events of this size. The strongest recent earthquake with a local magnitude of about 5.4 occurred in Waldkirch near Freiburg in 2005 (Schwarz et al. 2006), but no damages were caused. The largest documented event in the northern URG was recorded in Worms in February 1952 and had a local magnitude of 4.7 (Leydecker 2011). This earthquake marks the onset of a seismic sequence that shows a southward migration of the hypocenters. In September and October 1952, two events

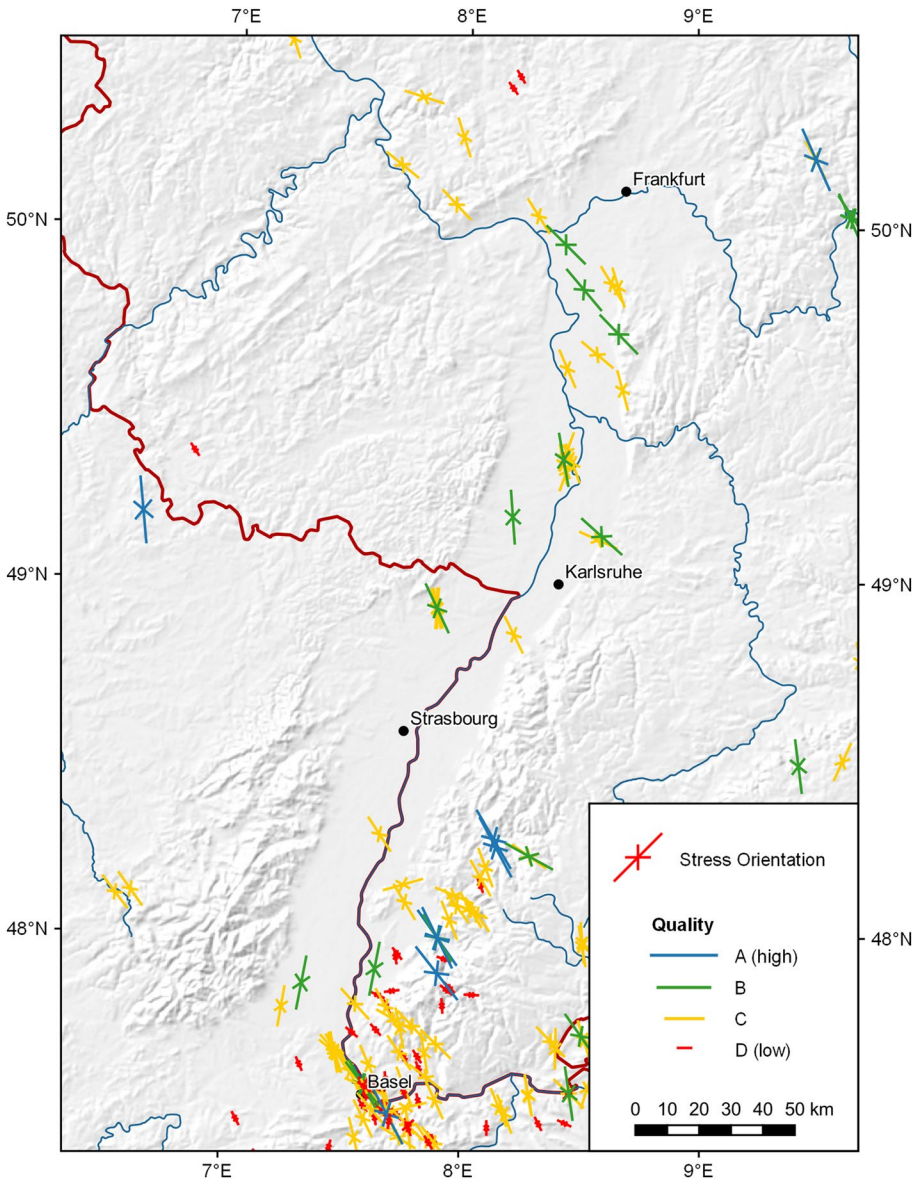

Fig. 7 Stress orientation map of the URG region (adapted from Reiter et al. 2016). The quality of stress measurements is indicated by the length of the symbol

of comparable magnitude followed between Landau and Wissenbourg and Wissenbourg and Haguenau, respectively (Doubre et al. 2021).

The URG exhibits significant lateral variations in the number and size of seismic events (Fig. 8) (Bonjer et al. 1984; Bonjer 1997; Homuth et al. 2014; Henrion et al. 2020). The largest cluster of epicenters is located south of Strasbourg, which according to Barth et al. (2015) can be explained by an increase of tectonic stresses related to convergence in the Alpine Orogen and the steep topography in this area. The central URG section between the Palatinate and Kraichgau is a seismically quiet zone, whereas seismicity increases again to the north. Barth et al. (2015) identified four sections of varying b-values (ranging from 0.83 to 1.42) in the URG. These differences can most likely be attributed to the local segmentation of the fault systems. In areas with relatively small-scale

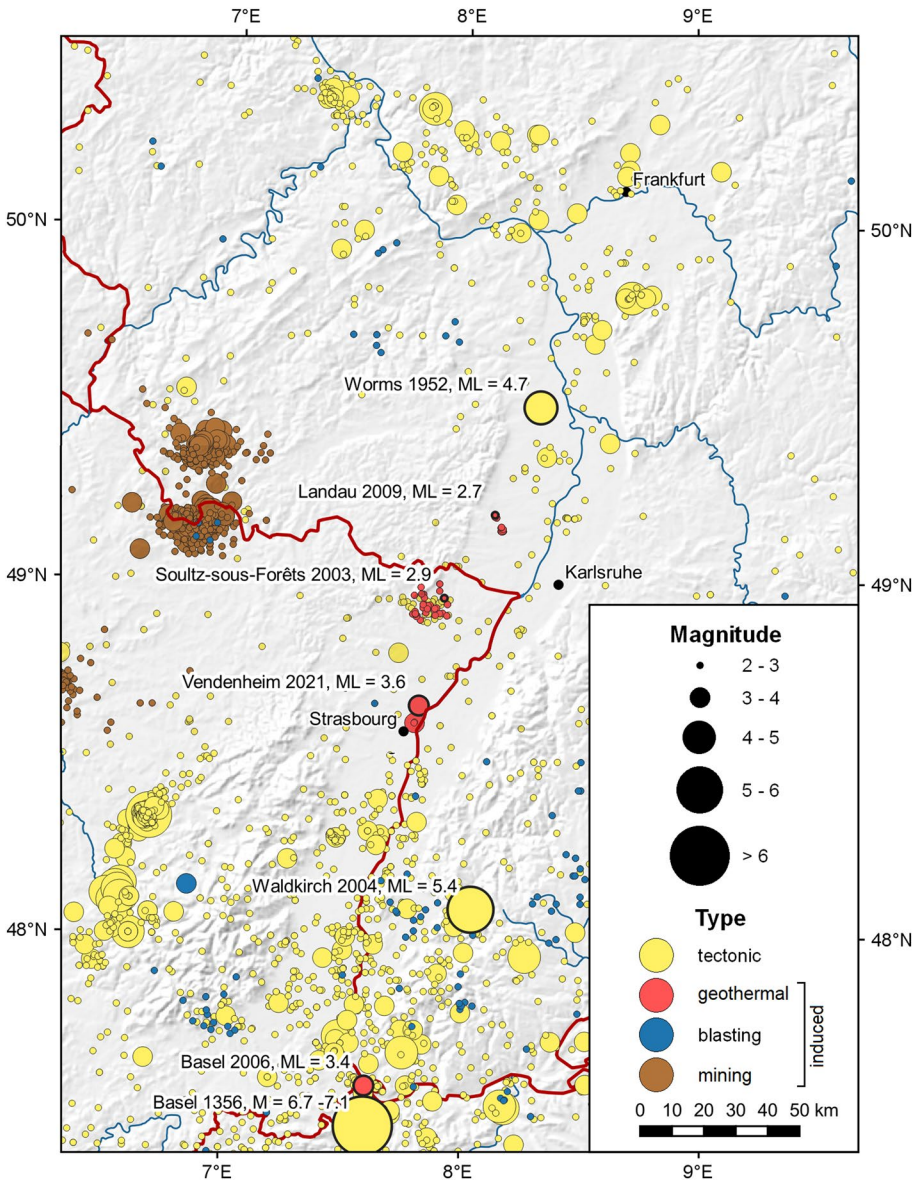

Fig. 8 Earthquakes with a local magnitude larger than 2 for the years between 1900 and 2021 observed in the wider region of the Upper Rhine Graben (data source: BGR (2021)). The 1356 Basel event is also included as the largest known earthquake in the region. Natural and induced events are distinguished

geological structures, e.g., between Mulhouse and Freiburg, accumulation of large tectonic stresses is limited, resulting in a smaller number of strong earthquakes. In general, the location of epicenters correlates well with larger fault zones, but the main border faults do not seem to be distinctly active (Grünthal et al. 2018).

Like the size of earthquake, the focal depth is also subject to variations across the URG region (Bonjer 1997; Edel et al. 2006). In the URG, earthquakes are observed in the upper crust down to depths of 13 to 16 km. The seismogenic zone is thinnest above the Moho uplift close to the Kaiserstuhl. Below the Black Forest and the Jura Mountains, the maximum focal depth increases to 20 km. N- to NNE-striking normal faulting and steep NNW- to WNW-striking strike–slip faulting are the predominant focal mechanisms

(Ahorner and Schneider 1974; Plenefisch and Bonjer 1997; Deichmann and Ernst 2006; Ritter et al. 2009; Grimmer et al. 2017). Thrust events occur rarely, hence the URG represents an overall transtensional regime.

Crustal temperature field

A significant increase in subsurface temperatures can be observed almost throughout the entire URG, with the highest geothermal gradients of up to 100 K/km being measured in the areas of Soultz-sous Forêts and Landau (Pribnow and Schellschmidt 2000; Agemar et al. 2012; Baillieux et al. 2013). The region represents a classical non-magmatic convection-dominated and fault-controlled geothermal play system (Moeck 2014) in an extensional domain. Fluid flow and effective heat transport are predominant along active fault zones bearing high fracture permeability. Upwelling of deep groundwater is hence the main reason for localized thermal anomalies.

Besides, several factors are influencing the crustal temperature field on a broader scale, resulting in a complex pattern of conductive and convective elements. Due to the Cenozoic rifting activities, the URG shows a considerable thinning of the crust and lithospheric mantle of up to 25% (Brun et al. 1992). This leads to a regional increase in the heat flux compared to the rest of Central Europe. Additionally, the radiogenic heat production of the crust is a major heat source controlled mainly by the thickness, structure and composition of the Variscan basement (Freymark et al. 2017). Different thermal properties of the Mesozoic and Tertiary sediments cause furthermore spatial variations in the conductive heat transport. Especially thermal insulation ('thermal blanketing effect') by thick clay-rich sediments results in increased geothermal gradients within the Tertiary formations (Zhang 1993; Wangen 1995; Freymark et al. 2019). A reversed effect occurs within salt deposits, such as the Weinstetter Diapir (Esslinger 1968). These are characterized by a particularly high thermal conductivity, which leads to a local chimney effect with high temperatures at the top and relatively low temperatures at the base of the salt structure.

Temperature measurements have been performed in c. 1000 wells throughout the URG so far, most of which are collected in the Geophysics Information System (FIS Geophysik) of the LIAG (Kühne 2006). Different measuring techniques were applied, resulting in significant quality variations. The most reliable results are provided by undisturbed temperature logs, where the thermal field reached equilibrium after drilling. However, disturbed temperature logs or bottom-hole temperature measurements are also common. In addition, temperature data were acquired in production tests and hydrochemical analyses. It is therefore necessary to correct disturbed temperature measurements before they are implemented in a model (Hermanrud et al. 1990; Schulz and Schellschmidt 1991; Agemar 2022). Moreover, it is recommended to weight the data according to their quality (Agemar et al. 2012; Rühaak 2015).

To create a comprehensive temperature model of the URG based on the measurements, geostatic interpolation is often applied. The most common method is kriging, which accounts for the closeness, redundancy and spatial continuity of the data. This has been used for example by Agemar et al. (2012) for the whole of Germany (Fig. 9), by Arndt et al. (2011) and Rühaak (2015) for Hesse and by the GeORG Projektteam (2013) for the central and southern URG. However, the disadvantage is that

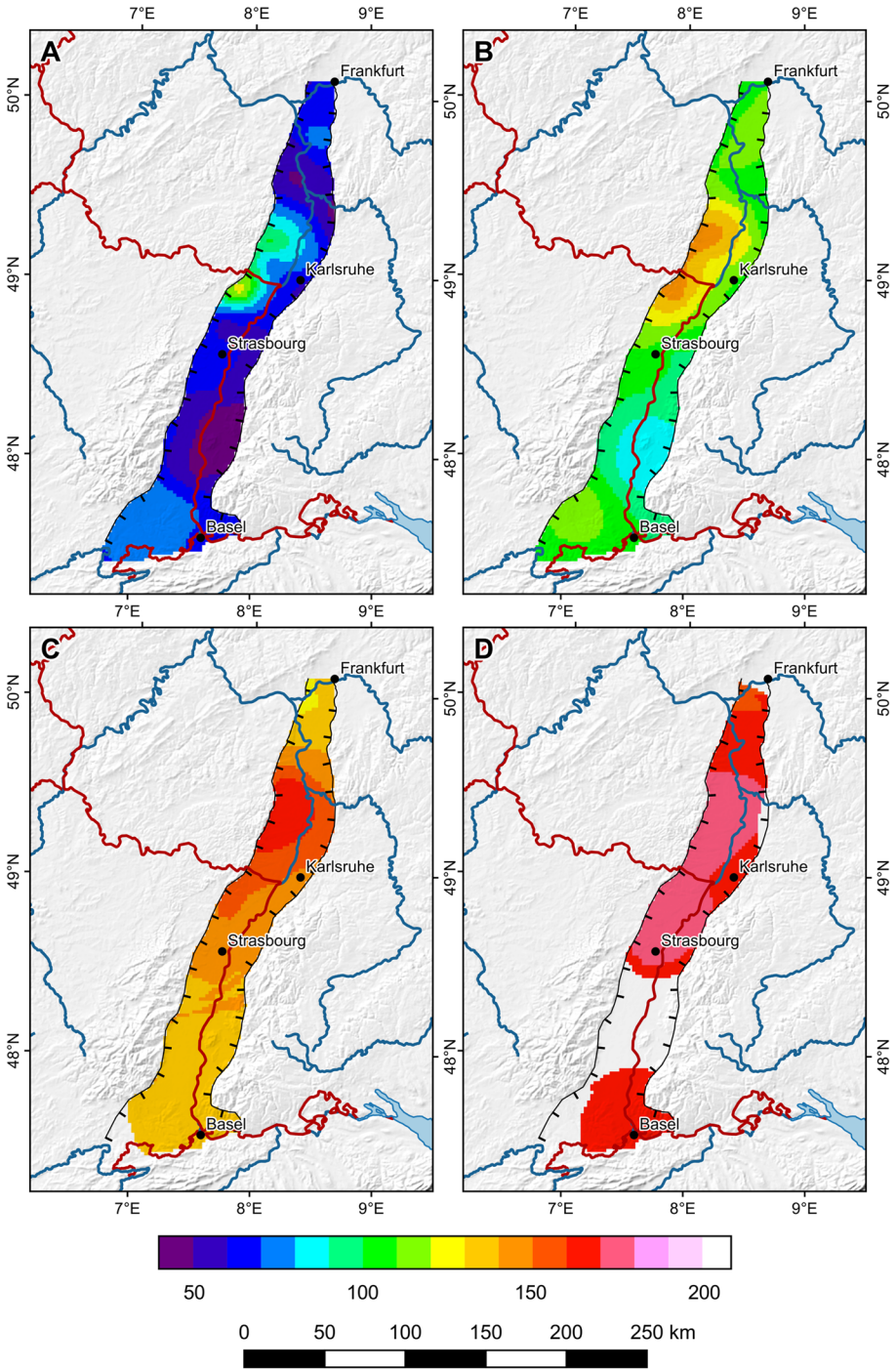

Fig. 9 Depth slices through the temperature model of Agemar et al. (2012) at **A** 1000 m, **B** 2000 m, **C** 3000 m and **D** 4000 m below sea level

discontinuities in the geological structure or the rock properties are not included in the interpolation, which can lead to an incorrect estimate of the subsurface temperatures. Furthermore, the results of the interpolation are uncertain in areas of low data density and for depths greater than about 2 km. Alternatively, the 3D temperature

distribution can also be calculated by numerical simulation (GeORG Projektteam 2013; Guillou-Frottier et al. 2013; Freymark et al. 2019, 2017, 2016; Koltzer et al. 2019). As shown by validation of these examples by measured temperatures, the mismatch for regional models can be kept below 20 °C with proper parametrization and carefully selected boundary conditions. A better fit is up to now not possible for regional-scale models due to the complex geometry of the faults acting as vertical and horizontal conduits, the variability of the other governing rock properties and due to the computational limits of most numerical simulation tools. However, numerical simulation of the subsurface temperature field can provide more accurate results especially on the local scale, where based on sufficiently accurate exploration data (3D seismics, reference wells) detailed models can be developed (Bär et al. 2021). To summarize, for regional scale assessment of the temperature field geostatistical interpolation is currently the primary method while numerical simulation has a much better potential for accurate temperature prediction at field scale.

Geothermal reservoir horizons

The investigation of deep geothermal potentials in the URG began already in the 1970s with the "Geothermische Synthese" (Sauer and Munck 1979). Since then, numerous studies have been carried out to characterize the subsurface and in particular the potential of geothermal target horizons (Dornstadter et al. 1999; Bär 2008, 2012; Stober and Jodocy 2009; GeORG Projektteam 2013; Bär et al. 2016; Frey et al. 2021a, 2021b). Based on that, in total nine geological units were identified, which show sufficient temperature, thickness and hydraulic permeability for the exploitation of heat at levels of more than 90 °C. In the following, these horizons are described with regard to their lithological properties and spatial distribution. Figure 2 summarizes the respective reservoir horizons and indicates the individual importance for deep geothermal projects in the URG.

Due to consolidation of the sediments with reduced porosity and permeability compared to their outcropping analogues, deep geothermal exploitation of intact rocks comes with a high risk of not reaching sufficient flow rates. For this reason, hydraulically active fault zones cross-cutting the geothermal reservoir horizons are usually targeted, which can exhibit significantly higher permeabilities and therefore allow high flow rates. In addition, as vertical conduits, they may be associated with natural upwelling of hot groundwater, resulting in increased geothermal gradients. Exceptions to this are to some extent the Mesozoic carbonates (Muschelkalk-Keuper, Hauptrogenstein and Upper Jurassic Limestones), which are locally karstified and thus sufficiently permeable. In addition, high permeabilities may also be reached in the coarse-grained initial as well as marginal facies of the graben filling (e.g., Pechelbronn Formation) and the double-porosity horizon of the Lower and Middle Buntsandstein.

Crystalline basement

According to the definition of the Variscan Orogenic Belt by Kossmat (1927), the crystalline basement of the URG is divided from north to south into the Rhenohercynian Zone, the Northern Phyllite Zone, the Mid-German Crystalline High (MGCH), the Saxothuringian Zone and the Moldanubian Zone. In deep geothermal exploration and research, interest in the crystalline basement is high, as it holds an almost inexhaustible potential

due to the favorable temperatures and large potential reservoir volume. In addition, it is the main source of radiogenic heat production (Vilà et al. 2010) and thus influences the thermal state of the crust to a considerable extent. Along the URG, the basement is already successfully used by the four power plants in Landau, Insheim, Rittershoffen and Soultz-sous-Forêts for electricity and heat generation (Vidal and Genter 2018) and was also the target of the abandoned projects in Basel and Vendenheim. Target reservoirs are generally related to large fault zones, where the fractured rocks show elevated natural permeability. However, for an economic operation of a geothermal system, hydraulic and chemical stimulation is necessary in most cases to increase the connectivity and permeability of the fracture network. A detailed description of the hydraulic, hydrochemical and petrophysical properties is given in chapter 6 for the main basement lithologies.

The limited availability of structural geologic information on the subsurface beneath sedimentary formations poses a significant challenge to the exploration, modeling and utilization of the basement. There is a total of 20 deep boreholes in the URG, which penetrate the top basement, whereas most of them are connected to the geothermal projects mentioned above. Figure 10 shows the location of these wells including the main rock type that was encountered. Likewise, the basement in the URG was surveyed by only a few large-scale seismic profiles, such as the DEKORP 9N and 9S lines. The latter was recently reprocessed and reinterpreted as part of the Hessen 3D 2.0 project (Homuth et al. 2021a, 2021b). The resolution and penetration depth of old seismic campaigns are usually not sufficient, but faults in shallower horizons may be traced into the basement. Crystalline outcrops at the graben shoulders, e.g., in the Black Forest, the Vosges, the Odenwald, the Palatinate or the Taunus, allow detailed investigations of petrophysical and thermal rock properties as well as the structural framework (Weinert et al. 2020; Bossennec et al. 2021; Frey et al. 2022). In addition, gravimetric and magnetic data sets (Rotstein et al. 2006; Edel and Schulmann 2009; Baillieux et al. 2014; Edel et al. 2018; Frey et al. 2021b) are suitable to study the structures, composition and properties of the basement beneath the sedimentary cover. These data sets are available in sufficiently high resolution for regional-scale models throughout the entire URG region.

Rhenohercynian and Northern Phyllite Zone

The Rhenohercynian and Northern Phyllite Zone are located at the northernmost rim of the URG (Blundell et al. 1992; Brun et al. 1992; Franke 2000). They make up only a small part of the region's basement and are therefore of rather subordinate importance for the deep geothermal power and heat production. But especially at the southern margin of the Taunus, there are several thermal springs (e.g., in Wiesbaden, Bad Nauheim, Bad Soden) related to large faults within these zones, which are used for balneological purposes (e.g., Loges et al. 2012).

The Rhenohercynian Belt is exposed in the Rhenish Massif (Taunus and Hunsrück) as well as in the Harz Mountains and Cornwall (Franke 1995b). The zone is mainly characterized by clastic shelf sediments, which were deposited from the Silurian onwards at the southern continental margin of Laurussia on top of Cadomian paragneisses (Molzahn et al. 1998; Franke 1995a). The unit further consists of subordinate reef carbonates, pelagic sediments, mid-ocean ridge basalts, and felsic volcanics (Huckriede et al. 2004; Stets and Schäfer 2011; Grösser and Dörr 1986; Floyd 1995). During the main

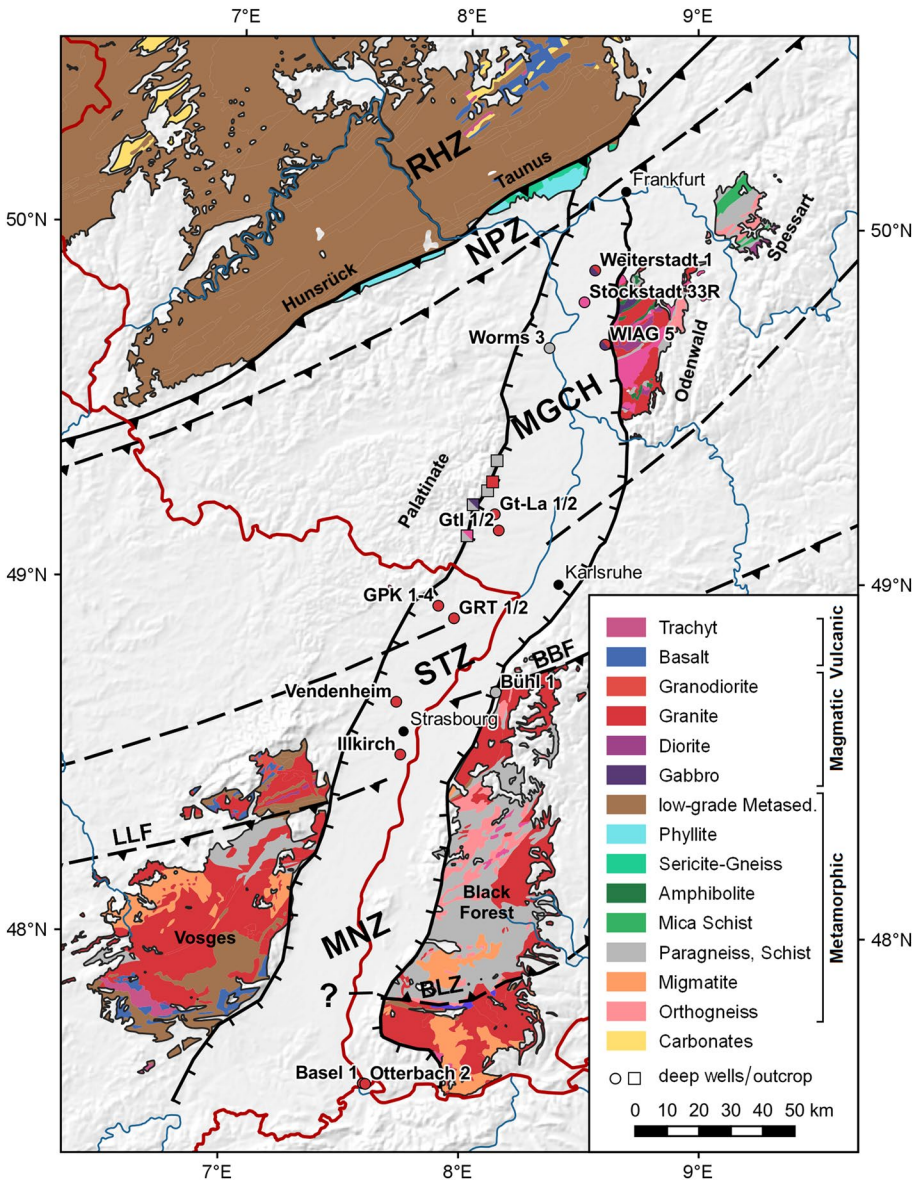

Fig. 10 Map of the Variscan basement outcrops around the URG (adapted from BGR 2016) including the location of deep boreholes that intersect the top basement. *BBF* Baden-Baden Zone, *BLZ* Badenweiler-Lenzkirch Zone, *LLF* Lalaye-Lubine Fault Zone, *MGCH* Mid-German Crystalline High, *MNZ* Moldanubian Zone, *NPZ* Northern Phyllite Zone, *RHZ* Rhenohercynian Zone, *STZ* Saxothuringian Zone

collision phase in the Carboniferous, far-reaching thrust sheets of marine sediments were established in the northern foreland of Variscan Orogeny (Edel and Weber 1995; Oncken et al. 1999), which show mainly low- to very low-grade metamorphic overprint (Doublier et al. 2012).

The Northern Phyllite Zone is a narrow belt on the plate boundary between Laurussia and the Armorican Terrain Assemblage. This zone is exposed at the southern Taunus and Hunsrück (Klügel 1997), but mostly covered by post-Variscan sediments. It is a heterogeneous tectonic mélange of 60 to 70% sedimentary rocks and 30 to 40% volcanic rocks (Klügel et al. 1994; Anderle et al. 1995). The Northern Phyllite was predominantly

overprinted by pressure-dominated greenschist facies metamorphism (Massonne 1995), which is intermediate between the P-/T-conditions in the Rhenohercynian Zone and the MGCH.

Mid-German Crystalline High

The MGCH is the deeply exposed basement of the northern active continental margin of the Armorican Terrain Assemblage, which consists mostly of plutonic rocks related to the southward subduction of the Rheic Ocean and Rhenohercynian Basin during the Carboniferous (Hirschmann 1995; Oncken 1997; Franke 2000). In addition, remnants of the Lower Paleozoic host rocks and earlier volcanic arc-related plutons with high-grade metamorphic overprint are found in this zone (Altenberger and Besch 1993; Zeh and Gerdes 2010).

The largest outcrop of the MGCH is the Odenwald at the northeastern shoulder of the URG, which is devided into the metamorphic Böllsteiner Odenwald in the east and the predominantly igneous Bergsträßer Odenwald in the west (Stein 2001). The latter is subdivided from north to south into the subunits Frankenstein Complex, Flaser-Granitoid Zone and Southern Granites/Granodiorites. From north to south, the plutons become gradually younger (from around 360 Ma in the north (Kirsch et al. 1988) to 325 Ma in the south (Kreuzer and Harre 1975; Anthes and Reischmann 2001)) and the SiO_2 increases (Okrusch et al. 1995). The westernmost exposure of the MGCH is situated in the Palatinate at the northwestern margin of the URG (Flöttmann and Oncken 1992). In contrast to the Odenwald, there are only a few local outcrops with the largest one in Albersweiler. At this location, orthogneisses derived from 369 ± 5 Ma old magmatic protoliths are predominant, that are vertically intercalated by metabasites (Frenzel 1971; Okrusch et al. 1995; Anthes and Reischmann 1997). Besides, granitoid intrusions with an age of about 340 Ma as well as metapelite and metagreywacke are found in the Palatinate basement (e.g., in Waldhambach).

Apart from surface outcrops, insights are derived from samples of several deep boreholes of the hydrocarbon and geothermal industries that penetrated the top MGCH in the URG (Fig. 10). The exploration wells Stockstadt 33R, Weiterstadt 1 and Wiag Hessen 5 reached mainly granitoids and subordinate amphibolites in depths between 2180 and 2490 m (Marell 1989; Lippolt et al. 1990; Müller 1996). In the well Worms 3 located about 20 km westbound in the graben, a cataclastic zone is intersected at 2170 m depth which is composed of strongly fractured gneisses, pegmatites and isolated granitoids. A mostly granitic basement was moreover encountered in the geothermal wells west of the Rhine River, Soultz-sous Forêts, Rittershoffen, Landau, Insheim, Vendenheim and Illkirch. However, it is still unsettled how far south the MGCH actually extends in this area. The Saar 1 well in the Saar-Nahe Basin is the westernmost borehole of the MGCH. Here, the deformed granitic basement was encountered under about 5.6-km-thick Carboniferous sediments (Weber 1995b).

Saxothuringian Zone

The Saxothuringian Zone or Saxothuringian Basin is located to the south of the MGCH. This unit is largely covered by sedimentary formations in the URG, leaving the course of the tectonic boundary unknown. However, geophysical data provide insights about

the lateral extent of the zone (Behr and Heinrichs 1987; Edel and Fluck 1989; Rotstein et al. 2006; Edel and Schulmann 2009; Frey et al. 2021b). The largest outcrop of the Saxothuringian Zone is situated in eastern Germany in the Thuringian Forest, the Fichtel Mountains and the Ore Mountains (Franke 1995c). There are two main facies types: the (para-)autochthonous Thuringian Facies is characterized by a sequence of Lower Paleozoic shelf sediments overlying the Precambrian gneiss basement of the Armorican Terrane Assemblage (Bankwitz and Bankwitz 1990; Behr et al. 1994; Falk et al. 1995). The autochthon is overlain by the allochthonous Bavarian Facies, which is a stack of tectonic nappes with varying metamorphic overprint (Behr et al. 1982; Martin 2003; Bahlburg et al. 2010). This unit consists of Upper Devonian to Lower Carboniferous deep marine deposits and intraplate volcanic as well as distal flysch in the uppermost part.

It is mostly unresolved how the Saxothuringian Zone continues to the west. Traditionally, the northern margins of the Vosges and the Black Forest are seen as outcrops of this unit (Kossmat 1927). The northern Vosges and the northern Black Forest (the so-called Baden-Baden Zone) are lithologically and structurally very heterogeneous, comprising gneisses intercalated with amphibolites, mica schist and quartzites as well as low-grade sedimentary and volcanic rocks, that are intruded by granites (e.g., Wickert et al. 1990).

Moldanubian Zone

The Moldanubian Zone is the southernmost unit of the Variscan basement in central Europe (Kossmat 1927; Franke 2000; Ziegler and Dèzes 2005). It is a heterogeneous and highly overprinted assemblage of Gondwana derived terranes that were juxtaposed during the Variscan Orogeny. Major outcrops of this zone are located in the Massif Central, in the Bohemian Massif as well as in the Vosges and Black Forest along the southern margin of the URG (Lardeaux et al. 2014).

The Moldanubian part of the Black Forest (Schwarzwald in German) is dominated by large gneiss complexes in the center and south (Central Schwarzwald Gneiss Complex (CSGC) and Southern Schwarzwald Gneiss Complex (SSGC)) (Eisbacher et al. 1989; Chen et al. 2000; McCann et al. 2008). CSGC and SSGC are further subdivided into a series of nappes consisting of Lower Paleozoic meta-granitoids and meta-sediments (Geyer et al. 2011). Large granitic plutons intruded at the boundaries of these nappes between 334 and 332 Ma (Schaltegger 2000). As in the Black Forest, the Vosges Mountains are divided into a northern, presumably Saxothuringian part and a central and southern Moldanubian part (McCann et al. 2008). The central Vosges consist of high-grade metamorphic zones that were intruded by large granitoid plutons in the Mid-Carboniferous. Granulites, migmatitic gneisses and meta-sediments are predominant in this region (Lardeaux et al. 2014). In general, the central Vosges show great similarities with the CSGC, but are shifted relatively southwards by about 30 km. The southern Vosges are a locally confined extensional basin (Eisbacher et al. 1989), filled with a Upper Devonian to Lower Carboniferous marine sequence of shales and greywackes, partly intruded by basalts and rhyolites (Schaltegger 2000).

In total three deep boreholes reached the Moldanubian basement in the URG. The geothermal well Bühl 1 encountered gneiss close to the eastern boarder fault. In the southernmost URG, the two wells Basel 1 and Otterbach 2 intersected a granitic basement.

Permo-Carboniferous

From the Westfalian onwards, Permo-Carboniferous (Rotliegend, r) sediments were deposited in numerous SE–NW oriented intramontane basins (Henk 1993; Weber 1995b; Schäfer and Korsch 1998; Scheck-Wenderoth et al. 2008). A thickness that allows an economic geothermal exploitation is only known from the northern URG (Sass et al. 2011; Arndt 2012; Bär 2012), whereas the extent and thickness of additional basins in the middle and southern URG is largely unknown and not confirmed by any deep wells (Rupf and Nitsch 2008). The largest exposure of the Permo-Carboniferous is located in the Saar-Nahe Basin (Schäfer 1989). Smaller outcrops can be found at the Sprendlinger Horst (Marell 1989), the Wetterau (Kowalczyk 2001) and in several location in the Vosges and Black Forest (e.g., near Baden-Baden where the thermal spas are fed by hot groundwater from this horizon or in the Badenweiler-Lenzkirch-Zone). The outcrops in the Saar-Nahe Basin and the Sprendlinger Horst and Wetterau can be correlated by several deep wells (Weiterstadt 1, Stockstadt 33R, Gimbsheim 2, Worms 3 and Trebur GT1) in the northern URG and show several suitable reservoir rock horizons (Bär 2012; Boy et al. 2012; Aretz et al. 2016). Accordingly, the highest thickness of presumably more than 2000 m is reached in the area west of Groß-Gerau.

In the Saar-Nahe Basin, the Permo-Carboniferous is divided into the lower Glan and upper Nahe Subgroups (Schäfer 2005; Deutsche Stratigraphische Kommission 2016). The former, also known as the pre-volcanic syn-rift phase, is further divided into the Kusel, Lebach and Tholey Layers (Stapf 1990) and consists of fine-to-coarse clastic sediments, which are occasionally interlayered by carbonates. The Nahe Subgroup comprises the volcanic syn-rift phase and the post-rift phase. Increased volcanic activity between 300 and 290 Ma led to the deposition of the up to 1100 m thick Donnersberg formation, which comprises basaltic-to-rhyolitic lava flows, tuffs and pyroclastics alternate with fluviatile and playa-like sediments (Stollhofen 1994; Stollhofen and Stanistreet 1994). During the post-rift phase mainly aeolian and playa-like sand-, silt- and claystones were deposited in a very hot-dry climate, known as the Standenbühl and Kreuznach formations (Aretz et al. 2016). Significant alluvial deposits of coarse clastics were simultaneously deposited at the basin margins in the Wadern formation. At the Sprendlinger Horst, sedimentation began during the active volcanic syn-rift phase (Marell 1989; Müller 1996). Here, however, alluvial fans as well as meandering and intertwined river systems are predominant.

The strong lithologic heterogeneity, both temporally and spatially, of the Permo-Carboniferous makes a general statement about the suitability of specific horizons for deep geothermal use very challenging. Broadly speaking, the coarse-grained fluviatile, aeolian and volcanoclastic sediments have higher permeabilities than the fine-grained lacustrine and playa deposits. However, because of the limited number of wells drilled into the Permo-Carboniferous of the URG, a detailed reservoir characterization can in most areas and especially to the south only be performed with larger uncertainties so far. The matrix of the sedimentary rocks is usually cemented, thus large-scale fault zones are again the main target of exploration as potential fluid pathways.

Buntsandstein

At the base of the Mesozoic, the Buntsandstein (s) was deposited in the Germanic Basin, which is dominated by terrigenous siliciclastic sediments (Backhaus 1974; Valeton 1953; Klapperer 2009; Meisel 1995). During the Lower Triassic, the depositional environment was similar to in the Permo-Carboniferous, with the Variscan Orogen still being the main sediment source (Paul et al. 2008). However, the deposition was not limited to the SW–NE trending molasse basins anymore but took place throughout the whole Germanic basin (Doebl and Olbrecht 1974; Ziegler 1990). The fluvio-lacustrine succession is therefore generally more homogeneous. Large outcrops of the Buntsandstein can be found across the entire URG area, but especially in the Palatinate, Buntsandstein Odenwald and Kraichgau (Fig. 1).

The lithostratigraphic unit is subdivided into the Lower, Middle and Upper Buntsandstein (Röhling et al. 2016). In the southern Germanic Basin, the Lower Buntsandstein comprises the Gelnhausen and Salmünster Sequences (Fazies 1966). The boundary to the fine-grained deposits of the Upper Zechstein is marked by boulder-bearing coarse sandstones, also known as Eck Formation. This horizon is overlain by fine and medium sandstones interlayered by clay and silt (Paul 1982). Towards the south, the grain size is steadily increasing, and the sediments are less sorted, which indicates a shorter transport distance. In the Middle Buntsandstein, the Volprihausen, Detfurth, Hardegsen and Solling Sequences are distinguished, which represent a cyclic sequence of fine- to coarse-grained clastic sediments (Dersch-Hansmann and Hug 2004). The Upper Buntsandstein is characterized by a gradual decrease in grain size. Fine and medium sandstones (Plattensandstein Formation) are overlain by silt and clay, referred to as Rötton Formation (Backhaus and Heim 1995).

In the URG, the thickness of the Buntsandstein increases continuously from about 65 m near Basel to 500 m in Karlsruhe. In a deep borehole in the Kraichgau, 539 m of Buntsandstein were intersected (Jodocy and Stober 2010a). North of Karlsruhe, a gradual thinning to a maximum of 300 m can be observed, caused by pre-Tertiary uplift of the Rhenish Shield and associated erosion processes (e.g., Sissingh 1998). The Buntsandstein is a double-porosity reservoir, where the main contribution to flow is provided by the fracture network (Haffen et al. 2012; Bossennec et al. 2021). In sandstone layers, the permeability of the rock matrix (e.g., measured on cores from oil and gas wells) is still comparatively high even at depths of more than 3 km, therefore contributing to the well productivity in addition to the fracture network (Bär 2012). However, the necessary data to quantify the respective contribution to fluid flow are currently missing, since hydraulic test data in deep wells always provide an integral value for the permeability. One possibility to determine the matrix permeability under reservoir conditions would be, e.g., drill stem tests in open borehole sections without hydraulically active fractures. In contrast to the coarse-grained layers, the clay-rich layers, mainly in the Upper Buntsandstein, exhibit overall low permeabilities.

Upper Muschelkalk

After the widespread transgression of the Tethys Ocean during the Middle Triassic, limestones, claystones and evaporites were predominantly deposited (Szulc 2000; Feist-Burkhardt et al. 2008; Götz and Gast 2010). The Upper Muschelkalk aquifer

(kuL/mo), which also includes the upper part of the Middle Muschelkalk and lowermost Keuper, is suitable for deep geothermal utilization (Wicke 2009; Stober and Bucher 2015). This lithostratigraphic unit consists mainly of banked lime- and dolostones, reflecting a full marine sedimentary environment. These rocks often contain larger amounts of trochites and oolites that lead to a high primary porosity. Furthermore, they are intensely fractured and karstified at fault zones. The Upper Muschelkalk is exposed on a large scale in the Kraichgau, where the highest thickness of more than 100 m is reached. In contrast, the thickness ranges from about 50 to 100 m in the central and southern URG (Boigk and Schöneich 1974; Jodocy and Stober 2010b; GeORG Projektteam 2013). In the north, the unit is thinned or not present at all, because, like the Buntsandstein, these rocks were eroded by Cretaceous uplift.

Jurassic carbonates

During the Middle Jurassic, the so-called Burgundy Carbonate Platform, in their sedimentary environment and extent comparable to today's Bahama Banks, developed in Central Europe (e.g., Brigaud et al. 2014). In the eastern part of this platform, mainly shallow marine carbonates were deposited in the Middle and Upper Mid-Jurassic (Dogger, jm), which are referred to as Hauptrogenstein (bjHR) (Ernst 1991; Gonzalez and Wetzel 1996; Pienkowski et al. 2008; Köster 2010). This formation consists of cross-bedded oolite-limestones and is bounded by clay and marl horizons. The deposits are interlayered by clay, marl and bioclastic horizons. Large outcrops of the Hauptrogenstein are located in the Swiss Jura Mountains and the eastern part of France. In the URG, it is present south of Hagenau and is exposed along the main graben faults at the Black Forest and the Vosges. The thickness increases continuously towards the south and reaches its maximum of about 120 to 140 m near Mulhouse (Jodocy and Stober 2010a, 2010b; GeORG Projektteam 2013).

Beside the Hauptrogenstein, also the Upper Jurassic carbonates (jo) represent potential targets for deep geothermal projects. This horizon is preserved only south of Mulhouse and consists of grey limestones interlayer with marlstones. The maximum thickness of about 100 m is reached at the southern URG margin. Like the Upper Muschelkalk, the Jurassic carbonates are often characterized by a comparatively large pore volume and a high fracture density. Moreover, they are usually karstified close to large fault zones, potentially allowing economic flow rates in geothermal wells (Stober and Bucher 2015).

Tertiary graben fill

The Tertiary (t) fill of the URG was intensively investigated by the hydrocarbon exploration, resulting in a large number of deep wells and seismic lines. Based on this, detailed characterization of the lithostratigraphic units was developed by various authors (Straub 1962; Doebl 1967, 1979; Rothe and Sauer 1967; Illies and Mueller 1970; Sauer and Munck 1979; Illies and Fuchs 1974; Doebl and Olbrecht 1974; Teichmüller 1979; Clauser and Villinger 1990; Durst 1991; Gaupp and Nickel 2001; Derer et al. 2003; Hurter and Schellschmidt 2003; Grimm 2005; Grimm et al. 2011; Jodocy and Stober 2011; GeORG Projektteam 2013; Reinhold et al. 2016; Hintze et al. 2018). It should be noted, however,

that the stratigraphic classification of the individual horizons has been regularly adapted over the last decades. Consequently, there are in many cases different names for identical geological units, which makes for example the correlation of formations between

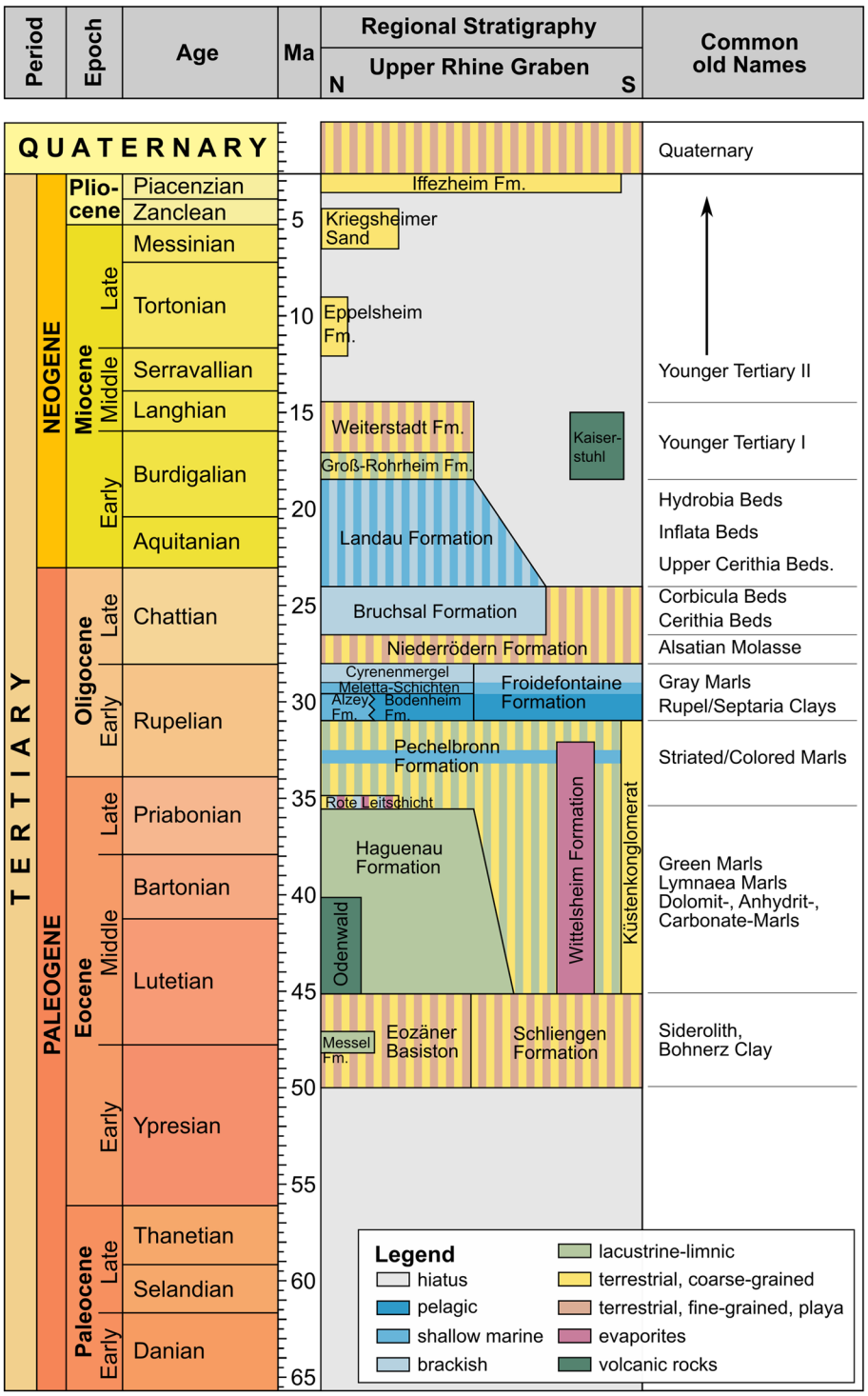

Fig. 11 Extract from the stratigraphic table of Germany, Tertiary lithostratigraphy of the URG (Deutsche Stratigraphische Kommission 2016)

wells sometimes challenging. In the following, we refer to the current nomenclature according to the German Stratigraphic Table (Fig. 11).

In the central and northern URG, the Cenozoic graben filling is usually characterized by a thickness of 1 to more than 3 km. Especially in local depositional centers, such as the Rastatt depression and the Heidelberg Trough ("Heidelberger Loch"), large amounts of Quaternary and Tertiary sediments were deposited. The highest thickness of more than 3300 m is reached between Heidelberg and Worms (Doebl and Olbrecht 1974), up to 2 km of which were deposited during the Miocene and Pliocene. In the southern URG, thick Tertiary sediments are limited to restricted basins, like the Hartheim Basin or the Kehl Basin (Jodocy and Stober 2010b). Particularly low sediment thicknesses are reached in the area of the so-called Rhenish Hauptschwelle north of the Kaiserstuhl.

The Cenozoic sediments of the URG contain partly high amounts of pelitic components, which are unfavorable for the utilization of geothermal resources due to their low permeability. Clay minerals also pose challenges for deep drilling operations, as they tend to fill cavities by swelling processes (Löschan et al. 2017). Furthermore, in fault and fracture zones, hydraulic contact can be interrupted by the accumulation of pelites or clay-smear development (Morrow et al. 1984; Jolley et al. 2007; Faulkner et al. 2010). The targets of geothermal exploration in the URG are therefore mainly medium- and coarse-grained horizons, which exhibit sufficiently high permeability and temperature. The Pechelbronn Formation seems to be most suitable in this context, particularly in the northern URG (Hintze et al. 2018; Stricker et al. 2020). In addition, the Niederrödern Formation and the Meletta Beds of the Froidefontaine Formation may also be a target for deep geothermal projects and underground thermal energy storages (UTES). Please note that the syn-sedimentary tectonics caused strong lateral changes of the depositional conditions and thus limit lateral reservoir amalgamation and hydraulic connectivity. Especially in the marginal areas and internal highs, considerable facies changes occur.

Pechelbronn Formation

The Pechelbronn Formation, also known as Pechelbronner Schichten or Pechelbronn Group, comprises syn-rift sediments of the Upper Eocene to Lower Oligocene that occur almost throughout the entire URG (Derer et al. 2003; Gaupp and Nickel 2001; Grimm 2005; Hintze et al. 2018). Due to the locally high oil content within this unit, it has been intensively studied since the nineteenth century. The Pechelbronn Formation generally overlies the Hagenau or Schliengen Formations in the southern and central URG (Grimm 2005). In the northern part, pre-tertiary rocks or Eocene base clays are located at the lower boundary. The top is marked by the onset of marine clays of the Bodenheim Formation (old name: Rupelton). The sequence can be divided into the Lower, Middle and Upper Pechelbronn Formation based on litho- and biostratigraphic characteristics. The Lower and Upper Pechelbronn Formation are characterized by fluvio-lacustrine conditions, which led to the formation of an alternation of colorful to gray, dolomitic marlstones with siltstones, sandstones and conglomerates. Coarser sedimentary rocks are mainly located in former channel structures. In subsidence centers like the Rastatt Basin, fine-clastic sediments are predominant (GeORG Projektteam 2013). The deposition of the Middle Pechelbronn Formation took place under brackish-marine conditions

after a transgression during the Uppermost Eocene (Doebl 1967). In the graben center, deep marine basins formed, in which grey to brown clay marl stones and subordinately fine sandstone layers and lenses were deposited. Due to the high proportion of pelites, the middle Pechelbronn Formation is rather unsuitable for geothermal utilization.

The Pechelbronn Formation is interlocked with the so-called Küstenkonglomerat (= costal conglomerate) Layer towards the URG margin (Geyer et al. 2011). This horizon consists of coarse sandstones and conglomerates of former alluvial and debris compartments or channels, containing boulders with diameters of locally more than 0.5 m. In the southern section of the Graben, the Haguenau and Pechelbronn Formations are moreover intercalated with halite sequences of up to 200 m thickness and several hundred meters thick marl stones, which are summarized under the term Wittelsheim Formation. The thickness of the Pechelbronn Formation ranges from a few meters in the Mainz Basin to 810 m in the Hagsfeld I well east of Karlsruhe (Doebl 1967). On average, the sediments are about 200 to 400 m thick (GeORG Projektteam 2013).

Froidefontaine Formation

The Lower Oligocene Froidefontaine Formation, also called Froidefontaine Subgroup or Grey Marl Formation, occurs throughout the whole URG (Grimm 2005). It is located on top of the Pechelbronn Formation and is overlain by the Niederrödern Formation. This subgroup is further divided into the Alzey and Bodenheim Formations, the Meletta Beds and the Cyrena Marl. The last two are sometimes also referred to as the Karlsruhe Formation. The Alzey Formation represents marine coastal facies, accordingly, it consists of mostly yellow sandstones and conglomerates (Grimm et al. 2000; Grimm 2005). At the same time, the basin facies of the Bodenheim Formation was deposited, which is characterized by alternating dark claystones and marl deposits. Alzey and Bodenheim Formation are overlain by the laminated, blue to grey clay- and marlstones of the Meletta Beds. In these, the proportion of carbonate-bearing sandstones increases continuously towards the top. The Froidefontaine Formation is completed by the Cyrene Marl, which consists mainly of colorful marlstones that contain thin layers of fine sandstones. The total thickness of the sequence ranges usually from 250 to 400 m, but locally up to 1250 m are reached (GeORG Projektteam 2013).

Niederrödern Formation

The Niederrödern Formation, which deposited during the Upper Oligocene, occurs also in the entire URG (Grimm et al. 2011). It overlays concordantly the Froidefontaine Formation. At the upper boundary, it is overlain by the Bruchsal Formation and south of Karlsruhe by unconsolidated tertiary sediments. The sequence consists of a colorful alternation of limnic marl and claystones with intercalated sandstones and siltstones. Especially in the upper half, sand horizons can be found that might be suitable for the deep geothermal exploration. The sequence is laterally variable and shows intercalations of carbonate banks, sulfate nodules and marginal conglomerates. The Niederrödern Formation is on average about 200 to 400 m thick. Locally, however, a thickness of up to 1 km is reached (GeORG Projektteam 2013; van der Vaart et al. 2021).

Reservoir characterization

Geohydrological and hydrochemical properties

Hydrogeological and hydrochemical data from laboratory investigations of drill cores from several hundred wells—mostly oil and gas drillings—within deep siliciclastic, carbonate and crystalline reservoirs of the URG area in France, Switzerland and Germany and their respective outcrop analogues have been compiled, examined, validated and analyzed with the aim to characterize fluid, rock and reservoir properties. This chapter compiles furthermore assessed, validated and analyzed hydrogeological and hydrochemical data from about 200 deep wells in different reservoirs in the URG and adjacent regions. Solely in situ testing data are presented from tests in single reservoirs; data from tests hydraulically connecting different reservoir formations with each other are excluded herein. The data have been collected from wellbores of some hundred to more than 3500 m depth. Bottom hole temperatures range from 60–160 ˚C. The prominent hard-rock reservoirs in the URG include sandstone, carbonate rock, a mixed lithology reservoir and the crystalline basement. Petrophysical properties were compiled from studies on cores from deep oil and gas as well as geothermal wells, as well as from outcrop analogue studies on the main reservoir horizons exposed in the Eastern and Western Graben shoulders.

Hydrogeological properties

Deeply buried sedimentary formations may contain and conduct water. Consequently, some formations at several km depths can behave as reservoirs, particularly limestones and sandstones. However, most of the subcritical liquid H_2O in fractured continental crust resides in the fracture pore space of the crystalline basement, which was only investigated during some local studies in the URG (e.g., Soultz, Rittershoffen and Basel). Thus, a compilation of hydraulic well test data in crystalline rocks of the Black Forest and from deep wells in northern Switzerland is introduced here. Data measured before stimulation in up to 5 km deep geothermal wells in the URG are included. For the influence of stimulation on the hydraulic properties, see e.g., Schill et al. (2017), Reinecker et al. (2019) and Stober et al. (2022).

The key data on the hydraulic conductivity of the reservoir formation of the reservoir are typically obtained from hydraulic well tests. The well yield depends not exclusively on the hydraulic properties of the reservoir formation (mainly hydraulic conductivity, storage coefficient) but to some degree also on the hydraulic properties of the wellbore itself (skin, wellbore storage), which were taken into account (Stober 1996). Hydraulic well tests also provide water samples for hydrochemical investigations and isotope studies.

A large number of hydraulic tests were completed in the different fractured and/or karstified deep reservoirs of the URG. Oil and gas industry tested most boreholes hydraulically several times within the same stratigraphic horizon. So, the results could be verified, and implausible results were rejected. Concept, approach and realization of most of the tests were dictated by the needs of the oil and gas industry. Tests included drill stem tests (DST), slug-tests and pumping-tests depending on the specific requirements. Most of these tests were typically of short duration and were performed in

relatively narrow packer-isolated test-sections. In contrast, tests in hydrothermal or geothermal wells were conducted over significantly longer time periods in longer borehole sections. Stober and Jodocy (2009) give general information on test realization and chosen evaluation methods. The straightforward evaluation of these hydraulic tests results in a value for the transmissivity (T [m^2/s]). The hydraulic conductivity (K [m/s]) can be retrieved from the transmissivity and the thickness of the tested formation (H [m]) as K = T/H assuming a homogeneous and isotropic tested formation.

The examined geothermal reservoir formations are characterized by relatively high hydraulic conductivity reflecting the active tectonic setting of the rift valley and its fractured and karstified reservoirs (Fig. 12).

The highest hydraulic conductivity with a median value of about $K = 1 \cdot 10^{-6}$ m/s is derived from the double porous (fractured and karstified) limestone reservoir of the Upper Muschelkalk (kuL/mo) and the lowest median value from the double porous Hauptrogenstein (bjHR) reservoir ($K = 6 \cdot 10^{-8}$ m/s). Five locations in the Buntsandstein (s) revealed high hydraulic conductivity, three wells provided low to very low conductivity (median: $K = 2.4 \cdot 10^{-7}$ m/s). The Buntsandstein typically is fractured with few fractures per meter, however, the fractures have relatively increased apertures ranging from approximately 1 to 10 mm (measured on cores) (Bossennec 2019). In addition to the fracture network, the hydraulic of the Buntsandstein is influenced by the matrix permeability, which depends strongly on the degree of diagenesis.

Figure 12 illustrates typical ranges of K, which indicate different flow-behaviors of the reservoirs. The two limestone reservoirs (Hauptrogenstein and Muschelkalk) are narrowly fractured, whereas in the Buntsandstein reservoir the distance between single water conducting fractures is much wider. Thus, it has to be considered that the test-length, especially for tests of the oil and gas industry, was too short in the Buntsandstein reservoir to fulfill always the criterions of an representative elementary volume (REV)

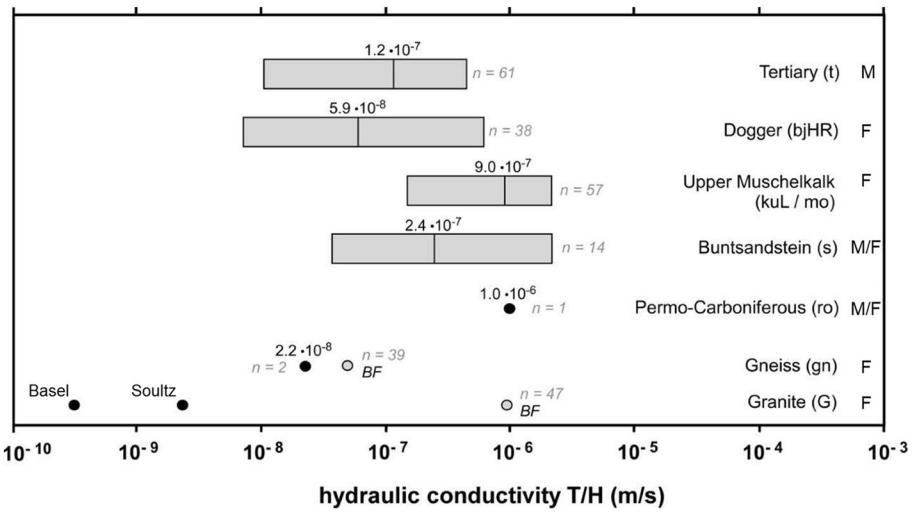

Fig. 12 Hydraulic conductivity of different deep reservoirs in the Upper Rhine Graben presented as boxplot; shown are the median values (*n* number of different boreholes, *BF* data of Black Forest and deep wells in N-Switzerland). It is indicated whether the fluid flow in the reservoir horizon is dominated by fractures (F) or matrix (M)

(Bear 1979) for fractured reservoirs and might only be representative for the rock matrix. The Tertiary (t) sediments (Fig. 12) on the other hand comprise hydraulic conductivity data of several hydraulically independent sedimentary strata (also compare Stober and Jodocy 2009). The retrieved hydraulic properties may not represent a single reservoir but several layers with heterogeneous properties. The vertical and lateral connectivity of permeable layers within the Tertiary strata can differ significantly from one location to another depending on the sedimentary environment and subsidence to accommodation space ratio.

In most reservoirs, the measured hydraulic conductivities show no regional variations or trend. The data also reveal that hydraulic conductivity decreases only marginally with depth in each of the reservoirs (Stober and Bucher 2015), probably a result of the young and still active tectonics in the Graben leading to intensified joint and fissure production rate or reactivation and thus to increased hydraulic conductivity even at greater depth. The data also clearly show that the Upper Muschelkalk- and Buntsandstein reservoir (with the exception of a few outliers) have the highest hydraulic conductivity, which might allow cross formations advective flow of thermal waters.

The crystalline basement is poorly investigated in the URG, since hydraulic data are only available from the deep wells of the Soultz-sous-Forêts geothermal project, while most other projects produce water from additional reservoirs on top of the crystalline (Vidal and Genter 2018; Reinecker et al. 2019). Thus, Fig. 12 presents additional hydraulic data of crystalline basement rocks from the Black Forest and deep wells in northern Switzerland (Stober 1996). Generally, hydraulic conductivity of the crystalline basement varies over several orders of magnitude. Some volumes of the continental crust are essentially impervious; other areas are highly conductive and (Stober and Bucher 2007) may hydraulically behave like near surface reservoirs (Ingebritsen and Manning 1999; Manning and Ingebritsen 1999; Scibek 2020; Achtziger-Zupančič et al. 2017; Stober et al. 2022). Deep geothermal wells in the URG often revealed a surprisingly high hydraulic conductivity at the top of the crystalline basement, e.g., at the former Paleozoic land surface. However, granite seems to be more permeable than gneiss (Fig. 12). The observed nearly depth-independent conductivity structure of the sediments in the Rhine Rift Valley is in marked contrast to the significant conductivity decrease with depth observed in the crystalline basement of the Black Forest (Stober and Bucher 2007).

Hydrochemical properties

Generally, the chemical data of water samples presented here are old data from archives reported from samples collected during production tests performed by the oil and gas industry. The original, tested and sampled boreholes are closed now, so that resampling is not possible anymore. A few recently collected samples from thermal spas and geothermal wells have been added to the data set. A total of more than 200 water analyses have been compiled (Pauwels et al. 1993; He et al. 1999; Stober and Jodocy 2009; Stober and Bucher 2015; Sanjuan et al. 2016; Stober et al. 2022). In some wells several samples had been taken from the same formation. So, on the one hand the hydrochemical data could be verified and implausible analyses could be rejected and on the other hand the best analyses for further investigations could be used, onsidering standard criteria given, e.g., in Hölting and Coldewey (2009).

The composition of the fluids from all four investigated reservoirs show systematic variations with increasing TDS corresponding to increasing depth (Fig. 13). The chemical composition of water from shallow sedimentary formations (< 800 m depth) typically reflects the mineral inventory of the sediments:

- Tertiary sedimentary formations: Ca-HCO_3 water, controlled by sediments with carbonate components. Locally SO_4 is enriched probably because of the occurrence of gypsum/anhydrite in some strata.
- Hauptrogenstein: Ca-HCO_3 water, related to fractured, karstified limestone (calcite)
- Upper Muschelkalk: Ca-SO_4-HCO_3 water, due to fractured, karstified limestone, containing gypsum/anhydrite-bearing strata beneath the reservoir (Middle Muschelkalk).
- Buntsandstein: Ca-HCO_3 waters with elevated SO_4 concentration, resulting from gypsum lenses in the fractured sandstone, locally cemented with calcite and abundant calcite veins.

Also, near-surface conditions such as recharge rate and REDOX conditions control the water composition. It is therefore not surprising that water residing in limestone reservoirs is strongly influenced by the carbonate minerals present in the rock (Fig. 13).

Deep thermal groundwater in the URG is always highly mineralized (Pauwels et al. 1993), with the total of dissolved solids (TDS) typically exceeding 5 g/kg in groundwaters below 800 m depth. TDS furthermore drastically increases with depth in all investigated reservoirs. The highest overall TDS-value of 300 g/kg is observed in brines from the Hauptrogenstein. In the Buntsandstein brine, the highest TDS is 127 g/kg, in Upper Muschelkalk 79 g/kg and in the Tertiary strata 240 g/kg. Na-Cl brines are the dominant chemical character irrespective of the rock forming minerals (Fig. 13) and the salinity of thermal waters in sedimentary formations is most commonly higher than in seawater (35 g/kg) (Stober and Bucher 2015), reflecting worldwide observations (Carpenter 1978; Grasby and Betcher 2002; Karro et al. 2004; Kharaka and Hanor 2004).

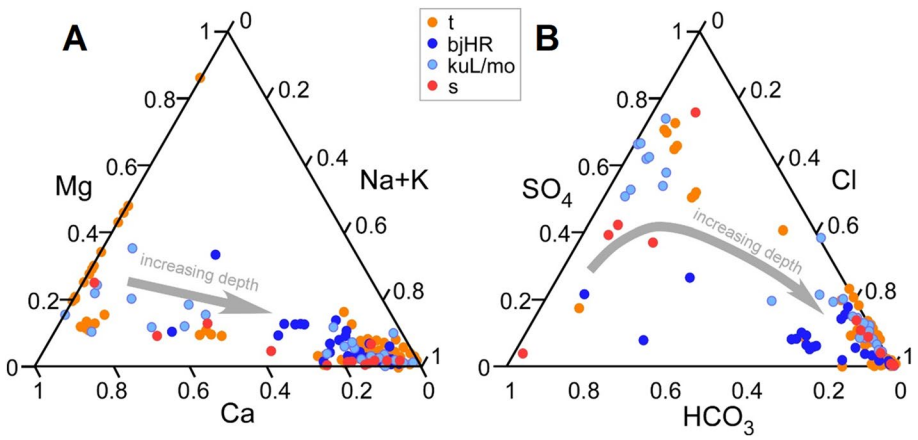

Fig. 13 **A** cations and **B** anions in different reservoirs of the URG (t—Tertiary, bjHR—Hauptrogenstein, kuL/mo—Upper Muschelkalk, s—Bundsandstein). With increasing depth, the main water components are Na and Cl

In the URG, the sulphate (SO_4) concentration first increases with TDS and becomes the dominant anion in some waters. At very high TDS, the SO_4 concentration relatively decreases in favor of Cl. Bicarbonate (HCO_3) is typically higher concentrated than sulphate in shallow, low TDS water. With depth and increasing TDS (increasing Cl concentration) also the SO_4 concentration increases and strongly outweighs HCO_3. Almost all deep high Cl (high TDS) water exhibits a higher concentration in SO_4 than in HCO_3. Thus, in all deep URG-reservoirs, the fluids evolve to a Na-Cl dominated brine, independent of the rock composition and the minerals of the reservoir rocks (Fig. 13).

Despite the very high salinity of brines in the URG, deep groundwaters within the Graben are still below saturation with respect to halite. However, waters reach saturation with respect to various minerals including calcite and quartz at much lower concentrations. Saturation of the water with some low-solubility minerals controls the composition of the fluid at depth. Since solubility depends on temperature and pressure, the water composition changes during flow along pressure and temperature gradients, that is during up- or downward flow or during uplift (decompression) or burial of the rock masses. The solubility changes may leave mineral precipitates (scales) on fracture surfaces or may cause dissolution corrosion on mineral surfaces. All deep waters of all reservoirs are saturated with respect to calcite. Calcium is increasing with increasing TDS and depth, whereas HCO_3 is decreasing as a consequence of the inverse concentration of Ca and carbonate at equilibrium with calcite ($CaCO_3$ solid $\Leftrightarrow Ca^{2+} + CO_3^{2-}$). All deep waters are moreover saturated with respect to dolomite, quartz and barite (Parkhurst and Appelo 1999). Thus, the waters have a certain scaling potential if pumped and used in geothermal energy applications as already proven for Soultz, Bruchsal, Insheim and other operating projects.

Buntsandstein water (e.g., in Cronenbourg and Bruchsal) is rich in strontium and lithium (> 0.1 g/kg) and arsenic may reach several 10^{-3} g/kg. Similar strontium- and lithium-concentrations were only measured in several crystalline basement and Tertiary wells (Sanjuan et al. 2016; Drüppel et al. 2020).

Water from a number of wells in Buntsandstein, Upper Muschelkalk and Hauptrogenstein showed CO_2-gas concentrations of more than 1 g/kg, while in the Tertiary sediments most CO_2-gas concentrations are on the order of several 0.1 g/kg. Generally, in all reservoirs the H_2S concentrations are low, often below detection limit.

The origin of salinity and major water components in deep sedimentary URG-reservoirs and in the crystalline basement was in detail investigated by Stober and Bucher (2015). Chloride can apart from external sources (fossil seawater, halite deposits) be found in the crystal lattice of minerals, in fluid inclusions and along grain boundaries. In magmatic rocks of the Black Forest chloride and lithium are typically found in biotite (Drüppel et al. 2020). During alteration, Cl and Li are (among others) removed from the solid into the fluid phase. Both elements behave rather conservatively, leading to enrichment in water. The high TDS of deep crystalline basement waters is not a consequence of prolonged acid–base reaction of water with the primary unstable minerals of the basement rocks, but rather the mechanism of zeolite formation from feldspar that generates saline neutral waters. Zeolitization does not affect pH and chemically binds free H_2O into the structure of a framework silicate, increasing passively the TDS of the remaining water (Stober and Bucher 2004; Brady et al. 2019). Zeolites have been

observed and mineralogically analyzed in drill cores from the Black Forest (Walenta 1992). Similar observations were, for example made in the Gotthard Massif (Zangerl et al. 2006; Weisenberger 2009). In addition, the formation of zeolites as hydrothermal transformation products has also been demonstrated in laboratory experiments under reservoir conditions (Schmidt et al. 2017, 2018, 2019).

Based on profound hydrochemical indicators (like Cl/Br, (Na + K)/Cl) and additional hydrochemical and geochemical indications (e.g., geothermometry), precipitation of specific minerals in cores (Vidal et al. 2018; Drüppel et al. 2020), on enhanced temperatures in the URG and temperature profiles in deep wells (e.g., Vidal et al. 2017), on heat flow anomalies (e.g., Clauser 1989) and on numerical modeling (Person and Garven 1992; Freymark et al. 2019; Koltzer et al. 2019) it is known that there are areas with (even recent) ascending thermal brines from deeper into shallower parts of the crystalline basement and in the central URG into the Buntsandstein and even in higher formations. The strong topography (Black Forest, Vosges Mountains) in combination with the fault-bound vertical fluid pathways induces fluid flow over long distances not only from the graben shoulders to the center, but also from south to the north within the graben. The deep hydrothermal flow system is both topography (Tóth 1978) and buoyancy driven and the upwelling water is focused and channeled along zones of higher permeability (faults, fractures, etc.). Upwelling waters with enhanced temperature and TDS, with significant amounts of Na, Cl, etc., are typically found in the foot hills or valleys of these mountains as thermal springs (Stober et al. 1999) and along major faults within the crystalline and in deep sedimentary layers in the URG as shown in the conceptual sketch in Fig. 14a.

Thus, the salinity of the Buntsandstein brine seems to be at least partly influenced by upwelling water from the crystalline basement. This assumption is supported by temperature profiles, barite precipitation, and numerical simulations, among others. In contrast, Sanjuan et al. (2016) argue, based on the Na/Li ratio and Sr isotopy, that fluids discharged from the crystalline basement mainly originate from the Buntsandstein. In any case, mixing of fluids from these two reservoirs is to be expected, depending on the local circulation system. Further upwelling of hot water from the Buntsandstein preferentially along fractures and fault systems is possible, especially in the halite-rich Middle Muschelkalk, thus leading to high salinity in the Upper Muschelkalk reservoir (Fig. 14a). Since particularly the Lower Jurassic (in addition to parts of the Keuper and Middle Jurassic) is very compartmentalized, circulation in the upper system (Hauptrogenstein, Tertiary sediments) is more or less separated and decoupled from the lower system (Crystalline basement, Buntsandstein, Upper Muschelkalk) (Stober and Bucher 2015). In the Tertiary sediments, the high salinity is mainly caused by dissolution of halite present in some of the Tertiary layers. Saline water in Tertiary sediments may possibly migrate into the Hauptrogenstein. However, fluid circulation from the lower into the upper system seems merely possible in areas with huge vertical displacement within the Graben, e.g., along prominent graben/horst-structures. Near the rim of the Graben the waters seem to be hydrochemically influenced by adjacent layers, being in line with the findings of the modeling of the temperature field by Clauser (1989), Person and Garven (1992), Rühaak et al. (2014) and (Freymark et al. 2019). Nevertheless, a systematic temperature trend with colder values at the two rims of the Graben and higher ones more in

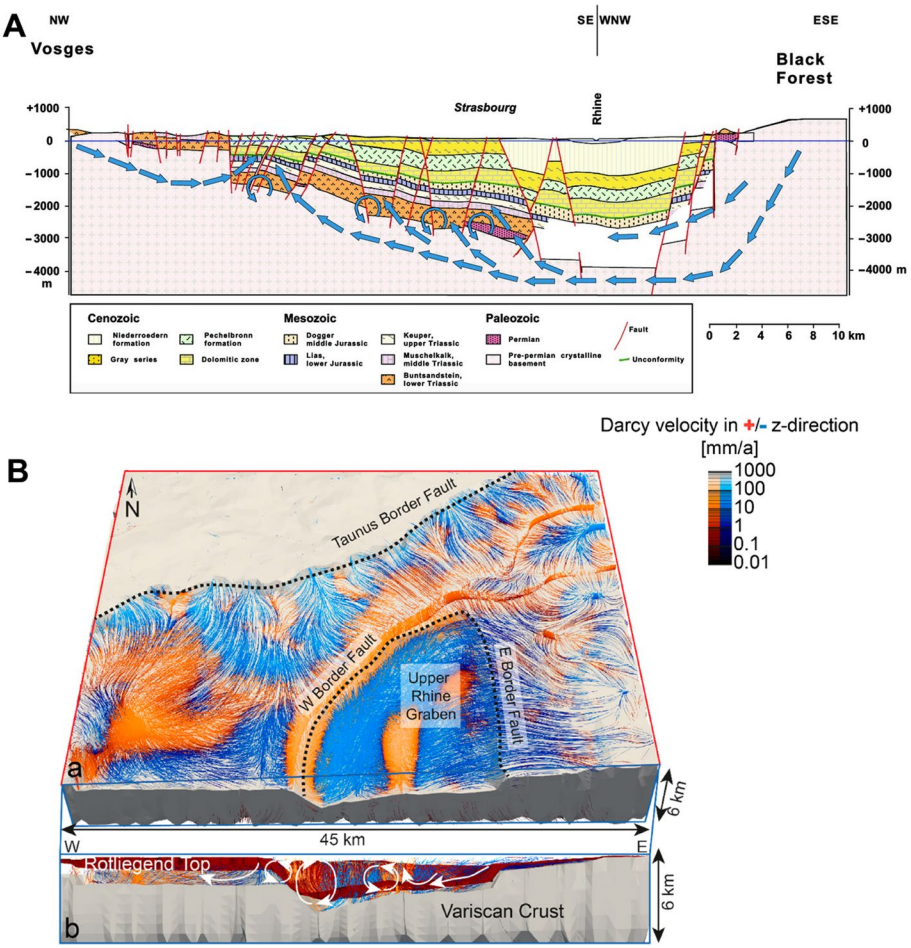

Fig. 14 **A** Schematic illustration of deep topography driven, hydrothermal flow systems with upwelling of saline water in the central URG (Stober and Bucher 2015), blue arrows showing the generalized fluid pathways within the basement and lower situated sedimentary horizons; **B** 3D visualization of simulated streamlines in the northern URG (Koltzer et al. 2019). The color code shows in red Darcy velocities in the positive z-direction (upflow) and in blue in the negative z-direction (downflow). With velocities from black over dark colors to light colors into white. **a** Streamlines above the Variscan crust in a block in South-West Hesse; **b** profile perpendicular to the Upper Rhine Graben with streamlines in Cenozoic and Rotliegend sediments. White arrows highlight the simulated fluid circulation in the URG

the center of the Graben is not visible in the temperature model of Agemar et al. (2013), which might also be a result of spatial data distribution and the interpolation approach.

Conceptual 2D profiles (as in Fig. 14a) can only describe to some degree the hydraulic processes in a complex system such as the URG, where small-scale changes in groundwater flow regime are expected. Therefore, attempts have been made in the past, e.g., by Koltzer et al. (2019), to refine the picture using 3D numerical modeling (Fig. 14b). The results suggest that the URG is characterized by a large number of locally confined convection cells tied to hydraulically active fault zones, an observation which matches very well with known geothermal anomalies present in the URG mainly along major graben internal faults. However, also this approach can only represent a limited geologic complexity (e.g., number of faults, spatial variation of hydraulic properties) with regard to the computational effort and data availability. For

this reason, the exact paths of fluid flow throughout the URG remain uncertain until new data are collected and combined in complex integrated models as proposed by Bär et al. (2021a).

Petrophysical properties

To assess and review the petrophysical properties of the sedimentary and basement reservoirs in various depths of the URG (Fig. 15), published data were compiled and structured following the guidelines of P^3—the PetroPhysical Property Database (Bär et al. 2020). Therefore, the data compiled and presented here only stem from lab measurements on core samples and not from any kind of borehole geophysical logging. Borehole geophysical logs in the URG are usually confidential and in most cases too old to determine the relevant petrophysical properties directly. Since petrophysical data from actual samples of reservoir depth is very sparse due to the high costs of drilling cores and often also confidential, results from various outcrop analogue investigations (mostly active and abandoned quarries) performed around the URG were included as well. An exception for data and core availability are the research wells of Soultz-sous-Forêts, where multiple investigations were performed both on logs as well as on drill cores.

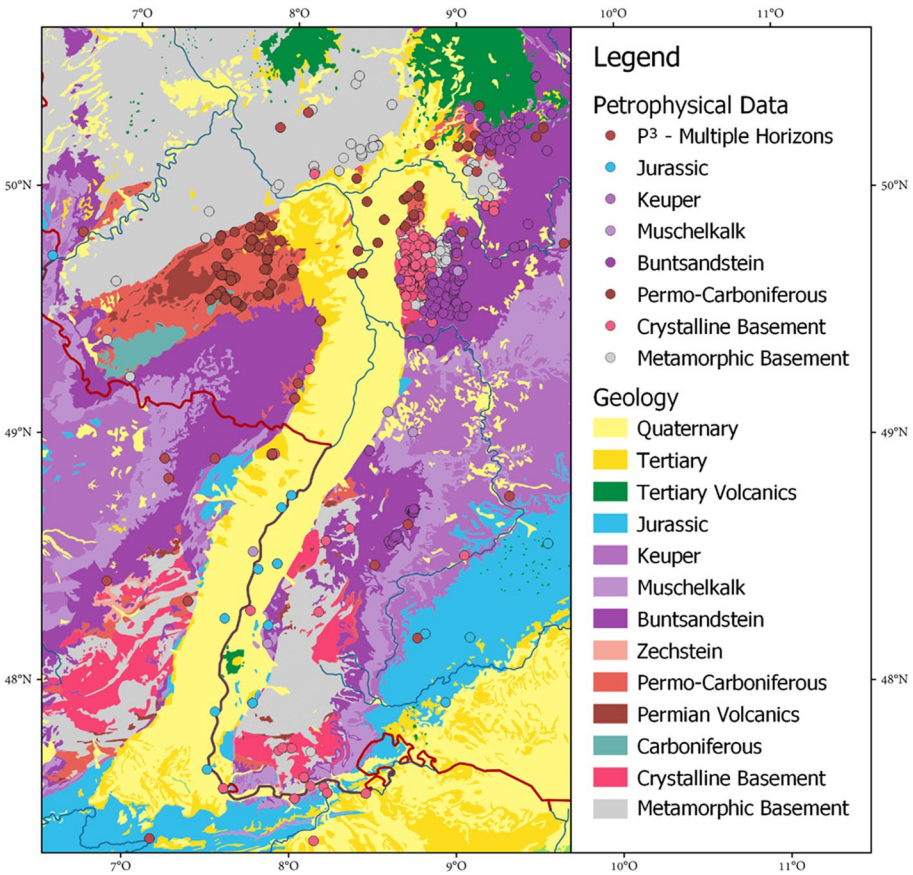

Fig. 15 Location of datapoints with petrophysical property data measured on samples from drill cores or outcrop analogues of the deep geothermal reservoir units of the Upper Rhine Graben

Overall, more than 19,000 single or averaged measurement values were compiled. Data evaluation was performed for each reservoir formations and for the main lithologies of the crystalline and metamorphic basement. Naturally, for such a large and diverse dataset, documentation of the original sources is very heterogeneous and of different quality, resulting in the need to compare and statistically assess results of single measurements together with mean values of multiple measurements of the same rock type.

Data availability also differs quite a lot depending on the particular properties to be assessed. While density, porosity and permeability are most abundant as well as thermal conductivity, data for other properties like specific heat capacity and thermal diffusivity are rather sparse. Direct measurements of mechanical rock properties like p-and s-wave velocities, Poisson ratio, uniaxial compressive strength, shear strength, cohesion, angle of internal friction are very rare and restricted to cores from less than three wells and only a couple of outcrop analogues. Mechanical rock properties are thus not yet included in the compilation here and need to be investigated in more detail in the future.

Depth trends and influence of alteration and weathering were not assessed in detail due to the heterogeneity of the dataset but are well known and investigated for the crystalline basement (Ledésert et al. 1999; Surma and Geraud 2003; Griffiths et al. 2016) and its weathering zone at the top and strongly hydrothermally altered sections as well as for the Buntsandstein, where hydrothermal bleaching is well known to reduce primary porosity and intrinsic permeability of the rock matrix (Gaupp et al. 1998; Haffen et al. 2013, 2015; Bossennec et al. 2021). For the Permo-Carboniferous, a thorough comparison of reservoir and outcrop analogue samples is presented by Aretz et al. (2016), where it is shown that the depositional facies plays an important role on the preservation of primary porosity at reservoir depth. Heap et al. (2017) and Kushnir et al. (2018a) investigated the influence of paleo-weathering on Soultz core samples of the Buntsandstein, Permo-Carboniferous and the crystalline basement and showed the positive influence of the associated processes on the reservoir properties.

As presented in Figs. 16 and 17 all reservoirs and reservoir lithologies show a large data spread reflecting the internal heterogeneity of the reservoirs with a wide range of different rock types (e.g., pelites to coarse sandstones; gabbro to granite, meta-pelites to quartzites). For the plutonic basement rocks, granites and granodiorites exhibit the best petrophysical properties for geothermal utilization. They both have considerably high thermal conductivities and thermal diffusivities and according to Vilà et al. (2010) also the highest internal radiogenic heat production. Additionally, from outcrop analogue investigation, strongly increased effective porosities and intrinsic permeabilities are known, resulting mainly from weathering effects and hydrothermal alteration. A more detailed statistic assessment is for example presented in Weinert et al. (2020) for the crystalline basement of the northern URG. For the less dominant metamorphic basement rocks, the gneiss and quartzites show the best thermal properties, but lowest porosities and intrinsic or apparent permeabilities. The hydraulic rock properties are seemingly better for meta-volcanics and meta-pelites, while still completely insufficient to provide the flow rates needed for geothermal utilization.

The Paleo- to Cenozoic reservoir units of the sedimentary units of the URG also cover a large spread of rock properties. The Tertiary, Buntsandstein, Zechstein and Permo-Carboniferous reservoir rocks have porosities, which are interesting for deep geothermal

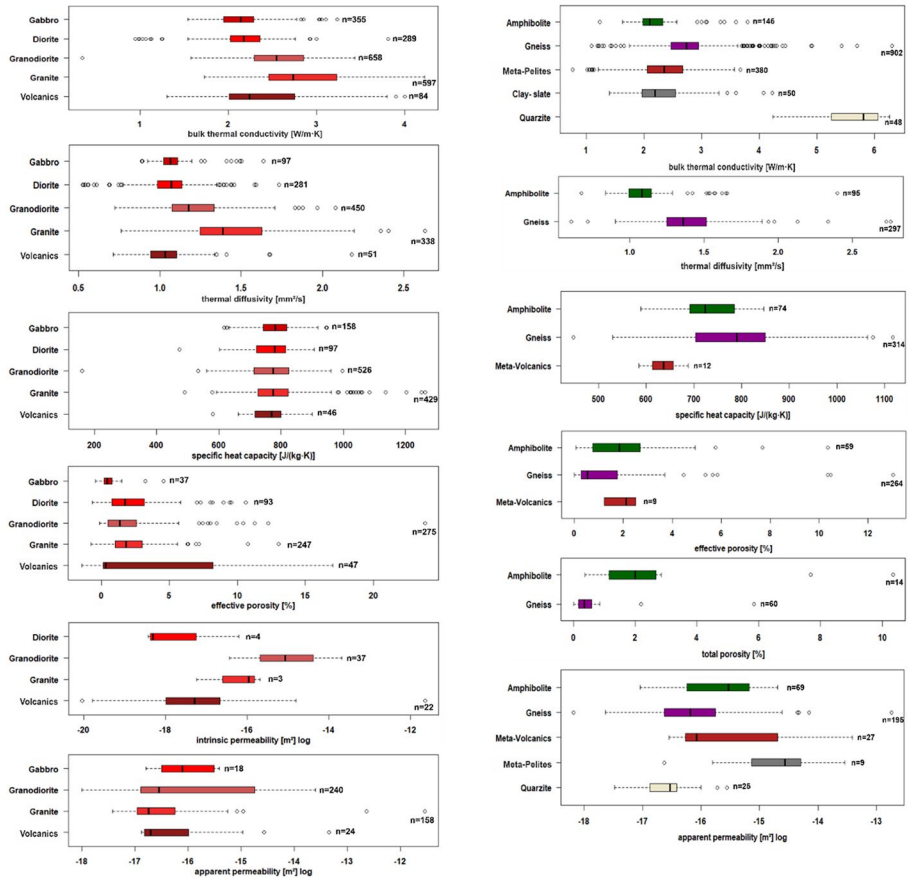

Fig. 16 Petrophysical properties (thermal conductivity, thermal diffusivity, specific heat capacity, effective and/or total porosity and intrinsic and/or apparent permeability) of different lithologies of the basement reservoirs in the Upper Rhine Graben from outcrop analogue and deep drill core investigations presented as box-whisker plots; shown are the average, Q25, Q75 and minimum and maximum values (n – number of data points per property and lithology). Data compiled from (Wenk and Wenk 1969; Kappelmeyer and Haenel 1974; Schärli and Kohl 2002; Surma 2003; Stober and Bucher 2007; Pei 2009; Kraus 2009; Faridfar 2010; Kläske 2010; Klumbach 2010; Vilà et al. 2010; Hoffmann 2011, 2015; Welsch 2011; Bär 2012; GeORG Projektteam 2013; Maire 2014; Hückel and Kappelmeyer 1966; Orendt 2014; Wiesner 2014; Weber 2014; Aretz et al. 2016; Lambert 2016; Schintgen 2016; Vogel 2016; Schäffer et al. 2018; Weinert et al. 2021)

utilization concerning their heat storage potential. The Jurassic, Keuper and Muschelkalk reservoir rocks have significant lower effective porosities and thus can mainly be classified as fracture-flow or karstified reservoirs. This observation is proven by the intrinsic or apparent permeabilities of the different reservoir rocks. Here, the Tertiary, Buntsandstein, Zechstein and Permo-Carboniferous have average values of more than $5{\cdot}10^{-15}$ m^2, which can be sufficient for deep geothermal utilization even if the contribution of the fracture network is not considered.

The petrophysical properties of the Tertiary succession is described in more detail, by e.g., Gaupp and Nickel (2001), Jodocy and Stober (2011), GeORG Projektteam (2013), Reinhold et al. (2016), Hintze et al. (2018), Stricker et al. (2020) and Bär et al. (2021b).

The petrophysical properties of the Buntsandstein as a double-porosity reservoir is well described by Bär (2012), Haffen et al. (2012), Haffen et al. (2015) and Bossennec et al. (2021).

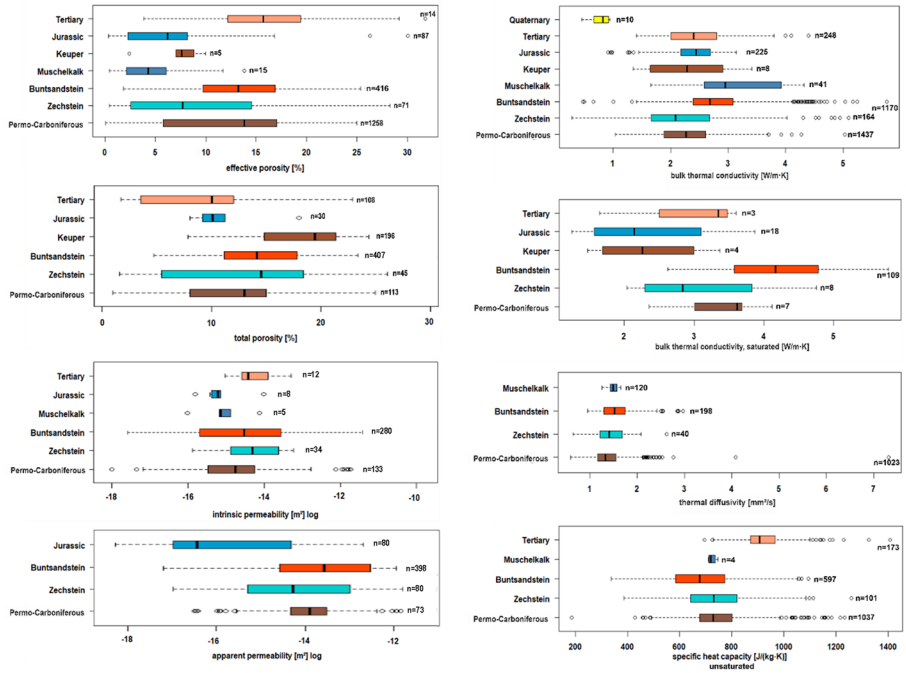

Fig. 17 Petrophysical properties (effective and total porosity, intrinsic and apparent permeability, thermal conductivity (dry and saturated), thermal diffusivity and specific heat capacity, of the different sedimentary reservoirs in the Upper Rhine Graben from outcrop analogue and deep drill core investigations presented as box-whisker plots; shown are the average, Q25, Q75 and minimum and maximum values (*n* number of data points per property and reservoir). Data compiled from (Leu et al. 1999; Mack 2007; Schumann 2008; Gu 2010; Klumbach 2010; Vilà et al. 2010; Hesse 2011; Jodocy and Stober 2011; Nehler 2011; Schubert 2011; Welsch 2011; Bär 2012; GeORG Projektteam 2013; Schöpflin 2013; Homuth 2014; Jensen 2014; Müller 2014; Weber 2014; Betten 2015; El Dakak 2015; Esteban et al. 2015; Sandkühler 2015; Aretz et al. 2016; Schintgen 2016; Heap et al. 2017; Kushnir et al. 2018b; Schäffer et al. 2018)

The petrophysical properties of the Permo-Carboniferous are described by e.g., Aretz et al. (2016), Gu et al. (2017), Molenaar et al. (2015), Reinecker et al. (2015) and Heap et al. (2017).

Geothermal projects

For centuries, deep thermal groundwaters have been used for balneological purposes along the margin of the URG starting with the Romans. Since the beginning of the twentieth century, this application has been further expanded by the drilling of numerous shallow or middle deep wells (Fig. 18). The large-scale exploration of deep geothermal resources for the generation of heat and electrical power began in the late 1970s and 1980s with the projects in Bühl, Cronenbourg and Bruchsal (Table 1).

This first phase was followed by the extensive European EGS (Enhanced Geothermal Systems) project at Soultz-sous-Forêts, which to date has provided extremely valuable insights into the hydraulic, mechanical and chemical properties of fractured reservoirs and the potential for economic exploitation. At this location in total 5 deep wells (GPK1-4 and EPS1), partly with a depth of more than 5 km, were drilled between 1987 and 2004 (Genter and Traineau 1996; Dezayes et al. 2005b; Baujard et al. 2017). Multiple hydraulic and chemical stimulation experiments were conducted, some of which

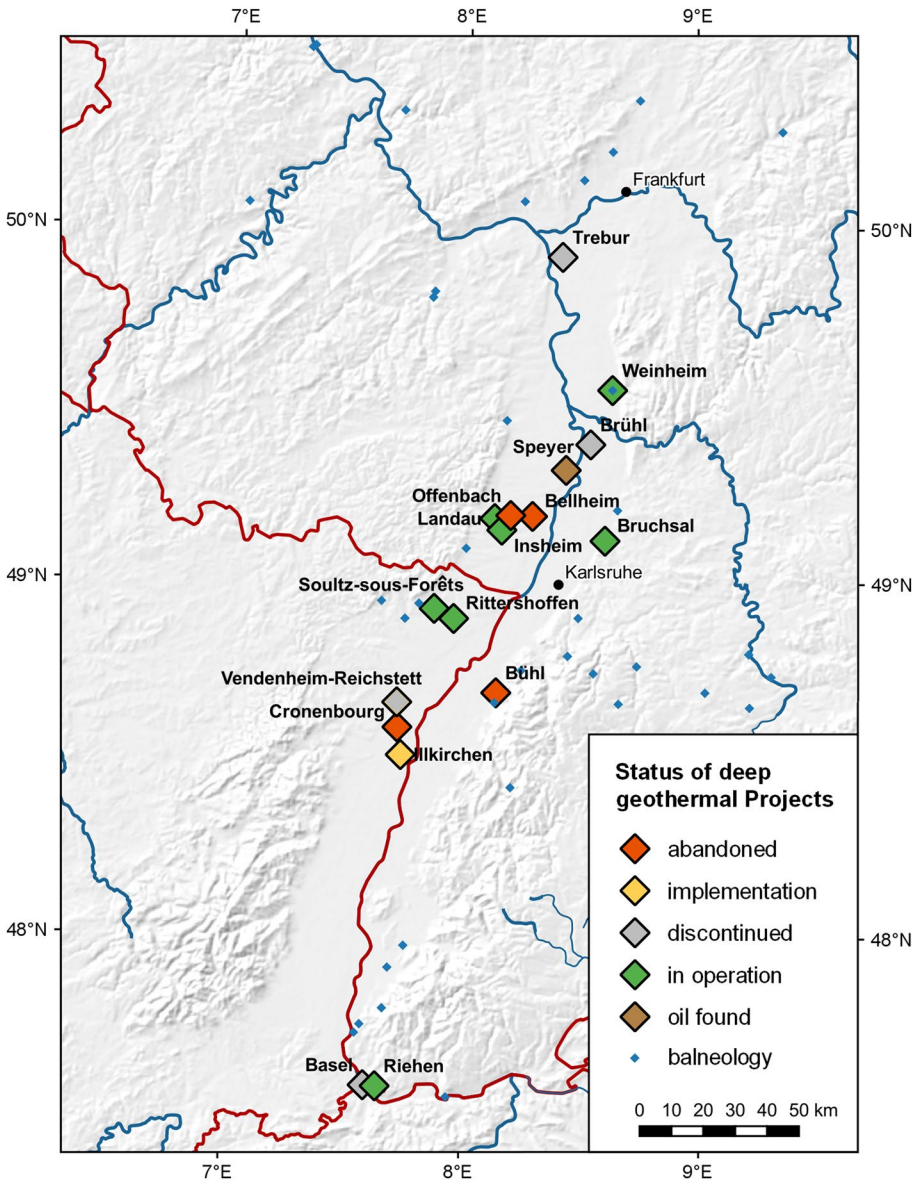

Fig. 18 Overview of the geothermal projects in the URG and their current status (adapted from Agemar et al. 2010). The geothermal wells in Weinheim are used for balneological and heating purposes, but the project has an exceptional position because a doublet was implemented here instead of a single production well

significantly improved the permeability of the fractured reservoir (Evans et al. 2005; Portier et al. 2009; Schill et al. 2017). Subsequently, the hydraulic properties of the subsurface were then investigated through long-term circulation tests.

Further successful projects were realized in Riehen, Landau, Weinheim, Insheim and Rittershoffen. Two additional projects near Strasbourg, Vendenheim and Illkirch, were in development until all operations were halted by political decisions after induced seismic events in Vendenheim. Besides, many projects are currently being planned, but will not be discussed here in detail. By 2020, geothermal power plants with a total capacity of about 50 MWth and 10 MWel have been installed in the URG, which is only a minor fraction of the total technical potential (Paschen et al. 2003; Kock and Kaltschmitt 2012).

Table 1 Summary of the major deep geothermal projects with drilled wells in the URG in 2020

Project location	Status	Target reservoir	Number of wells	Year of drilling	Max. depth TVD [m]	Max. temp [°C]	Power generation [MW]		References
							Thermal	Electrical	
Basel	Discontinued	Basement	1	2006	4992	190	–	–	Häring et al. (2008), Ladner et al. (2008)
Bellheim	Abandoned	Muschelkalk	1	2005–2006	2606	–	–	–	Internal reports
Bruchsal	In operation	Buntsandstein, Rotliegend	2	1983–1985	2542	123	5.5	0.55	Bertleff et al. (1988), Rettenmaier et al. (2013), Herzberger et al. (2010)
Brühl	Discontinued	Buntsandstein	1	2012–2013	3281	153	–	–	Reinecker et al. (2015)
Bühl	Abandoned	Dogger, Keuper, Basement	1	1979–1980	2699	120	–	–	Bertleff et al. (1988), Pauwels et al. (1993)
Cronenbourg	Abandoned	Buntsandstein	1	1980	2870	140	–	–	Housse (1984), Pauwels et al. (1993), Vidal and Genter (2018)
Illkirch	In implementation	Basement	1	2018–2019	3400	150	–	–	https://www.geothermie-illkirch.es.fr/le-projet/
Insheim	In operation	Muschelkalk to Basement	2	2008 -2010	3750	165	–	4.8	Baumgärtner et al. (2013)
Landau	In operation	Buntsandstein to Basement	2	2005–2006	3256	159	6	3.8	Teza et al. (2008), Schindler et al. (2010)
Offenbach a. d. Queich	Discontinued	Muschelkalk, Buntsandstein	1	2004	2732	–	–	–	Internal reports
Riehen	In operation	Muschelkalk	2	1988	1550	65	5.25	–	Bertleff et al. (1988), Hauber (1993), Mégel and Rybach (2000), Klingler (2010)
Rittershoffen	In operation	Buntsandstein, Basement	2	2012, 2014	2750	170	24	–	Baujard et al. (2017), Mouchot et al. (2018), Duringer et al. (2019)
Soultz-sous Forêts	In operation	Basement	3 + 2	1987–2003	5260	170	-	1.7	Dezayes et al (2005a), Cuenot et al. (2008), Schill et al. (2017), etc.

Table 1 (continued)

Project location	Status	Target reservoir	Number of wells	Year of drilling	Max. depth TVD [m]	Max. temp [°C]	Power generation [MW]		References
							Thermal	Electrical	
Speyer	Oil found	Buntsandstein, Rotliegend	1	2004	?	?	–	–	Internal reports
Trebur	Discontinued	Rotliegend	1	2016	3697	–	–	–	Internal reports
Vendenheim	Discontinued	Basement	2	2017–2019	5393 MD	200	–	–	Boissavy et al. (2019), Sanjuan et al. (2021), Schmittbuhl et al. (2021)
Weinheim	In operation	Hydrobia Beds (Tertiary)	2	2006	1145	65	?	–	Internal reports

Wells for mainly balneological purposes are not included, except for the project in Weinheim where a geothermal doublet was installed

In total, seven realized deep geothermal projects have not been successful in the URG so far due to a variety of technical and political reasons. First of all, induced seismicity, in particular during the enhancement of geothermal systems, but also during operation of the power plant, poses a major risk to these projects (e.g., Majer et al. 2007). The main reason for the seismic activity is the increase in pore pressure due to the reinjection of large volumes of water into the fractured reservoir. This reduces friction along joints and fault zones, which can lead to shear failure if the natural stress state is already critical. The resulting earthquakes are usually of magnitudes less than 2 and thus rarely perceptible. Cornet et al. (1997) could furthermore show for Soultz-sous-Forêts that most of the slip during injection is actually aseismic. Nevertheless, larger events have been detected at various sites in the URG: Basel ($M_L = 3.4$), Landau ($M_L = 2.7$), Insheim ($M_L = 2.4$), Soultz-sous-Forêts ($M_L = 2.9$) and Vendenheim ($M_L = 3.6$) (Deichmann and Giardini 2009; Dorbath et al. 2010; Leydecker 2008; Evans et al. 2012; Schmittbuhl et al. 2021; BGR 2021). In Basel and Vendenheim, seismic activity even led to the complete stop of the projects. Based on these experiences, different methods have been developed to reduce the pore pressure during reinjection. One option is the further decrease of the temperature of the re-injection fluid, which causes the rock to contract and consequently the fracture to open. Alternatively, chemicals can be added to the injection fluid to dissolve mineral precipitates on the joint and fault planes, resulting in increased hydraulic permeability (Portier et al. 2009). Other possibilities to minimize the seismic risk are geomechanical modeling in advance (e.g., Rathnaweera et al. 2020), i.e., to optimize the drilling path and to limit the injection flow rate and pressure and to monitor seismicity before and during drilling, stimulation and production to predict the reaction of the subsurface.

In other projects like Bühl, Bellheim, Cronenbourg, Offenbach a.d. Queich and Trebur, technical problems, insufficient permeability or not reaching the target horizon were the reason for unsuccessful projects. Here it became evident that a detailed

geological and geophysical exploration is essential for the success of deep geothermal projects (Reinecker et al. 2019; Bär et al. 2021a). Especially for the localization of the targeted fault zones, the use of existing or acquisition of new 3D seismic data sets and of data form old oil/gas wells is highly recommended, as they provide a much better spatial resolution than 2D seismic profiles (e.g., Reinhold et al. 2016). Nevertheless, the classical input data (seismic and borehole data) provide only limited information about the hydraulic conditions in targeted aquifers and faults. Integration of secondary geophysical data offer additional insight to characterize the reservoir (e.g., Frey et al. 2021b). Electromagnetic methods (magnetotelluric or controlled source EM, Volpi et al. 2003; Newman et al. 2008; Darnet et al. 2020), for example, can be used to identify high saline fluid flow in the subsurface. Likewise, gravimetric measurements can reveal zones of increased fracture porosity (Guglielmetti et al. 2013; Baillieux et al. 2014; Frey et al. 2022).

Finally, public acceptance is critical to the success of any deep geothermal power plant. The project in Brühl, for example, was stopped in response to poor public acceptance, even though drilling the first well has been successful and a very high flow rate was achieved during a first pumping and injection test (Reinecker et al. 2015). It has been shown that public opinion and knowledge regarding this energy form as well as the perception of potential risks can vary greatly between different locations (Chavot et al. 2019). Chavot et al. (2018) distinguish between "locally anchored" projects, where experiences with geothermal use are already existing and an intensive dialogue takes place, and "unbound" projects, where site selection is purely based on political-economic factors. The latter have a much higher risk of failure, as they are disconnected from local needs. Consequently, it is essential to involve the public in the planning of geothermal projects at an early stage and to communicate the benefits but also the possible risks in a transparent way (Meller et al. 2018). The support of local politicians can have a particularly positive effect on acceptance.

One good example of a transparent communication policy was the one implemented in the Trebur project (https://www.risiko-dialog.ch/projekt/dialoggeo/). The project developers started a public information campaign directly with the first steps of the project and formed a public stakeholder forum (Bürgerbeirat). They developed an own scientific and technical assessment of the project and a list of recommendations and requirements, the project developers declared themselves to fulfill. Additionally, the public information campaign included a detailed project website and six public information workshops, where regional and international experts where invited to present all associated risks and benefits to the public.

To conclude, with every drilling the risk of failure decreases because the technical challenges and the complex geological structure (van der Vaart et al. 2021) become more known. Moreover, as the risks become increasingly controllable and awareness of geothermal energy grows, public acceptance can be expected to improve in the future.

3D models

In the last two decades, a variety of geological 3D models of the URG serving different purposes has been developed. Some of these models cover the whole rift valley, whereas others focus on local structures, e.g., in the area of Soultz-sous-Forêts. Additionally, a lot

of 2D sections reaching the basement rocks through the URG exist and are implemented in GeotIS (Agemar et al. 2010). For a better overview, a selection of models is shown in Fig. 19.

The so far most detailed regional-scale models for geothermal potential assessment were developed during the GeORG (GeORG Projektteam 2013) and Hessen 3D (1.0 and 2.0) (Sass et al. 2011; Arndt et al. 2011; Bär 2012; Bär et al. 2016, 2021b) projects. The first covers the central and southern, the latter the northernmost part of the URG and they include the main geothermal reservoir horizons in the respective region. Modeling of the horizons was mostly based on the available borehole and reflection seismic data

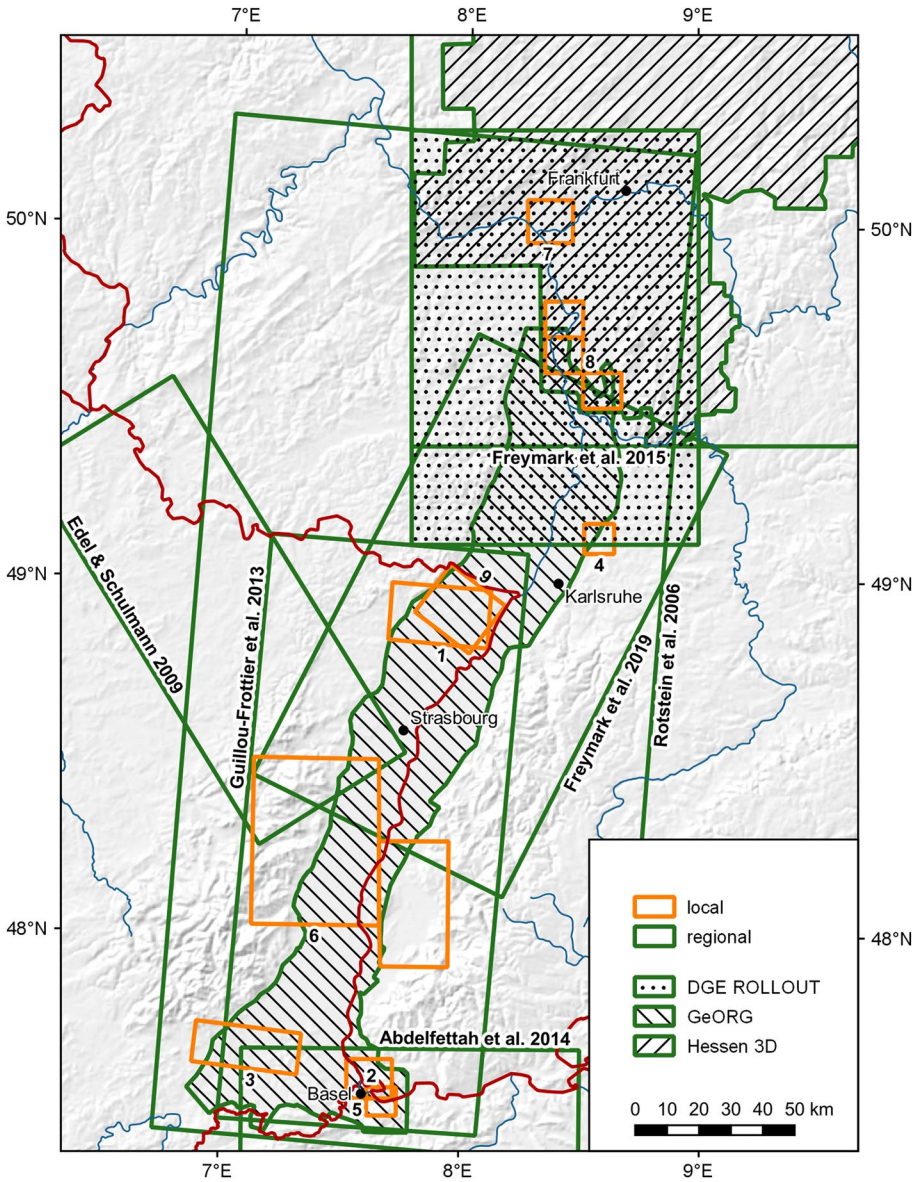

Fig. 19 Selection of published 3D geological models in the URG region. 1 = Dezayes et al. (2011), 2 = Spottke et al. (2005), 3 = Le Carlier de Veslud et al. (2005), 4 & 5 = Meixner et al. (2016), 6 = Bertrand et al. (2005), 7 = Deckert et al. (2017), 8 = Wächter et al. (2018), 9 = Abdelfettah et al. (2020). Note that the Freymark et al. (2020) model area is larger than the map section shown here

(for an overview of the available data see e.g., FIS Geophysik: www.fis-geophysik.de, GeotIS: www.geotis.de, GEORG-Portal: www.geopotenziale.org,). Afterward, the models were parameterized with temperature, hydrogeological and petrophysical data to quantify the deep geothermal potential. Within the framework of the EU-NW-Interreg project DGE-Rollout, these models are being merged and the potential estimation will be carried out again using also newly collected data (Frey et al. 2021b) and uncertainty modeling techniques (van der Vaart et al. 2021). Additional potential assessments on a regional scale in the URG have been performed by e.g., Dornstadter et al. (1999) and Paschen et al. (2003).

Since the classical input data, such as boreholes and 2D and 3D seismics, are not evenly distributed in the URG and only cover certain depth ranges, gravity and magnetic data were additionally used in several models. Particularly noteworthy are the regional studies by Rotstein et al. (2006), Edel and Schulmann (2009), Freymark et al. (2017) and Frey et al. (2021a). The potential field data are often applied to map crustal-scale structures. However, in the case of high-resolution surveys, also near-surface features, for example fault networks (e.g., Deckert et al. 2017; Abdelfettah et al. 2020) or even petrophysical properties can be explored (Frey et al. 2021b). By applying frequency filters to the observed potential fields, information about specific depth ranges can be obtained (pseudo-tomography, Baillieux et al. (2014)).

The numerous deep-reaching fault zones in the URG represent hydraulic pathways for hydrothermal fluids, which significantly increases the influence of convective heat transport. Both up- and downflow of the groundwater can be observed, leading to the formation of locally distinct temperature anomalies, e.g., in Soultz-sous Forêts or Landau. To further investigate this factor, comprehensive 3D groundwater flow models have been developed (Freymark et al. 2019; Guillou-Frottier et al. 2013; Koltzer et al. 2019; Les Landes et al. 2019). These showed a general flow direction from the graben flanks towards the center and from south to north, following the topographic gradient. Moreover, pronounced upflows occur mainly at the central graben axis, where the Rhine river represents the lowest hydraulic head.

Finally, it should be mentioned that a variety of local models exist that aim to explore specific reservoirs or target areas (Bertrand et al. 2005; Spottke et al. 2005; Cornu et al. 2007; Sausse et al. 2010; Dezayes et al. 2011; Lehne et al. 2013; Meixner et al. 2016; Deckert et al. 2017). In most cases, borehole and reflection seismic data served as primary input data, in some cases also gravity data as well as earthquake tomography and hypocenter locations were integrated.

Discussion

Future of geothermal energy in the URG

In the medium to long term, man-made climate change will have a severe impact on all aspects of life through a rise in mean temperatures, an increase in extreme weather events and a rising sea level. To mitigate the consequences of this process, 195 nations committed themselves in the Paris Climate Agreement to limit global warming to well below 2 °C (United Nations 2015). In order to achieve this goal, a rapid reduction of greenhouse emissions is inevitable. Geothermal energy can make an important contribution, since greenhouse gas emissions per unit of energy are

one to two orders of magnitude smaller than for fossil fuels (Lacirignola and Blanc 2013; Douziech et al. 2021). In recent years, the share of renewable energy forms in Germany's electricity production has increased to over 50% in 2020, mainly due to the expansion of wind and solar energy (Frauenhofer ISE 2021). In contrast, the proportion of renewables in the heat supply, which accounts for about half of Germany's energy consumption, stagnates at about 15% (BMWK 2021), leaving a large potential for savings in this sector. This could be enhanced through the large-scale development of deep geothermal power and heating plants, as the technical potential of geothermal energy considerably exceeds the demand in Germany (e.g., Jain et al. 2015).

The URG offers a unique framework of high population densities with several large cities (Frankfurt, Mainz, Wiesbaden, Mannheim, Heidelberg, Strasbourg, Karlsruhe, Basel, Freiburg, etc.), well-established district heating networks and large geothermal resources. Thus, the potential to use deep geothermal energy for the decarbonization of the heating sector is extraordinarily high. The combination of deep geothermal heat generation with medium-deep seasonal heat storage, especially in urban areas with existing district heating networks, allows the inclusion of other renewable energy heat sources. Excess heat can be stored in the summer and extracted again in the winter, when demand is much higher. By doing this, the peak loads can be met more easily by renewable sources without the need of additional fossil fuel or expensive hydrogen boilers. One possible implementation type is the use aquifers in medium depth especially in the Tertiary (aquifer thermal energy storage—ATES, e.g., Dickinson et al. 2009; Fleuchaus et al. 2018, 2021). Here, horizons which have been used in the past for oil and gas production or storage have suitable properties and usually a sufficient impermeable cap-rock to be used for ATES systems even at high temperatures of more than 120 °C (Stricker et al. 2020). Furthermore, deep and hot thermal underground storage is gaining a certain interest and upcoming projects have been reported already (Banks et al. 2021).

So far, deep geothermal energy occupies a rather small niche in the total heat and power supply, because of the comparatively high investment costs and risks. However, modern drilling methods are expected to become more affordable in the near future, which will make this technology much more attractive to investors. Upscaling of geothermal power plants by drilling multiple wells from one drill pad and wells with multilaterals allow to increase the inflow at lower relative costs and thereby ensures economic reservoir operation.

Coproduction and extraction of lithium (or other mineral resources contained in the thermal water) adds a significant economic value and can help to make deep geothermal energy economic without any subsidies in the very near future (e.g., Saevarsdottir et al. 2014). Similarly, the hydrocarbon reservoirs of the URG offer potentials for co-production of heat and oil, which would optimize the use of natural resources (e.g., Ziabakhsh-Ganji et al. 2018). In addition, unsuccessful or exhausted oil and gas wells can be geothermally exploited, e.g., by retrofitting deep borehole heat exchangers (van Horn et al. 2020).

Data availability and uncertainties

To successfully plan and realize any geothermal project accurate knowledge of the subsurface conditions is key. Nowadays, 3D geological models of the concession areas are developed as standard, which are used for potential assessment, planning of well paths or the numerical simulation of reservoir behavior during development and operation. For the URG, a large variety of datasets and models are already available, as presented above. However, it must be considered that all data are subject to some errors. They create uncertainties in models, which can significantly elevate the risk of project failure (Witter et al. 2019). Commonly, three types of errors are distinguished in geological modeling (Cox 1982; Mann 1993): all input datasets are affected by inaccuracies inherent to each individual measurement, which are referred to as Type 1 errors. For example, errors arise with respect to the well path due to wireline stretching or due to precision and accuracy limits of the measurement. On the other hand, seismic interpretation commonly suffers from errors of migration and velocity uncertainty, cumulating in a depth conversion error. Each of these errors need to be analyzed individually to understand and account for them in the final model. While this error is usually small for well data, variations in the velocity model might produce errors of more than 100 m in seismic profiles or cubes. Type 2 errors are associated with the inter- and extrapolation between available data points. Depending on the interpolation method, vastly different results can be obtained, especially where the data density is low. Geostatistical methods such as kriging have been developed to account for the uncertainties (Chilès et al. 2004). Type 3 errors stem from our lack of knowledge and inability to model nature accurately. A typical example is the existence of a fault between two wells, which could not be detected with the available data (e.g., wells and 2D seismic) so far. Here, a 3D seismic survey may close this gap of knowledge considerably and allow for a much better prediction of the fault position, fault type and detailed geometry and orientation in the recent stress field. Type 1 and 2 errors can be quantitatively described as probability density functions and be included in a stochastic uncertainty modeling, whereas type 3 errors are considered as purely qualitative components (Mann 1993).

Within the URG, the presented data and models are subject to all 3 types of errors to varying degrees, as they are based on different source datasets with different levels of accessibility. Depending on whether commercial or open-access data are used, the quality and density may vary substantially. Secondly, when only interpreted data like well markers are available, commonly it cannot be verified or checked for quality against the source. The limited access to source data leads to a significant reduction in the model reliability. Indeed, spatial uncertainties on the vertical position of horizons have been reported with standard deviations of nearly 130 m for the potential Tertiary geothermal reservoirs in the northern URG (van der Vaart et al. 2021). For the older reservoir units, uncertainties are most likely much higher, as the depth is considerably greater, input data sparser and data suitability (e.g., target horizon of seismic exploration) is not always given. However, this situation is subject to change with the new geological data law (Geologiedatengesetz, (Bücker 2021)) which has come into effect in 2021. This law requires geological surveys, institutions and companies to make their data publicly available within 5–10 years after acquisition completion through the respective state authorities, depending on data source and purpose. This should allow for a better understanding

of the subsurface and a reduction of uncertainties. Indeed, Perner (2018) shows a deviation of 30 m between 3D seismic and well data near Stockstadt in the northern part of the URG, indicating unpublished data could decrease errors in many of the public models.

Evaluation of geothermal reservoirs in the URG

For the URG, a total of nine horizons were identified that are suitable for deep geothermal exploitation due to their favorable thermal–hydraulic properties. The question remains which of these reservoirs is locally the most promising considering the local project context, the financial framework conditions and the planned type of utilization. In the following, the pros and cons of the different reservoir horizons will be discussed based on the data presented here and the experiences of past projects.

The crystalline basement presents an attractive target horizon for deep geothermal applications because it is usually is the deepest potential reservoir and thus has the highest reservoir temperatures. Additionally, due to its longest tectonic history it has both several fracture sets and a comparable high fracture density, which are prone to reactivation by recent tectonic events. The large-scale fault zones as targeted in Soultz and Rittershoffen proved to locally act as hydraulic conduits making them primary targets for geothermal exploitation. On the other hand, large-scale fault zones can also lead to the development of high fault core thicknesses with significant hydrothermal alteration and mineral precipitation, decreasing horizontal permeabilities orthogonal to the fault strike direction. However, the likelihood of permeable faults or fractures in the vicinity of large-scale fault zones is significantly increased if the fault has been recently active and has a preferential orientation in the present stress field (high slip- and dilation tendencies). Especially the upper, hydrothermally altered part of the basement, where additional secondary porosity was developed during alteration exhibits a higher hydraulic conductivity than the unaltered basement, where permeability is only controlled by the fracture network. As shown in chapter 6.1 the hydraulic properties of the basement strongly depend on the predominant rock type. Granites, for example, have on average about 1 to 2 magnitudes higher hydraulic conductivities than gneisses (Stober and Bucher 2007). Therefore, crystalline basement reservoirs are more suitable targets where granitic lithologies are predominant compared to metamorphic rock types. Using geophysical exploration data as presented by Frey et al. (2021b) are therefore key to identify suitable areas before selecting a drill site, especially since the lithologic composition of the basement is still subject to large uncertainties in most parts of the URG due to the low density of wells reaching the basement. The encountered natural permeability of the basement is usually not sufficient for an economic operation of a power plant, thus measures to enhance the geothermal reservoir are necessary. The hydraulic stimulation, as well as the regular geothermal operation, of crystalline rocks often induces seismicity, which, in severe cases, led to the termination of a geothermal project (e.g., Basel in 2006/2007 or Vendenheim in 2020/2021). Worldwide research activities (e.g., Grimsel Rock Laboratory, Bedretto Tunnel Laboratory, Äspö, GeoLAB) are currently and in future scientifically addressing this problem at various scales of investigation (Bossart et al. 1991; Schill et al. 2016; Zimmermann et al. 2019; Hertrich et al. 2021), so new stimulation procedures and techniques are in development to enhance the understanding of

hydro- or thermomechanical interactions and can provide the basis to reduce or mitigate induced seismicity in the future. In addition, improved geomechanical models will help to select the most appropriate borehole path, or paths in case of wells with multilateral reservoir completion. In any project, seismic monitoring is required to start well ahead before drilling and accompany testing, stimulation and operation together with a pre-defined reaction plan approved by the respective authorities to mitigate induced seismicity. Another measure to mitigate induced seismicity during reservoir development is chemical stimulation or 'acid cleaning', which has proven to be effective in several projects in the URG (e.g., Soultz, Vendenheim, Rittershoffen).

The Permo-Carboniferous and Triassic sandstones are to be expected in almost the entire URG with varying thicknesses. While the Permo-Carboniferous heterogeneous fine-to-coarse siliciclastic and volcanic rocks are mainly present in the position of SW–NE-striking molasse basins of the Variscan Orogen, the Triassic sandstones are limited in their northern extent by pre-Tertiary erosion roughly at the position of Worms-Bensheim. Again, high reservoir temperatures are usually encountered, allowing for both heat and power production throughout the entire URG. As a result of the strong compaction and cementation, the sandstone matrix shows a permeability one or two orders lower than the permeability created by the connected fracture network (e.g., Bär 2012). Matrix permeability is often additionally reduced by hydrothermal alteration (sandstone bleaching) associated to long-term hydraulically active fault zones further reducing the primary porosity by secondary precipitations (Gaupp et al. 1998). Fluid flow thus occurs mainly along fractures and faults. Based on outcrop analogue studies in the Odenwald and the Palatinate it can be concluded, that compared to the basement, the fracture density is often lower (e.g., Gottschalk 2010), resulting in highly variable lateral hydraulic properties. In the vicinity of faults, very high hydraulic conductivities can be achieved (e.g., in Brühl 1, Reinecker et al. 2019). In order to minimize the exploration risk, drilling inclined wells respecting the fault and fracture set orientation and recent in situ stress field is recommended, which significantly increases the probability of intersecting hydraulically active steeply dipping fault zones and fracture sets. Hydraulic stimulation of the sandstones is associated with reduced seismic risks, since the rock strength is smaller than that of the crystalline basement and part of the pore pressure increase by injection is resulting in poroelastic response of the rock matrix. But inducing seismicity is still possible, especially when faults are targeted that extend into the basement where a pore pressure increase is mainly restricted to the fault zone itself. Additionally, chemical stimulation is a useful reservoir stimulation technique, in particular if carbonatic fracture mineralization has been proven by core or cutting analysis. In these cases, both mineralized fractures and fault zones can be treated and even the connectivity to the rock matrix can be increased (Wiedemann 2021).

The strongly fractured and karstified Upper Muschelkalk features the highest hydraulic conductivity of all investigated units in the URG and thus represents a very interesting reservoir for deep geothermal projects. However, the degree of karstification is highly variable from one to another location. A borehole might easily miss karst cavities and only encounter unkarstified rock. Additionally, the Upper Muschelkalk is only present in the central and southern URG with a thickness of usually less than 100 m which might locally be insufficient to achieve sustainable economic flow

rates. Furthermore, karstification poses an additional risk to drilling operations and well stability during drilling, testing and operation which needs to be accounted for. Similarly, high permeabilities are expected in the karstified Jurassic carbonates, which are limited to the southern URG and are also limited in thickness. Here as well as for the Upper Muschelkalk, karstification is usually fault-bound, while the tectonic block between the faults only show a very limited degree of karstification and thus comparatively lower hydraulic conductivities.

The Cenozoic infill of the URG includes at least three formations with coarse-grained clastic sediments of sufficient thickness that may allow deep geothermal exploitation. Due to the shallower depth, power production might not be feasible with the obtained reservoir temperatures, whereas heat production or seasonal heat storage are promising utilizations. So far, only the installed doublet in Weinheim uses Tertiary sandstones for geothermal heat production. From the oil and gas industry, an extensive dataset including numerous wells, core investigations and seismic lines exists, which can significantly minimize exploration costs and risks (Hintze et al. 2018; Van der Vaart et al. 2021). In contrast to the deeper reservoirs, the matrix permeability of the coarse-grained clastic Tertiary sediments of the Pechelbronn Formation, the Froidefontaine Formation and the Niederrödern Formation could allow for sufficient flow rates in geothermal wells. The frequently occurring interlayering by clay and silt horizons may have a negative effect on conductivity, especially along fault zones, where clay smear effects might seal the fault. Of particular interest are the Tertiary marginal facies along the eastern and western boundary fault of the URG, which often have a much higher share of coarse-grained sediments and a much higher lateral reservoir connectivity compared to the clay dominated basinal facies along the graben axis.

In summary, all geological units suitable as deep geothermal reservoirs in the URG have been identified with certain pros and cons. The approach of exploiting multiple reservoirs with one well, e.g., Landau, Insheim, Illkirch and Rittershoffen, also appears to be an adequate method for increasing the flow rates. In the past, the goal was in many cases to drill as deep as possible in order to obtain maximum temperatures produced at wellhead. However, convective heat transport along recently active fault zones in the URG leads to a significant increase in the geothermal gradient (up to more than 10 K/100 m) above the convection cells. In these areas, adequate reservoir temperatures may prevail even at shallow depths. In contrast, in the convection-dominated interval, the geothermal gradient is usually very small (e.g., Soultz-sous-Forêts), meaning that greater well depths do not result in a significant increase in heat production. Note that convection can also lead to negative temperature anomalies when dense near-surface groundwater is transported downwards along faults. In areas of the URG that are less influenced by active fault zones, conductive heat transport dominates, with gradients between about 3 and 6 K/100 m. Thus, the aim of exploration should be primarily to identify the reservoirs in areas of positive geothermal anomalies in the vicinity of the above-mentioned fault zones (Bär et al. 2021). High-temperature heat pumps can be used if necessary to raise the temperature level, especially in the combined utilization of deep geothermal reservoirs and medium deep reservoirs for seasonal heat storage.

Conclusions

In this review, a comprehensive overview of the geological and geothermal situation of the URG is given. The region exhibits an overall very high potential for deep geothermal utilization. Nine potential reservoir horizons have been identified and were characterized with respect to their distribution and thickness, lithology, structural geology, hydrochemistry, hydraulics and petrophysics. These include the crystalline basement, the Permo-Carboniferous sandstones, the Buntsandstein, the Upper Muschelkalk, the Hauptrogenstein, the Upper Jurassic Limestones, the Pechelbronn Formation, the Froidefontaine Formation and the Niederrödern Formation, showing suitable temperatures and permeabilities depending on the location. However, as a result of the multistage tectonic and diagenetic evolution and hydrothermal alteration, complex reservoirs with double porosity (fracture-matrix, fracture-karstification) have formed. The strong heterogeneity of relevant properties between and within geologic units remains therefore a key challenge in defining the exploration and drilling target.

The abundant, hydraulically active fault zones in the URG can serve as major fluid conduits and thus also contribute significantly to the development of temperature anomalies in the subsurface. Compared to the intact rock matrix, large-scale faults often show significantly increased permeabilities, making them preferred targets for geothermal projects. In this context, the location of fault planes in the ambient stress field may be used as a proxy for permeability (slip and dilatation tendency). That said, mineral precipitation, particularly in the fault core, can also act as a natural fluid barrier. In order to reduce exploration risks as much as possible, new comprehensive exploration concepts combining different methods (3D seismics, electromagnetic methods, gravimetry, magnetics, hydrochemistry, gradient wells, slim hole exploration wells) are required. This includes also rigorous statistical modeling of uncertainties that takes into account the intrinsic errors of individual measurements.

In addition to geological uncertainties, economic aspects of course play a crucial role in the realization of geothermal projects. Upscaling power plants through multiwell systems and multilateral drilling can help to save costs and thus increase economic efficiency. Besides, co-production of lithium presents an additional revenue stream that could enable economic power and heat production even without subsidies. Apart from the classical deep geothermal system for power and heat supply, the URG offers a high potential for seasonal heat storage via ATES, which can compensate the mismatch between production and demand of heat at the surface.

Abbreviations

ATES	Aquifer thermal energy storage
BO	Borehole breakouts (BO)
CSGC	Central Schwarzwald Gneiss Complex
DST	Drill stem tests
ECRIS	European Cenozoic Rift System
EGS	Enhanced geothermal system
EM	Electromagnetic methods
EMBF	Eastern Main Boundary Fault
FMS	Earthquake focal mechanisms
LOT	Leak-off tests
DIFT	Drilling-induced tensile fractures
MGCH	Mid-Germany Crystalline High
REV	Representative elementary volume
SSGC	Southern Schwarzwald Gneiss Complex

TDS	Total dissolved solids
Td	Dilation tendency
Ts	Slip tendency
URG	Upper Rhine Graben
WMBF	Western Main Boundary Fault

Acknowledgements
We acknowledge support by the Deutsche Forschungsgemeinschaft (DFG—German Research Foundation) and the Open Access Publishing Fund of Technical University of Darmstadt.

Author contributions
MF: conception, analysis and interpretation of data, drafting and revision of the text; KB: conception, analysis and interpretation of data, drafting and revision of the text; IS: analysis and interpretation of data, drafting and revision of the text; JR: analysis and interpretation of data, drafting and revision of the text; JV: drafting and revision of the text; IS: revision of the text. All authors read and approved the final manuscript.

Funding
Open Access funding enabled and organized by Projekt DEAL. This study was funded by the Interreg NWE Program through the Roll-out of Deep Geothermal Energy in North-West Europe (DGEROLLOUT) Project www.nweurope.eu/DGE-Rollout). The Interreg NWE Program is part of the European Cohesion Policy and is financed by the European Regional Development Fund (ERDF).

Availability of data and materials
A large quantity of research data were presented in this review, most of which are freely available. The respective studies have been cited accordingly. Detailed information on the individual datasets is provided in the main text.

Declarations

Competing interests
We have no conflicts of interest to disclose.

Received: 16 February 2022 Accepted: 17 August 2022
Published online: 29 September 2022

References

Abdelfettah Y, Hinderer J, Calvo M, Dalmais E, Maurer V, Genter A. Using highly accurate land gravity and 3D geologic modeling to discriminate potential geothermal areas: application to the Upper Rhine Graben. France GEOPHYSICS. 2020;85(2):G35–56.
Achtziger-Zupančič P, Loew S, Mariéthoz G. A new global database to improve predictions of permeability distribution in crystalline rocks at site scale. J Geophys Res. 2017;122(5):3513–39. https://doi.org/10.1002/2017JB014106.
AG Energiebilanzen. Energieverbrauch in Deutschland im Jahr 2021; 2022. https://ag-\.de/wp-content/uploads/2022/04/AGEB_Jahresbericht2021_20220524_dt_Web.pdf. Accessed 29 Aug 2022.
Agemar T. Bottom hole temperature correction based on empirical correlation. Geothermics. 2022;99: 102296. https://doi.org/10.1016/j.geothermics.2021.102296.
Agemar T, Schellschmidt R, Schulz R. Subsurface temperature distribution of Germany. Geothermics. 2012;44:65–77. https://doi.org/10.1016/j.geothermics.2012.07.002.
Agemar T, Brunken J, Jodocy M, Schellschmidt R, Schulz R, Stober I. Untergrundtemperaturen in Baden-Württemberg. ZDGG. 2013;164(1):49–62. https://doi.org/10.1127/1860-1804/2013/0010.
Agemar T, Hese F, Moeck I, Stober I. Kriterienkatalog für die Erfassung tiefreichender Störungen und ihrer geothermischen Nutzbarkeit in Deutschland. ZDGG. 2017;168(2):285–300. https://doi.org/10.1127/zdgg/2017/0084.
Agemar T, Alten JA, Ganz B, Kuder J, Kühne K, Schumacher S, Schulz R. GeotIS–das Geothermische Informationssystem für Deutschland. In: Der Geothermiekongress, 17–19 November 2010, Karlsruhe, Germany; 2010. https://www.geothermie.de/fileadmin/useruploads/aktuelles/Geothermiekongress/2010/Programmuebersicht_DGK_2010_1009_2.pdf. Accessed 29 August 2022.
Ahlers S, Henk A, Hergert T, Reiter K, Müller B, Röckel L, et al. 3D crustal stress state of Germany according to a data-calibrated geomechanical model. Solid Earth. 2021;12(8):1777–99. https://doi.org/10.5194/se-12-1777-2021.
Ahorner L. Historical seismicity and present-day microearthquake activity of the Rhenish Massif, Central Europe. In: Fuchs K, Gehlen K, Mälzer H, Murawski H, Semmel A, editors. Plateau uplift: the rhenish shield—a case history. Berlin: Springer, Berlin Heidelberg; 1983. p. 198–221 (**10.1007/978-3-642-69219-2_27**).
Ahorner L, Schneider G. Herdmechanismen von Erdbeben im Oberrheingraben und in seinen Randgebirgen. In: Illies JH, Fuchs K, editors. Approaches to taphrogenesis. Stuttgart: Schweizerbart; 1974. p. 104–17.
Aigner T, Bachmann GH. Sequence-stratigraphic framework of the German Triassic. Sed Geol. 1992;80(1–2):115–35. https://doi.org/10.1016/0037-0738(92)90035-P.
Altenberger U, Besch T. The Böllstein Odenwald: evidence for pre- to early Variscan plate convergence in the Central European variscides. Int J Earth Sci. 1993;82(3):475–88. https://doi.org/10.1007/BF00212411.
Anderle H-J, Franke W, Schwab M. III.C.1 stratigraphy. In: Dallmeyer RD, Franke W, Weber K, editors. Pre-Permian geology of Central and Eastern Europe. Berlin: Springer, Berlin Heidelberg; 1995. p. 99–107.
Andres J, Schad A. Seismische Kartierung von Bruchzonen im mittleren und nördlichen Teil des Oberrheintalgrabens und deren Bedeutung für die Ölansammlung. Erdöl Und Kohle. 1959;5:323–34.

Anthes G, Reischmann T. New 207Pb/206Pb single zircon evaporation ages from the central part of the Mid German Crystalline Rise. Terra Nostra. 1997;97(5):10.
Anthes G, Reischmann T. Timing of granitoid magmatism in the eastern mid-German crystalline rise. J Geodyn. 2001;31(2):119–43. https://doi.org/10.1016/S0264-3707(00)00024-7.
Aretz A, Bär K, Götz AE, Sass I. Outcrop analogue study of Permocarboniferous geothermal sandstone reservoir formations (northern Upper Rhine Graben, Germany): impact of mineral content, depositional environment and diagenesis on petrophysical properties. Int J Earth Sci. 2016;105(5):1431–52. https://doi.org/10.1007/s00531-015-1263-2.
Arndt D, Bär K, Fritsche J-G, Sass I, Hoppe A. 3D structural model of the Federal State of Hesse (Germany) for geopotential evaluation. ZDGG. 2011;162(4):353–69. https://doi.org/10.1127/1860-1804/2011/0162-0353.
Arndt D. Geological structural modelling of Hesse to determine geopotentials (Geologische Strukturmodellierung von Hessen zur Bestimmung von Geopotenzialen) [PhD thesis]: Technische Universität Darmstadt; 2012.
Azzola J, Valley B, Schmittbuhl J, Genter A. Stress characterization and temporal evolution of borehole failure at the Rittershoffen geothermal project. Solid Earth. 2019;10(4):1155–80. https://doi.org/10.5194/se-10-1155-2019.
Bächler D, Kohl T, Rybach L. Impact of graben-parallel faults on hydrothermal convection-–Rhine Graben case study. Phys Chem Earth. 2003;28:431–41. https://doi.org/10.1016/S1474-7065(03)00063-9.
Backhaus E. Limnische und fluviatile Sedimentation im südwestdeutschen Buntsandstein. Int J Earth Sci. 1974;63(3):925–42. https://doi.org/10.1007/BF01821318.
Backhaus E, Heim D. Die fluvio-lakustrine Fazies des Übergangsbereichs Plattensandstein/Rötquarzit (Oberer Buntsandstein) im mittleren Odenwald unter besonderer Berücksichtigung der Violetten Zone. Geol Jb Hessen. 1995;123:49–68.
Bahlburg H, Vervoort JD, DuFrane SA. Plate tectonic significance of Middle Cambrian and Ordovician siliciclastic rocks of the Bavarian Facies, Armorican Terrane Assemblage, Germany—U-Pb and Hf isotope evidence from detrital zircons. Gondwana Res. 2010;17(2–3):223–35. https://doi.org/10.1016/j.gr.2009.11.007.
Baillieux P, Schill E, Edel JB, Mauri G. Localization of temperature anomalies in the Upper Rhine Graben: insights from geophysics and neotectonic activity. Int Geol Rev. 2013;55(14):1744–62. https://doi.org/10.1080/00206814.2013.794914.
Baillieux P, Schill E, Abdelfettah Y, Dezayes C. Possible natural fluid pathways from gravity pseudo-tomography in the geothermal fields of Northern Alsace (Upper Rhine Graben). Geotherm Energy. 2014. https://doi.org/10.1186/s40517-014-0016-y.
Banks J, Poulette S, Grimmer J, Bauer F, Schill E. Geochemical changes associated with high-temperature heat storage at intermediate depth: thermodynamic equilibrium models for the deepstor site in the Upper Rhine Graben, Germany. Energies. 2021;14(19):6089. https://doi.org/10.3390/en14196089.
Bankwitz E, Bankwitz P. Lower Paleozoic series at the southern margin of the Central German Crystalline Zone. Terranes in the circum-Atlantic Paleozoic orogens.(Abstr vol, unpubl). 1990.
Bär K, Hintze M, Weinert S, Sippel J, Freymark J, Scheck-Wenderoth M, Sass I. Das Verbundprojekt Hessen 3D 20. Geotherm Energie. 2016;3(85):24–5.
Bär K, Reinsch T, Bott J. The PetroPhysical Property Database (P^3)—a global compilation of lab-measured rock properties. Earth Syst Sci Data. 2020;12(4):2485–515. https://doi.org/10.5194/essd-12-2485-2020.
Bär K, Reinecker J, Bott J, Cacace M, Frey M, van der Vaart J, et al. Integrated Exploration Strategy 'ConvEx' to detect Hydrothermal Convection in the Subsurface. In: World Geothermal Congress 2020; April - October 2021a; Reykjavik, Iceland; 2021a.
Bär K, Schäffer R, Weinert S, Sass I. Schlussbericht Verbundprojekt „Hessen 3D 2.0": 3D-Modell der geothermischen Tiefenpotenziale von Hessen: Technical University of Darmstadt; 2021b.
Bär K. 3D-Modellierung des tiefengeothermischen Potenzials des nördlichen Oberrheingrabens und Untersuchung der geothermischen Eigenschaften des Rotliegend [Diplomathesis]: Technical University Of Darmstadt; 2008.
Bär K. Assessment of the deep geothermal potentials of Hessen (Untersuchung der tiefengeothermischen Potenziale von Hessen) [PhD thesis]: Technische Universität Darmstadt; 2012.
Barnasch J. Der Keuper im Westteil des Zentraleuropäischen Beckens (Deutschland, Niederlande, England, Dänemark): diskontinuierliche Sedimentation, Litho-, Zyklo- Und Sequenzstratigraphie. SDGG. 2010;71:7–169. https://doi.org/10.1127/sdgg/71/2010/7.
Barth A, Ritter J, Wenzel F. Spatial variations of earthquake occurrence and coseismic deformation in the Upper Rhine Graben, Central Europe. Tectonophysics. 2015;651–652:172–85. https://doi.org/10.1016/j.tecto.2015.04.004.
Barth G, Franz M, Heunisch C, Ernst W, Zimmermann J, Wolfgramm M. Marine and terrestrial sedimentation across the T-J transition in the North German Basin. Palaeogeogr Palaeoclimatol Palaeoecol. 2018;489:74–94. https://doi.org/10.1016/j.palaeo.2017.09.029.
Barton CA, Zoback MD, Moos D. Fluid flow along potentially active faults in crystalline rock. Geology. 1995;23(8):683. https://doi.org/10.1130/0091-7613(1995)023%3c0683:FFAPAF%3e2.3.CO;2.
Baujard C, Genter A, Dalmais E, Maurer V, Hehn R, Rosillette R, et al. Hydrothermal characterization of wells GRT-1 and GRT-2 in Rittershoffen, France: implications on the understanding of natural flow systems in the Rhine graben. Geothermics. 2017;65:255–68. https://doi.org/10.1016/j.geothermics.2016.11.001.
Baumgärtner J, Teza D, Wahl G. Gewinnung geothermischer Energie durch Entwicklung und Zirkulation eines Störungssystems im Kristallin und deren mikroseismische Überwachung am Beispiel des Geothermieprojektes Insheim (Internal Report No. 0325158): Bestec GmbH; 2013.
Baumgärtner J, Kölbel T, Mergner H, Schlagermann P, Hettkamp T, Teza D, Lerch C. Betriebserfahrungen mit den Geothermiekraftwerken Landau, Insheim und Bruchsal. BBR Fachmagazine fur Brunnen und Leitungsbau. 2013:48–57.
Bear J. Hydraulics of groundwater. New York: McGraw-Hill Book Comp; 1979.
Behr HJ, Heinrichs T. Geological interpretation of DEKORP 2-S: a deep seismic reflection profile across the Saxothuringian and possible implications for the Late Variscan structural evolution of Central Europe. Tectonophysics. 1987;142(2–4):173–202. https://doi.org/10.1016/0040-1951(87)90122-3.
Behr H-J, Engel W, Franke W. Variscan wildflysch and nappe tectonics in the Saxothuringian Zone (Northeast Bavaria, West Germany). Am J Sci. 1982;282(9):1438–70. https://doi.org/10.2475/ajs.282.9.1438.

Behr H-J, Engel W, Franke W, Giese P, Weber K. The Variscan Belt in Central Europe: main structures, geodynamic implications, open questions. Tectonophysics. 1984;109(1–2):15–40. https://doi.org/10.1016/0040-1951(84)90168-9.
Behr H-J, Dürbaum H-J, Bankwitz P, Bankwitz E, Benek R, Berger H-J, et al. Crustal structure of the Saxothuringian Zone: Results of the deep seismic profile MVE-90 (East). Z Geol Wiss. 1994;22(6):647–770.
Behrmann JH, Hermann O, Horstmann M, Tanner DC, Bertrand G. Anatomy and kinematics of oblique continental rifting revealed: a three-dimensional case study of the southeast Upper Rhine graben (Germany). Bulletin. 2003;87(7):1105–21. https://doi.org/10.1306/02180300153.
Behrmann JH, Ziegler PA, Schmid SM, Heck B, Granet M. The EUCOR-URGENT Project. Int J Earth Sci. 2005;94(4):505–6. https://doi.org/10.1007/s00531-005-0513-0.
Belka Z, Narkiewicz M. Devonian. In: McCann T, editor. The Geology of Central Europe: Volume 1: Precambrian and Palaeozoic. London: Geological Society of London; 2008. p. 383–410.
Berger J-P, Reichenbacher B, Becker D, Grimm M, Grimm K, Picot L, et al. Paleogeography of the Upper Rhine Graben (URG) and the Swiss Molasse Basin (SMB) from Eocene to Pliocene. Int J Earth Sci. 2005;94(4):697–710. https://doi.org/10.1007/s00531-005-0475-2.
Bertleff B, Joachim H, Koziorowski G, Leiber J, Ohmert W, Prestel R, et al. Ergebnisse der Hydrogeothermiebohrungen in Baden-Württemberg. GLAB. 1988;30:27–116.
Bertrand G, Horstmann M, Hermann O, Behrmann JH. Retrodeformation of the southern Upper Rhine Graben: new insights on continental oblique rifting. Quatern Sci Rev. 2005;24(3–4):345–52. https://doi.org/10.1016/j.quascirev.2004.07.011.
Betten I. 3D-Laserscanning, DFN-Modellierung und Aufschlussaufnahme im Rotliegend des östlichen Saar-Nahe-Beckens [Masterthesis]. Darmstadt: Technische Universität Darmstadt; 2015.
BGR. Geologische Karte der Bundesrepublik Deutschland 1 : 1 000 000 (GK1000); 2016.
BGR. Der Geodatendienst für Erdbeben in Deutschland - GERSEIS. 2021. https://www.bgr.bund.de/DE/Themen/Erdbeben-Gefaehrdungsanalysen/Seismologie/Seismologie/GERSEIS/gerseis_node.html. Accessed 12 Dec 2021.
Blundell DJ, Freeman R, Mueller S, Button S. A continent revealed: the European Geotraverse, structure and dynamic evolution. Cambridge: Cambridge University Press; 1992.
BMWK. Energiedaten: Gesamtausgabe. Bundesministerium für Wirtschaft und Klimaschutz; 2022. https://www.bmwk.de/Redaktion/DE/Artikel/Energie/energiedaten-gesamtausgabe.html. Accessed 29 August 2022.
Böcker J. Petroleum system and thermal history of the Upper Rhine Graben - Implications from organic geochemical analyses, oil-source rock correlations and numerical modelling [PhD thesis]: RWTH Aachen; 2015.
Boigk H, Schöneich H. The Rhinegraben: geologic history and neotectonic activity—Perm, Trias und älterer Jura im Bereich der südlichen Mittelmeer-Mjösen-Zone und des Rheingrabens. In: Illies JH, Fuchs K, editors. Approaches to Taphrogenesis. Stuttgart: Schweizerbart; 1974. p. 60–72.
Boissavy C, Henry L, Genter A, Pomart A, Rocher P, Schmidlé-Bloch V. Geothermal Energy Use, Country Update for France. In: European Geothermal Congress; 11.-14. June; Den Haag; 2019.
Bonjer K-P. Seismicity pattern and style of seismic faulting at the eastern borderfault of the southern Rhine Graben. Tectonophysics. 1997;275(1–3):41–69. https://doi.org/10.1016/S0040-1951(97)00015-2.
Bonjer K-P, Gelbke C, Gilg B, Rouland D, Mayer-Rosa D, Massinon B. Seismicity and dynamics of the Upper Rhinegraben. J Geophys. 1984;55(1):1–12.
Bossart P, Mazurek M, Hellmuth KH, Siitari-Kauppi M, Schneebeli M. Grimsel Test Site: Structural geology and water flow-paths in the migration shear-zone: Nationale Genossenschaft fuer die Lagerung Radioaktiver Abfaelle (NAGRA); 1991. https://www.nagra.ch/de/technical-report-91-12. Accessed 29 Aug 2022.
Bossennec C, Géraud Y, Böcker J, Klug B, Mattioni L, Bertrand L, Moretti I. Characterisation of fluid flow conditions and paths in the Buntsandstein Gp. sandstones reservoirs. Upper Rhine Graben BSGF. 2021;192:35. https://doi.org/10.1051/bsgf/2021027.
Bossennec C, Géraud Y, Böcker J, Klug B, Mattioni L, Sizun J-P, et al. Evolution of diagenetic conditions and burial history in Buntsandstein Gp. fractured sandstones (Upper Rhine Graben) from in-situ δ18O of quartz and 40Ar/39Ar geochronology of K-feldspar overgrowths. Int J Earth Sci. 2021;110(8):2779–802. https://doi.org/10.1007/s00531-021-02080-2.
Bossennec C, Frey M, Seib L, Bär K, Sass I. Multiscale characterisation of fracture patterns of a crystalline reservoir analogue. Geosciences. 2021. https://doi.org/10.3390/geosciences11090371.
Bossennec C. Evolution of transfer properties of sandstones by diagenesis and deformation : Case study on Buntsandstein Gp. sandstones, Upper Rhine Graben: Évolution des propriétés de transfert des grès par diagénèse et déformation : application aux formations du Buntsandstein Gp., Graben du Rhin: Université de Lorraine; 2019.
Boy JA, Haneke J, Kowalczyk G, Lorenz V, Schindler T, Thum H. Rotliegend im Saar-Nahe-Becken, am Taunus-Südrand und im nördlichen Oberrheingraben. SDGG. 2012;61:254–377. https://doi.org/10.1127/sdgg/61/2012/254.
Brady P, Lopez C, Sassani D. Granite hydrolysis to form deep brines. Energies. 2019;12(11):2180. https://doi.org/10.3390/en12112180.
Brigaud B, Vincent B, Carpentier C, Robin C, Guillocheau F, Yven B, Huret E. Growth and demise of the Jurassic carbonate platform in the intracratonic Paris Basin (France): interplay of climate change, eustasy and tectonics. Mar Pet Geol. 2014;53:3–29. https://doi.org/10.1016/j.marpetgeo.2013.09.008.
Brun JP, Gutscher M-A. Deep crustal structure of the Rhine Graben from dekorp-ecors seismic reflection data: a summary. Tectonophysics. 1992;208(1–3):139–47. https://doi.org/10.1016/0040-1951(92)90340-C.
Buchmann TJ, Connolly PT. Contemporary kinematics of the Upper Rhine Graben: a 3D finite element approach. Global Planet Change. 2007;58(1–4):287–309. https://doi.org/10.1016/j.gloplacha.2007.02.012.
Buchner F. Rhinegraben: Horizontal stylolites indicating stress regimes of earlier stages of rifting. Tectonophysics. 1981;73(1–3):113–8. https://doi.org/10.1016/0040-1951(81)90178-5.
Bücker C. Das Geologiedatengesetz GeolDG—was ist neu? Geotherm Energie. 2021;99:28–30.
Caine JS, Evans JP, Forster CB. Fault zone architecture and permeability structure. Geology. 1996;24(11):1025. https://doi.org/10.1130/0091-7613(1996)024%3c1025:FZAAPS%3e2.3.CO;2.

Carpenter AB. Origin and chemical evolution of brines in sedimentary basins. In: SPE Annual Fall Technical Conference and Exhibition; October 1978; Houston, Texas. OnePetro: OnePetro; 1978. https://doi.org/10.2118/7504-MS.
Chavot P, Heimlich C, Masseran A, Serrano Y, Zoungrana J, Bodin C. Social shaping of deep geothermal projects in Alsace: politics, stakeholder attitudes and local democracy. Geotherm Energy. 2018. https://doi.org/10.1186/s40517-018-0111-6.
Chavot P, Masseran A, Bodin C, Heimlich C, Serrano Y, Zoungrana J. Public perception of geothermal projects in Alsace: between energy transition and territorial rooting. In: European Geothermal Congress; 11.-14. June; Den Haag; 2019.
Chen F, Hegner E, Todt W. Zircon ages and Nd isotopic and chemical compositions of orthogneisses from the Black Forest, Germany: evidence for a Cambrian magmatic arc. Int J Earth Sci. 2000;88(4):791–802. https://doi.org/10.1007/s005310050306.
Chilès J, Aug C, Guillen A, Lees T. Modelling the Geometry of Geological Units and its Uncertainty in 3D From Structural Data: The Potential-Field Method. In: Orebody Modelling and Strategic Mine Planning; 22 - 24 November; Perth; 2004. p. 313–320.
Clauser C. Conductive and convective heat flow components in the Rheingraben and implications for the deep permeability distribution. In: Beck AE, editor. Hydrogeological regimes and their subsurface thermal effects. Washington: DC; 1989. p. 59–64.
Clauser C, Villinger H. Analysis of conductive and convective heat transfer in a sedimentary basin, demonstrated for the Rheingraben. Geophys J Int. 1990;100(3):393–414. https://doi.org/10.1111/j.1365-246X.1990.tb00693.x.
Cloetingh S, Ziegler PA, Beekman F, Andriessen PAM, Hardebol N, Dèzes P. Intraplate deformation and 3D rheological structure of the Rhine Rift System and adjacent areas of the northern Alpine foreland. Int J Earth Sci. 2005;94(4):758–78. https://doi.org/10.1007/s00531-005-0502-3.
Commission of the European Communities. Geothermische Synthese des Oberrheingrabens. BRGM Alsace & Geologisches Landesamt Baden-Württemberg; 1979. https://lgrbwissen.lgrbbw.de/geothermische-synthese-des-oberrheingrabens-bestandsaufnahme. Accessed 29 Aug 2022.
Cornet FH, Helm J, Poitrenaud H, Etchecopar A. Seismic and aseismic slips induced by large-scale fluid injections. Pure Appl Geophys. 1997;150:563–83. https://doi.org/10.1007/978-3-0348-8814-1_12.
Cornet FH, Bérard T, Bourouis S. How close to failure is a granite rock mass at a 5km depth? Int J Rock Mech Min Sci. 2007;44(1):47–66. https://doi.org/10.1016/j.ijrmms.2006.04.008.
Cornu T, Cardozo GL, Cloetingh S, Beekman F. A structural model from local earthquake tomography: application to present-day tectonics of the Upper Rhine Graben. Global Planet Change. 2007;58(1–4):270–86. https://doi.org/10.1016/j.gloplacha.2007.03.008.
Coward MP. Structural and tectonic setting of the Permo-Triassic basins of northwest Europe. Geol Soc Spec Publ. 1995;91(1):7–39. https://doi.org/10.1144/GSL.SP.1995.091.01.02.
Cox LA. Artifactual uncertainty in risk analysis. Risk Anal. 1982;2(3):121–35. https://doi.org/10.1111/j.1539-6924.1982.tb01375.x.
Crowley QG, Floyd PA, Winchester JA, Franke W, Holland JG. Early Palaeozoic rift-related magmatism in Variscan Europe: fragmentation of the Armorican Terrane Assemblage. Terra Nova. 2000;12(4):171–80. https://doi.org/10.1046/j.1365-3121.2000.00290.x.
Cuenot N, Charléty J, Dorbath L, Haessler H. Faulting mechanisms and stress regime at the European HDR site of Soultz-sous-Forêts, France. Geothermics. 2006;35(5–6):561–75. https://doi.org/10.1016/j.geothermics.2006.11.007.
Cuenot N, Faucher J-P, Fritsch D, Genter A, Szablinski D. The European EGS project at Soultz-sous-Forêts: From extensive exploration to power production. In: 2008 IEEE Power & Energy Society General Meeting; 7/20/2008 - 7/24/2008; Pittsburgh, PA. Pittsburgh, Pa.: IEEE: IEEE; 2008. p. 1–8. https://doi.org/10.1109/PES.2008.4596680.
Dallmeyer RD, Franke W, Weber K, editors. Pre-Permian Geology of Central and Eastern Europe. Berlin: Springer, Berlin Heidelberg; 1995.
Darnet M, Wawrzyniak P, Coppo N, Nielsson S, Schill E, Fridleifsson G. Monitoring geothermal reservoir developments with the Controlled-Source Electro-Magnetic method—a calibration study on the Reykjanes geothermal field. J Volcanol Geoth Res. 2020;391: 106437. https://doi.org/10.1016/j.jvolgeores.2018.08.015.
Deckert H, Bauer W, Abe S, Horowitz F, Schneider U. Geophysical greenfield exploration in the permo-carboniferous Saar-Nahe basin—the Wiesbaden Geothermal Project, Germany. Geophys Prospect. 2017. https://doi.org/10.1111/1365-2478.12598.
Deichmann N, Ernst J. Earthquake focal mechanisms of the induced seismicity in 2006 and 2007 below Basel (Switzerland). Swiss J Geosci. 2009. https://doi.org/10.1007/s00015-009-1336-y.
Deichmann N, Giardini D. Earthquakes induced by the stimulation of an enhanced geothermal system below Basel (Switzerland). Seismol Res Lett. 2009;80(5):784–98. https://doi.org/10.1785/gssrl.80.5.784.
Derer C, Kosinowski M, Luterbacher HP, Schäfer A, Süß MP. Sedimentary response to tectonics in extensional basins: the Pechelbronn Beds (Late Eocene to early Oligocene) in the northern Upper Rhine Graben, Germany. Geological Society, London, Special Publications. 2003;208(1):55–69. https://doi.org/10.1144/GSL.SP.2003.208.01.03.
Derer CE, Schumacher ME, Schäfer A. The northern Upper Rhine Graben: basin geometry and early syn-rift tectono-sedimentary evolution. Int J Earth Sci. 2005;94(4):640–56. https://doi.org/10.1007/s00531-005-0515-y.
Dersch-Hansmann M, Hug N. Oberer und Mittlerer Buntsandstein im Untergrund des Dieburger Beckens. Geologisches Jahrbuch Hessen. 2004;131:81–95.
Deutsche Stratigraphische Kommission. Stratigraphische Tabelle von Deutschland 2016: Potsdam (Deutsches GeoForschungsZentrum); 2016. ISBN 978-3-9816597-7-1. https://gfzpublic.gfzpotsdam.de/pubman/item/item_2524907. Accessed 29 Aug 2022.
Dezayes C, Genter A, Valley B. Structure of the low permeable naturally fractured geothermal reservoir at Soultz. CR Geosci. 2010;342(7–8):517–30. https://doi.org/10.1016/j.crte.2009.10.002.
Dezayes C, Gentier S, Genter A. Deep Geothermal Energy in Western Europe: The Soultz-Project: Final Report. BRGM; 2005a. http://infoterre.brgm.fr/rapports/RP-54227-FR.pdf. Accessed 29 Aug 2022.

Dezayes C, Chevremont P, Tourlière B, Homeier G, Genter A. Geological study of the GPK4 HFR borehole and correlation with the GPK3 borehole (Soultz-sous-Forêts, France). BRGM; 2005b. http://infoterre.brgm.fr/rapports/RP-53697-FR.pdf. Accessed 29 Aug 2022.
Dezayes C, Beccaletto L, Oliviero G, Baillieux P, Capar L, Schill E. 3-D Visualization of a Fractured Geothermal Field: The Example of the EGS Soultz Site (Northern Upper Rhine Graben, France). In: Stanford University, ed. Thirty-Sixth Workshop on Geothermal Reservoir Engineering; 31. January—2. February; Stanford, California; 2011.
Dèzes P, Schmid SM, Ziegler PA. Evolution of the European Cenozoic Rift System: interaction of the Alpine and Pyrenean orogens with their foreland lithosphere. Tectonophysics. 2004;389(1–2):1–33. https://doi.org/10.1016/j.tecto.2004.06.011.
Dickinson JS, Buik N, Matthews MC, Snijders A. Aquifer thermal energy storage: theoretical and operational analysis. Géotechnique. 2009;59(3):249–60. https://doi.org/10.1680/geot.2009.59.3.249.
Doebl F. The Tertiary and Pleistocene sediments of the northern and central part of the Upper Rhinegraben. Abh Geol Landesamts Baden-Württemb. 1967;6:48–54.
Doebl F. Die tertiären und quartären Sedimente des südlichen Rheingrabens. In: Illies JH, Mueller S, editors. Graben problems. Stuttgart: Schweizerbart; 1970. p. 56–66.
Doebl F, Olbrecht W. An isobath map of the Tertiary base in the Rhinegraben. In: Illies JH, Fuchs K, editors. Approaches to Taphrogenesis. Stuttgart: Schweizerbart; 1974. p. 71–2.
Doebl F. Zur Geologie und Geothermik im mittleren Oberrheingraben. Fortschr. Geol. Rheinld. u. Westf. 1979;27:1–17.
Dorbath L, Evans K, Cuenot N, Valley B, Charléty J, Frogneux M. The stress field at Soultz-sous-Forêts from focal mechanisms of induced seismic events: Cases of the wells GPK2 and GPK3. CR Geosci. 2010;342(7–8):600–6. https://doi.org/10.1016/j.crte.2009.12.003.
Dornstadter J, Kappelmeyer O, Welter M. The geothermal potential in the Upper Rhine Graben valley. In: European Geothermal Conference Basel 1999; 28.-30. September; Basel, Switzerland; 1999.
Doublier MP, Potel S, Franke W, Roache T. Very low-grade metamorphism of Rheno-Hercynian allochthons (Variscides, Germany): facts and tectonic consequences. Int J Earth Sci. 2012;101(5):1229–52. https://doi.org/10.1007/s00531-011-0718-3.
Doubre C, Meghraoui M, Masson F, Lambotte S, Jund H, Bès de Berc M, Grunberg M. Seismotectonics in Northeastern France and neighboring regions. Comptes Rendus Géosci. 2021;353(S1):153–85. https://doi.org/10.5802/crgeos.80.
Douziech M, Tosti L, Ferrara N, Parisi ML, Pérez-López P, Ravier G. Applying harmonised geothermal life cycle assessment guidelines to the rittershoffen geothermal heat plant. Energies. 2021;14(13):3820. https://doi.org/10.3390/en14133820.
Drüppel K, Stober I, Grimmer JC, Mertz-Kraus R. Experimental alteration of granitic rocks: implications for the evolution of geothermal brines in the Upper Rhine Graben, Germany. Geothermics. 2020;88: 101903. https://doi.org/10.1016/j.geothermics.2020.101903.
Duringer P, Aichholzer C, Orciani S, Genter A. The complete lithostratigraphic section of the geothermal wells in Rittershoffen (Upper Rhine Graben, eastern France): a key for future geothermal wells. BSGF. 2019;190:13. https://doi.org/10.1051/bsgf/2019012.
Durst H. Aspects of exploration history and structural style in the Rhine graben area. Generation, accumulation and production of Europe's hydrocarbons. Eur Assoc Petrol Geosci Spec Publ. 1991;1:247–61.
Duwiquet H, Guillou-Frottier L, Arbaret L, Bellanger M, Guillon T, Heap MJ. Crustal Fault Zones (CFZ) as geothermal power systems: a preliminary 3D THM model constrained by a multidisciplinary approach. Geofluids. 2021;2021:1–24. https://doi.org/10.1155/2021/8855632.
Eckelmann K, Nesbor H-D, Königshof P, Linnemann U, Hofmann M, Lange J-M, Sagawe A. Plate interactions of Laurussia and Gondwana during the formation of Pangaea—constraints from U-Pb LA–SF–ICP–MS detrital zircon ages of Devonian and Early Carboniferous siliciclastics of the Rhenohercynian zone Central European Variscides. Gondwana Res. 2014;25(4):1484–500. https://doi.org/10.1016/j.gr.2013.05.018.
Edel JB, Fluck P. The upper Rhenish Shield basement (Vosges, Upper Rhinegraben and Schwarzwald): main structural features deduced from magnetic, gravimetric and geological data. Tectonophysics. 1989;169(4):303–16. https://doi.org/10.1016/0040-1951(89)90093-0.
Edel JB, Schulmann K. Geophysical constraints and model of the "Saxothuringian and Rhenohercynian subductions - magmatic arc system" in NE France and SW Germany. Bull Soc Geol Fr. 2009;180:545–58. https://doi.org/10.2113/gssgfbull.180.6.545.
Edel JB, Weber K. Cadomian terranes, wrench faulting and thrusting in the central Europe Variscides: geophysical and geological evidence. Int J Earth Sci. 1995. https://doi.org/10.1007/BF00260450.
Edel J-B, Whitechurch H, Diraison M. Seismicity wedge beneath the Upper Rhine Graben due to backwards Alpine push? Tectonophysics. 2006;428(1–4):49–64. https://doi.org/10.1016/j.tecto.2006.08.009.
Edel JB, Schulmann K, Rotstein Y. The Variscan tectonic inheritance of the Upper Rhine Graben: evidence of reactivations in the Lias, Late Eocene-Oligocene up to the recent. Int J Earth Sci. 2007;96(2):305–25. https://doi.org/10.1007/s00531-006-0092-8.
Edel JB, Maurer V, Dalmais E, Genter A, Richard A, Letourneau O, Hehn R. Structure and nature of the Palaeozoic basement based on magnetic, gravimetric and seismic investigations in the central Upper Rhinegraben. Geothermal Energy. 2018;6(1):13. https://doi.org/10.1186/s40517-018-0099-y.
Eisbacher GH, Lüschen E, Wickert F. Crustal-scale thrusting and extension in the Hercynian Schwarzwald and Vosges, central Europe. Tectonics. 1989;8(1):1–21. https://doi.org/10.1029/TC008i001p00001.
El Dakak W. Influence of Temporal Variation of Water Saturation on Shallow Geothermal Systems Using Numerical Modeling [Masterthesis]: TU Darmstadt; 2015.
Ernst M. Lithostratigraphische und fazielle Untersuchungen des Hauptrogensteins (Bajocium) im SE-Oberrheingraben. Jahresberichte und Mitteilungen des Oberrheinischen Geologischen Vereins. 1991:311–82. https://doi.org/10.1127/jmogv/73/1991/311.
Esslinger G. Rezente Bodenbewegungen über dem Salinar des südlichen Oberrheingrabens [PhD thesis]: TU Berlin; 1968.

Esteban L, Pimienta L, Sarout J, Piane CD, Haffen S, Geraud Y, Timms NE. Study cases of thermal conductivity prediction from P-wave velocity and porosity. Geothermics. 2015;53:255–69. https://doi.org/10.1016/j.geothermics.2014.06.003.
Evans JP, Forster CB, Goddard JV. Permeability of fault-related rocks, and implications for hydraulic structure of fault zones. J Struct Geol. 1997;19(11):1393–404. https://doi.org/10.1016/S0191-8141(97)00057-6.
Evans KF, Genter A, Sausse J. Permeability creation and damage due to massive fluid injections into granite at 3.5 km at Soultz: 1. Borehole observations. J Geophys Res. 2005. https://doi.org/10.1029/2004JB003168.
Evans K, Zappone A, Kraft T, Deichmann N, Moia F. A survey of the induced seismic responses to fluid injection in geothermal and CO2 reservoirs in Europe. Geothermics. 2012;41:30–54. https://doi.org/10.1016/j.geothermics.2011.08.002.
Fäh D, Gisler M, Jaggi B, Kästli P, Lutz T, Masciadri V, et al. The 1356 Basel earthquake: an interdisciplinary revision. Geophys J Int. 2009;178(1):351–74. https://doi.org/10.1111/j.1365-246X.2009.04130.x.
Falk F, Franke W, Kurze M. Stratigraphy. In: Dallmeyer RD, Franke W, Weber K, editors. Pre-Permian Geology of Central and Eastern Europe. Berlin: Springer, Berlin Heidelberg; 1995. p. 221–34.
Faridfar N. Untersuchung und Bewertung der geothermischen Eigenschaften der Gesteine der Noerdlichen Pyllitzone, Vordertaunus [Bachelorthesis]: TU Darmstadt; Goethe Universität Frankfurt am Main; 2010.
Faulkner DR, Jackson C, Lunn RJ, Schlische RW, Shipton ZK, Wibberley C, Withjack MO. A review of recent developments concerning the structure, mechanics and fluid flow properties of fault zones. J Struct Geol. 2010;32(11):1557–75. https://doi.org/10.1016/j.jsg.2010.06.009.
Fazies DG, Paläogeographie und Genese des unteren Buntsandsteins norddeutscher Auffassung im südlichen Beckenbereich. Notizbl. hess. L.-Amt Bodenforsch. 1966;94:132–57.
Fei L, Niu J, Linsel A, Hinderer M, Scheuvens D, Petschick R. Rock alteration at the post-Variscan nonconformity: implications for Carboniferous-Permian surface weathering versus burial diagenesis and paleoclimate evaluation. Solid Earth. 2021;12:1165–84. https://doi.org/10.5194/se-2020-221.
Feist-Burkhardt S, Götz A, Szulc J, Borkhataria R, Geluk M, Haas J, et al. Triassic. In: McCann T, editor., et al., The geology of Central Europe: Volume 2: Mesozoic and Cenozoic. London: Geological Society of London; 2008. p. 749–821.
Ferrill DA, Morris AP. Dilational normal faults. J Struct Geol. 2003;25(2):183–96. https://doi.org/10.1016/S0191-8141(02)00029-9.
Fleuchaus P, Godschalk B, Stober I, Blum P. Worldwide application of aquifer thermal energy storage—a review. Renew Sustain Energy Rev. 2018;94:861–76. https://doi.org/10.1016/j.rser.2018.06.057.
Fleuchaus P, Schüppler S, Stemmle R, Menberg K, Blum P. Aquiferspeicher in Deutschland. Grundwasser. 2021;26(2):123–34. https://doi.org/10.1007/s00767-021-00478-y.
Flöttmann T, Oncken O. Contraints on the evolution of the Mid German Crystalline Rise—a study of outcrops west of the river Rhine. Geol Rundsch. 1992;82(2):515–43. https://doi.org/10.1007/bf01828613.
Floyd PA. Igneous Activity. In: Dallmeyer RD, Franke W, Weber K, editors. Pre-Permian Geology of Central and Eastern Europe. Berlin: Springer, Berlin Heidelberg; 1995. p. 59–81.
Franke W. Tectonostratigraphic units in the Variscan belt of central Europe. Geol Soc Am Bull. 1989;230:67–90. https://doi.org/10.1130/SPE230-p67.
Franke W. III.B.1 Stratigraphy. In: Dallmeyer RD, Franke W, Weber K, editors. Pre-Permian Geology of Central and Eastern Europe. Berlin: Springer, Berlin Heidelberg; 1995a. p. 33–49.
Franke W. Rhenohercynian foldbelt: autochthon and nonmetamorphic units—stratigraphy. In: Dallmeyer RD, Franke W, Weber K, editors. Pre-Permian Geology of Central and Eastern Europe. Berlin: Springer, Berlin Heidelberg; 1995b. p. 33–49.
Franke W. Saxothuringian Basin. In: Dallmeyer RD, Franke W, Weber K, editors. Pre-Permian Geology of Central and Eastern Europe. Berlin: Springer, Berlin Heidelberg; 1995c. p. 217–8.
Franke W. The mid-European segment of the Variscides: tectonostratigraphic units, terrane boundaries and plate tectonic evolution. Geol Soc Spec Publ. 2000;179:35–61. https://doi.org/10.1144/GSL.SP.2000.179.01.05.
Franke W, Cocks LRM, Torsvik TH. The Palaeozoic Variscan oceans revisited. Gondwana Res. 2017;48:257–84. https://doi.org/10.1016/j.gr.2017.03.005.
Franz M, Bachmann GH, Barnasch J, Heunisch C, Röhling H-G. Der Keuper in der Stratigraphischen Tabelle von Deutschland 2016 – kontinuierliche Sedimentation in der norddeutschen Beckenfazies (Variante B). ZDGG. 2018;169(2):203–24. https://doi.org/10.1127/zdgg/2018/0114.
Frauenhofer ISE. Öffentliche Nettostromerzeugung in Deutschland im Jahr 2020. Fraunhofer-Institut für Solare Energiesysteme ISE. 2021. https://www.energy-charts.info/downloads/Stromerzeugung_2020_1.pdf. Accessed 29 Aug 2022.
Frenzel G. Die Mineralparagenese der Albersweiler Lamprophyre. Neues J Mineral Abh. 1971;115:164–91.
Frey M, Weinert S, Bär K, van der Vaart J, Dezayes C, Calcagno P, Sass I. Integrated 3D geological modelling of the northern Upper Rhine Graben by joint inversion of gravimetry and magnetic data. Tectonophysics. 2021b;813: 228927. https://doi.org/10.1016/j.tecto.2021.228927.
Frey M, Bossennec C, Seib L, Bär K, Schill E, Sass I. Interdisciplinary fracture network characterization in the crystalline basement: a case study from the Southern Odenwald, SW Germany. Solid Earth. 2022;13(6):935–55. https://doi.org/10.5194/se-13-935-2022.
Frey M, Weinert S, Bär K, van der Vaart J, Dezayes C, Calcagno P, Sass I. 3D Geological Model of the Crystalline Basement in the Northern Upper Rhine Graben Region. Technical University Of Darmstadt; 2021a. https://doi.org/10.48328/tudatalib-417.2.
Freymark J, Sippel J, Scheck-Wenderoth M, Bär K, Stiller M, Fritsche J-G, Kracht M. The deep thermal field of the Upper Rhine Graben. Tectonophysics. 2017;694:114–29. https://doi.org/10.1016/j.tecto.2016.11.013.
Freymark J, Bott J, Cacace M, Ziegler M, Scheck-Wenderoth M. Influence of the main border faults on the 3D hydraulic field of the Central Upper Rhine Graben. Geofluids. 2019;2019:1–21. https://doi.org/10.1155/2019/7520714.

Freymark J, Sippel J, Scheck-Wenderoth M, Bär K, Stiller M, Fritsche J-G, Kracht M. The thermal field of the Upper Rhine Graben – Temperature predictions based on a 3D model. In: European Geothermal Congress; 19.-23. September; Strasbourg, France; 2016.
Freymark J, Bott J, Scheck-Wenderoth M, Bär K, Stiller M, Fritsche J-G, et al. 3D-URG: 3D gravity constrained structural model of the Upper Rhine Graben; 2020. https://doi.org/10.5880/GFZ.4.5.2020.004.
Fritsche R, Rüter H. Seismizität. In: Bauer MJ, editor. Handbuch Tiefe Geothermie: Prospektion, Exploration, Realisierung, Nutzung. Berlin: Springer Spektrum; 2014. p. 397–427.
Gaupp R, Clauer N, Bauer A, Eynatten H von, Baaske U, Mezger J. Untersuchung des Einflusses von Diagenese im Bereich von Störungen anhand von Oberflächenaufschlüssen – Buntsandstein westlich der Rheingraben-Randstörung zwischen Bad Bergzabern und Leistadt / Bad Drükheim: Bericht zur Piotstudie 10/97 bis 5/98: Friedrich-Schiller-Universität Jena; CNRS Strasbourg; 1998.
Gaupp R, Nickel B. Die Pechelbronn-Schichten im Raum Eich-Stockstadt (Nördlicher Oberrheingra-ben; Blatt 6216 Gernsheim). Geol Jb Hessen. 2001;128:19–27.
Genter A, Traineau H. Analysis of macroscopic fractures in granite in the HDR geothermal well EPS-1, Soultz-sous-Fore^ts, France. J Volcanol Geoth Res. 1996;72(1–2):121–41. https://doi.org/10.1016/0377-0273(95)00070-4.
Genter A, Evans K, Cuenot N, Fritsch D, Sanjuan B. Contribution of the exploration of deep crystalline fractured reservoir of Soultz to the knowledge of enhanced geothermal systems (EGS). CR Geosci. 2010;342(7–8):502–16. https://doi.org/10.1016/j.crte.2010.01.006.
GeORG Projektteam. Geopotenziale des tieferen Untergrundes im Oberrheingraben: Fachlich-Technischer Abschlussbericht des INTERREG-Projekts GeORG; 2013. https://www.geopotenziale.org/products/fta?lang=1. Accessed 29 Aug 2022.
Gérard A, Kappelmeyer O. The Soultz-sous-Forêts project. Geothermics. 1987;16(4):393–9. https://doi.org/10.1016/0375-6505(87)90018-6.
Geyer G, Elicki O, Fatka O, Zylinska A. Cambrian. In: McCann T, editor. The Geology of Central Europe: Volume 1: Precambrian and Palaeozoic. London: Geological Society of London; 2008. p. 155–202.
Geyer OF, Gwinner MP, Simon T. Geologie von Baden-Württemberg. 5th ed. Stuttgart: Schweizerbart; 2011.
Giardini D, Wössner J, Danciu L. Mapping Europe's Seismic hazard. Eos Trans AGU. 2014;95(29):261–2. https://doi.org/10.1002/2014EO290001.
Gonzalez R. Response of shallow-marine carbonate facies to third-order and high-frequency sea-level fluctuations: Hauptrogenstein Formation, northern Switzerland. Sed Geol. 1996;102(1–2):111–30. https://doi.org/10.1016/0037-0738(95)00059-3.
Gonzalez R, Wetzel A. Stratigraphy and paleogeography of the Hauptrogenstein and Klingnau Formations (middle Bajocian to late Bathonian), northern Switzerland. Eclogae Geol Helv. 1996. https://doi.org/10.5169/seals-167921.
Gottschalk K. Oberflächenanaloge zu geothermischen Reservoiren im mittleren Oberrheingraben - Kristallin, Rotliegend und Buntsandstein im südlichen Pfälzerwald [Diplomathesis]: Universität Freiburg i. Br.; 2010.
Götz AE, Gast S. Basin evolution of the Anisian Peri-Tethys: implications from conodont assemblages of Lower Muschelkalk key sections (Central Europe). ZDGG. 2010;161(1):39–49. https://doi.org/10.1127/1860-1804/2010/0161-0039.
Götz AE. Zyklen und Sequezen im Unteren Muschelkalk des Germanischen Beckens. Hallesches Jb. Geowiss. 2004;Beih. 18:91–8.
Grasby SE, Betcher RN. Regional hydrogeochemistry of the carbonate rock aquifer, southern Manitoba. Can J Earth Sci. 2002;39(7):1053–63. https://doi.org/10.1139/E02-021.
Griffiths L, Heap MJ, Wang F, Daval D, Gilg HA, Baud P, et al. Geothermal implications for fracture-filling hydrothermal precipitation. Geothermics. 2016;64:235–45. https://doi.org/10.1016/j.geothermics.2016.06.006.
Grimm MC. Beiträge zur Lithostratigraphie des Paläogens und Neogens im Oberrheingebiet (Oberrheingraben, Mainzer Becken, Hanauer Becken). Geol JB Hessen. 2005;132:79–112.
Grimm KI, Grimm MC, Schindler T. Lithostratigraphic subdivision of the Rupelian and Chattian in the Mainz Basin. Germany Njgpa. 2000;218(3):343–97. https://doi.org/10.1127/njgpa/218/2000/343.
Grimm MC, Wielandt-Schuster U, Hottenrott M, Radtke G, Berger J-P, Ellwanger D, et al. Oberrheingraben (Tertiär des Oberrheingrabens). SDGG. 2011;75:57–132. https://doi.org/10.1127/sdgg/75/2011/57.
Grimmer JC, Ritter JRR, Eisbacher GH, Fielitz W. The Late Variscan control on the location and asymmetry of the Upper Rhine Graben. Int J Earth Sci. 2017;106(3):827–53. https://doi.org/10.1007/s00531-016-1336-x.
Grösser J, Dörr W. MOR-type basalts of the Eastern Rhenish Massif. NJGPM. 1986;1986(12):705–22. https://doi.org/10.1127/njgpm/1986/1986/705.
Grünthal G, Stromeyer D, Bosse C, Cotton F, Bindi D. The probabilistic seismic hazard assessment of Germany—version 2016, considering the range of epistemic uncertainties and aleatory variability. Bull Earthquake Eng. 2018;16(10):4339–95. https://doi.org/10.1007/s10518-018-0315-y.
Gu Y, Rühaak W, Bär K, Sass I. Using seismic data to estimate the spatial distribution of rock thermal conductivity at reservoir scale. Geothermics. 2017;66:61–72. https://doi.org/10.1016/j.geothermics.2016.11.007.
Gu Y. Calculations of the Optimized Design for an Existing Multifunction Building with Borehole Heat Exchangers [Masterthesis]: TU Darmstadt; 2010.
Gudmundsson A, Berg SS, Lyslo KB, Skurtveit E. Fracture networks and fluid transport in active fault zones. J Struct Geol. 2001;23(2–3):343–53. https://doi.org/10.1016/S0191-8141(00)00100-0.
Guglielmetti L, Comina C, Abdelfettah Y, Schill E, Mandrone G. Integration of 3D geological modeling and gravity surveys for geothermal prospection in an Alpine region. Tectonophysics. 2013;608:1025–36. https://doi.org/10.1016/j.tecto.2013.07.012.
Guillou-Frottier L, Carrè C, Bourgine B, Bouchot V, Genter A. Structure of hydrothermal convection in the Upper Rhine Graben as inferred from corrected temperature data and basin-scale numerical models. J Volcanol Geoth Res. 2013;256:29–49. https://doi.org/10.1016/j.jvolgeores.2013.02.008.
Guillou-Frottier L, Duwiquet H, Launay G, Taillefer A, Roche V, Link G. On the morphology and amplitude of 2D and 3D thermal anomalies induced by buoyancy-driven flow within and around fault zones. Solid Earth. 2020;11(4):1571–95. https://doi.org/10.5194/se-11-1571-2020.

Haffen S, Geraud Y, Diraison M, Dezayes C. Determination of fluid-flow zones in a geothermal sandstone reservoir using thermal conductivity and temperature logs. Geothermics. 2013;46:32–41. https://doi.org/10.1016/j.geothermics.2012.11.001.
Haffen S, Géraud Y, Diraison M, Dezayes C. Determining majors fluid-flow zones in a geothermal sandstone reservoir from thermal conductivity and temperature logs. In: EGU General Assembly; 2012. p. 9043.
Haffen S, Géraud Y, Diraison M. Geothermal, structural and petrophysical characteristics of Buntsandstein sandstone reservoir (Upper Rhine Graben, France). In: World Geothermal Congress; 19.-24. April; Melbourne, Australia; 2015.
Hagdorn H. Triassic Muschelkalk of Central Europe. In: Hess H, Ausich WI, Brett CE, Simms MJ, editors. Fossil crinoids. Cambridge: Cambridge University Press; 1999. p. 164–76.
Hann HP, Chen F, Zedler H, Frisch W, Loeschke J. The Rand Granite in the southern Schwarzwald and its geodynamic significance in the Variscan belt of SW Germany. Int J Earth Sci. 2003;92(6):821–42. https://doi.org/10.1007/s00531-003-0361-8.
Häring MO, Schanz U, Ladner F, Dyer BC. Characterisation of the Basel 1 enhanced geothermal system. Geothermics. 2008;37(5):469–95. https://doi.org/10.1016/j.geothermics.2008.06.002.
Hauber L. Der südliche Rheingraben und seine geothermische Situation. Bulletin der Vereinigung Schweiz. Petroleum-Geologen und -Ingenieure. 1993. doi:https://doi.org/10.5169/seals-216879.
He K, Stober I, Bucher K. Chemical evolution of thermal waters from limestone aquifers of the Southern Upper Rhine Valley. Appl Geochem. 1999;14(2):223–35. https://doi.org/10.1016/S0883-2927(98)00046-8.
Heap MJ, Kushnir ARL, Gilg HA, Wadsworth FB, Reuschlé T, Baud P. Microstructural and petrophysical properties of the Permo-Triassic sandstones (Buntsandstein) from the Soultz-sous-Forêts geothermal site (France). Geotherm Energy. 2017. https://doi.org/10.1186/s40517-017-0085-9.
Hegner E, Chen F, Hann H. Chronology of basin closure and thrusting in the internal zone of the Variscan belt in the Schwarzwald, Germany: evidence from zircon ages, trace element geochemistry, and Nd isotopic data. Tectonophysics. 2001;332(1–2):169–84. https://doi.org/10.1016/S0040-1951(00)00254-7.
Heidbach O, Rajabi M, Reiter K, Ziegler M, WSM Team. World Stress Map Database Release 2016; 2016. https://doi.org/10.5880/WSM.2016.001.
Henk A. Mächtigkeit und Alter der erodierten Sedimente im Saar-Nahe-Becken (SW-Deutschland). Int J Earth Sci. 1992;81(2):323–31. https://doi.org/10.1007/BF01828601.
Henk A. Late orogenic Basin evolution in the Variscan internides: the Saar-Nahe Basin, southwest Germany. Tectonophysics. 1993;223(3–4):273–90. https://doi.org/10.1016/0040-1951(93)90141-6.
Henk A. Late-Orogenic Burial and Exhumation at a Major Variscan Suture Zone. In: Oncken O, editor. Basement Tectonics 11 Europe and Other Regions. Dordrecht: Springer; 1996.
Henrion E, Masson F, Doubre C, Ulrich P, Meghraoui M. Present-day deformation in the Upper Rhine Graben from GNSS data. Geophys J Int. 2020;223(1):599–611. https://doi.org/10.1093/gji/ggaa320.
Hermanrud C, Cao S, Lerche I. Estimates of virgin rock temperature derived from BHT measurements: bias and error. Geophysics. 1990;55(7):924–31. https://doi.org/10.1190/1.1442908.
Hertrich M, Brixel B, Broeker T, et al. Characterization, Hydraulic Stimulation, and Fluid Circulation Experiments in the Bedretto Underground Laboratory for Geosciences and Geoenergies. In: 55th US Rock Mechanics/Geomechanics Symposium; 2021.
Herzberger P, Münch W, Kölbel T, Bruchmann U, Schlagermann P, Hötzl H, et al. The Geothermal Power Plant Bruchsal. In: World Geothermal Congress 2010; 25–29 April; Bali, Indonesia; 2010.
Hess JC, Schmidt G. Zur Altersstellung der Kataklasite im Bereich der Otzberg-Zone, Odenwald. Geol JB Hessen. 1989;117:69–77.
Hesse J. Untersuchung des geothermischen Potenzials der effusiven Vulkanite der permischen Donnersberg-Formation [Bachelorthesis]: TU Darmstadt; 2011.
Hinsken S, Ustaszewski K, Wetzel A. Graben width controlling syn-rift sedimentation: the Palaeogene southern Upper Rhine Graben as an example. Int J Earth Sci. 2007;96(6):979–1002. https://doi.org/10.1007/s00531-006-0162-y.
Hintze M, Plasse B, Bär K, Sass I. Preliminary studies for an integrated assessment of the hydrothermal potential of the Pechelbronn Group in the northern Upper Rhine Graben. Adv Geosci. 2018;45:251–8. https://doi.org/10.5194/adgeo-45-251-2018.
Hirschmann G. IV.B Lithological Characteristics. In: Dallmeyer RD, Franke W, Weber K, editors. Pre-Permian Geology of Central and Eastern Europe. Berlin: Springer, Berlin Heidelberg; 1995. p. 155–63.
Hoffmann H. Bestimmung von geothermischen Kennwerten an Gesteinen des Kellerwaldes [Bachelorthesis]: TU Darmstadt; Goethe Universität Frankfurt am Main; 2011.
Hoffmann H. Petrophysikalische Eigenschaften der Mitteldeutschen Kristallinschwelle im Bereich des Oberrheingrabens [Masterthesis]: TU Darmstadt; 2015.
Hölting B, Coldewey WG. Hydrogeologie: Einführung in die allgemeine und angewandte Hydrogeologie; 90 Tabellen. 7th ed. Heidelberg: Spektrum Akad. Verl; 2009.
Homuth B, Rümpker G, Deckert H, Kracht M. Seismicity of the northern Upper Rhine Graben—constraints on the present-day stress field from focal mechanisms. Tectonophysics. 2014;632:8–20. https://doi.org/10.1016/j.tecto.2014.05.037.
Homuth B, Stiller M, Schmidt B. Reprocessed deep seismic reflection profile DEKORP 1988–9N across the Northern Upper Rhine Graben. Southwest Germany. 2021a. https://doi.org/10.5880/GFZ.DEKORP-9N.002.
Homuth B, Bär K, Weinert S, Sass I. Reprocessing of the hessian DEKORP seismic profiles. In: DGG, ed. 81. Jahrestagung der Deutschen Geophysikalischen Gesellschaft; 01.-05. March 2021b; Kiel; 2021b. p. 182.
Homuth S. Aufschlussanalogstudie zur Charakterisierung oberjurassischer geothermischer Karbonatreservoire im Molassebecken [PhD thesis]. Darmstadt: Technische Universität Darmstadt; 2014.
Housse B-A. Reconnaisance du potentiel géothermique du Buntsadnstein à Strasbourg-Cronenbourg. Géothermie Actualités. 1984;1:36–41.
Hückel B, Kappelmeyer O. Geothermische untersuchungen im saarkarbon. ZDGG_ALT. 1966;117(1):280–311.

Huckriede H, Wemmer K, Ahrendt H. Palaeogeography and tectonic structure of allochthonous units in the German part of the Rheno-Hercynian Belt (Central European Variscides). Int J Earth Sci. 2004;93(3):414–31. https://doi.org/10.1007/s00531-004-0397-4.
Hug N, Vero G. Ein vollständiges Zechsteinprofil im südlichen Odenwald: die hydrogeologische Erkundungsbohrung Langenthal BK2/05. Geol JB Hessen. 2008;135:25–45.
Hug N. Sedimentgenese und Paläogeographie des höheren Zechstein bis zur Basis des Buntsandstein in der Hessischen Senke. Hessisches Landesamt für Umwelt; 2004.
Hurter S, Schellschmidt R. Atlas of geothermal resources in Europe. Geothermics. 2003;32(4–6):779–87. https://doi.org/10.1016/S0375-6505(03)00070-1.
Hüttner R. Bau und Entwicklung des Oberrheingrabens. Ein Überblick mit historischer Rückschau. Geol Jahrbuch. 1991;48:17–42.
Illies JH, Mueller S, editors. Graben problems. Stuttgart: Schweizerbart; 1970.
Illies JH, Fuchs K, editors. Approaches to Taphrogenesis. Stuttgart: Schweizerbart; 1974.
Illies JH. Ancient and recent rifting in the Rhinegraben. Geol En Mijnbouw. 1977;56(4):329–50.
Illies JH. Two Stages Rheingraben Rifting. In: Ramberg IB, Neumann ER, editors. Tectonics and geophysics of continental rifts. Dordrecht: D. Reidel Publ. Comp; 1978. p. 63–71.
Illies JH, Greiner G. Holocene movements and state of stress in the rhinegraben rift system. Dev Geotecton. 1979;13:349–59. https://doi.org/10.1016/B978-0-444-41783-1.50057-X.
Ingebritsen SE, Manning CE. Geological implications of a permeability-depth curve for the continental crust. Geology. 1999;27(12):1107. https://doi.org/10.1130/0091-7613(1999)027%3c1107:GIOAPD%3e2.3.CO;2.
Jafari A, Babadagli T. Effective fracture network permeability of geothermal reservoirs. Geothermics. 2011;40(1):25–38. https://doi.org/10.1016/j.geothermics.2010.10.003.
Jain C, Vogt C, Clauser C. Maximum potential for geothermal power in Germany based on engineered geothermal systems. Geotherm Energy. 2015. https://doi.org/10.1186/s40517-015-0033-5.
Jensen B. Geothermische Untersuchung des Hauptrogenstein im suedlichen Oberrheingraben [Bachelorsthesis]: TU Darmstadt; 2014.
Jodocy M, Stober I. Development of an internet based geothermal information system for Germany-region Baden-Wuerttemberg; Aufbau eines geothermischen Informationssystems fuer Deutschland-Landesteil Baden-Wuerttemberg. Erdoel Erdgas Kohle. 2008;124.
Jodocy M, Stober I. Geologisch-geothermische Tiefenprofile für den baden-württembergischen Teil des nördlichen und mittleren Oberrheingrabens. Erdöl Erdgas Kohle. 2010a;126(2):68–76.
Jodocy M, Stober I. Geologisch-geothermische Tiefenprofile für den südlichen Teil des Oberrheingrabens in Baden-Württemberg. Z Geol Wiss. 2010b;38(1):3–25.
Jodocy M, Stober I. Porositäten und Permeabilitäten im Oberrheingraben und südwestdeutschen Molassebecken. Erdöl Erdgas Kohle. 2011;127(1):20–7.
Jolley SJ, Dijk H, Lamens JH, Fisher QJ, Manzocchi T, Eikmans H, Huang Y. Faulting and fault sealing in production simulation models: Brent Province, northern North Sea. Pet Geosci. 2007;13(4):321–40. https://doi.org/10.1144/1354-079306-733.
Kappelmeyer O, Haenel R. Geothermics with special reference to application. Berlin: Gebrueder Borntraeger; 1974.
Karro E, Marandi A, Vaikme R. The origin of increased salinity in the Cambrian-Vendian aquifer system on the Kopli Peninsula, northern Estonia. Hydrogeol J. 2004. https://doi.org/10.1007/s10040-004-0339-z.
Kemnitz H, Romer RL, Oncken O. Gondwana break-up and the northern margin of the Saxothuringian belt (Variscides of Central Europe). Int J Earth Sci. 2002;91(2):246–59. https://doi.org/10.1007/s005310100209.
Kharaka YK, Hanor JS. Deep fluids in the continents: I. Sedimentary basins. In: Drever JI, ed. Surface and Groundwater, Weathering, and Soils. Treatise on Geochemistr. Elsevier Pergamon; 2003. p. 499–540. https://doi.org/10.1016/B0-08-043751-6/05085-4.
Kirsch H, Kober B, Lippolt HJ. Age of intrusion and rapid cooling of the Frankenstein gabbro (Odenwald, SW-Germany) evidenced by40Ar/39Ar and single-zircon207Pb/206Pb measurements. Int J Earth Sci. 1988;77(3):693–711. https://doi.org/10.1007/BF01830178.
Klapperer S. Zur Fazies des Buntsandsteins im Odenwald und nördlichen Oberrheingraben [Diplomathesis]: Universität Jena; 2009.
Kläske U. Bestimmung des geothermischen Potenzials des Kristallinen Odenwaldes [Bachelorthesis]: TU Darmstadt; 2010.
Klingler P. Charakterisierung des Geothermischen Reservoirs Riehen: 3D-Struktur und Tracer-Test [Masterthesis]. Neuchâtel: Université de Neuchâtel; 2010.
Klügel T, Ahrendt H, Oncken O, Käfer N, Schäfer F, Weiss B. Age and Provenance of the Sediments and the Detritus of the Northern Phyllite Zone (South Taunus). ZDGG_ALT. 1994;145(1):172–91. https://doi.org/10.1127/zdgg/145/1994/172.
Klügel T. Geometrie und Kinematik einer variszischen Plattengrenze: der Südrand des Rhenoherzynikums im Taunus. Hessisches Landesamt für Bodenforschung; 1997. ISBN: 3895318035.
Klumbach S. Petrophysical properties of geothermal reservoir rocks in the Upper Rhine Graben from surface outcrops [Masterthesis]: Albert-Ludwigs-Universität Freiburg; 2010.
Knaust D. Invertebrate trace fossils and ichnodiversity in shallow-marine carbonates of the German Middle Triassic (Muschelkalk). SEPM Special Publication. 2006;88:223–40.
Kock N, Kaltschmitt M. Geothermisch erschließbare Niedertemperaturwärmesenken in Deutschland—identifikation und Quantifizierung. Z Energiewirtsch. 2012;36(3):191–203. https://doi.org/10.1007/s12398-012-0079-z.
Kohl T, Signorelli S, Engelhardt I, Berthoud NA, Sellami S, Rybach L. Development of a regional geothermal resource atlas. J Geophys Eng. 2005;2(4):372–85. https://doi.org/10.1088/1742-2132/2/4/S11.
Koltzer N, Scheck-Wenderoth M, Bott J, Cacace M, Frick M, Sass I, et al. The effects of regional fluid flow on deep temperatures (Hesse, Germany). Energies. 2019;12(11):2081. https://doi.org/10.3390/en12112081.
Kossmat F. Gliederung des varistischen Gebirgsbaues. Abh Sächsischen Geol Landesamts. 1927;1:1–39.

Köster MH. Mikrofazies, Diagenese und Geochemie des Hauptrogensteins aus dem Pfirter Jura [PhD Thesis]: Freie Universität Berlin; 2010.
Kowalczyk G. Permokarbon des Sprendlinger Horstes und der westlichen Wetterau (Exkursion I am 20. April 2001). JBER_OBERRH. 2001;83:211–36. https://doi.org/10.1127/jmogv/83/2001/211.
Kraus E. 3D Modellierung des tiefengeothermischen Potentials und der Petrologie des westlichen Taunus, Rheinisches Schiefergebirge [Diplomathesis]: TU Darmstadt; 2009.
Krawczyk CM, McCann T, Cocks L, England R, McBride J, Wybraniec S. Caledonian tectonics. In: McCann T, editor. The Geology of Central Europe: Volume 1: Precambrian and Palaeozoic. London: Geological Society of London; 2008. p. 303–82.
Kreuzer H, Harre W. K/Ar-Altersbestimmungen an Hornblenden und Biotiten des Kristallinen Odenwalds. In: Amstutz GC, Meisl S, Nickel E, eds. Mineralien und Gesteine im Odenwald. Heidelberg; 1975. p. 70–78. https://hdl.handle.net/10013/epic.42772. Accessed 29 Aug 2022.
Krohe A. Structural evolution of intermediate-crustal rocks in a strike-slip and extensional setting (Variscan Odenwald, SW Germany): differential upward transport of metamorphic complexes and changing deformation mechanisms. Tectonophysics. 1992;205(4):357–86. https://doi.org/10.1016/0040-1951(92)90443-A.
Krohe A, Willner AP. IV.C.2 The Odenwald Crystalline Complex. In: Dallmeyer RD, Franke W, Weber K, editors. Pre-Permian Geology of Central and Eastern Europe. Berlin: Springer, Berlin Heidelberg; 1995. p. 182–5.
Kroner U, Mansy JL, Mazur S, Aleksandrowski P, Hann HP, Huckriede H. Variscan tectonics. In: McCann T, editor. The Geology of Central Europe: Volume 1: Precambrian and Palaeozoic. London: Geological Society of London; 2008. p. 599–664.
Kühne K. Das Fachinformationssystem Geophysik und seine Nutzung über das Internet. GIS. 2006;57:227–31.
Kushnir AR, Heap MJ, Baud P. Assessing the role of fractures on the permeability of the Permo-Triassic sandstones at the Soultz-sous-Forêts (France) geothermal site. Geothermics. 2018a;74:181–9. https://doi.org/10.1016/j.geothermics.2018.03.009.
Kushnir ARL, Heap MJ, Baud P, Gilg HA, Reuschlé T, Lerouge C, et al. Characterizing the physical properties of rocks from the Paleozoic to Permo-Triassic transition in the Upper Rhine Graben. Geotherm Energy. 2018b. https://doi.org/10.1186/s40517-018-0103-6.
Lacirignola M, Blanc I. Environmental analysis of practical design options for enhanced geothermal systems (EGS) through life-cycle assessment. Renew Energy. 2013;50:901–14. https://doi.org/10.1016/j.renene.2012.08.005.
Ladner F, Schanz U, Häring MO. Deep-Heat-Mining-Projekt Basel-Erste Erkenntnisse bei der Entwicklung eines Enhanced Geothermal System (EGS). Bull Für Angew Geol. 2008;13:41–54. https://doi.org/10.5169/seals-226675.
Lambert AD. Bestimmung der petrophysikalischen und felsmechanischen Kennwerte des Tromm-und Weschnitz-Plutons, Odenwald, Deutschland [Bachelorthesis]: TU Darmstadt; 2016.
Lardeaux JM, Schulmann K, Faure M, Janoušek V, Lexa O, Skrzypek E, et al. The Moldanubian Zone in the French Massif Central, Vosges/Schwarzwald and Bohemian Massif revisited: differences and similarities. Geol Soc Spec Publ. 2014;405(1):7–44. https://doi.org/10.1144/SP405.14.
Le Carlier de Veslud C, Bourgeois O, Diraison M, Ford M. 3D stratigraphic and structural synthesis of the Dannemarie basin (Upper Rhine Graben). Bull Soci Géol Fr. 2005;176(5):433–42. https://doi.org/10.2113/176.5.433.
Ledésert B, Berger G, Meunier A, Genter A, Bouchet A. Diagenetic-type reactions related to hydrothermal alteration in the Soultz-sous-Forêts granite. France Ejm. 1999;11(4):731–42. https://doi.org/10.1127/ejm/11/4/0731.
Ledésert B, Hebert R, Genter A, Bartier D, Clauer N, Grall C. Fractures, hydrothermal alterations and permeability in the Soultz Enhanced Geothermal System. CR Geosci. 2010;342(7–8):607–15. https://doi.org/10.1016/j.crte.2009.09.011.
Lehne RJ, Hoselmann C, Heggemann H, Budde H, Hoppe A. Geological 3D modelling in the densely populated metropolitan area Frankfurt/Rhine-Main. ZDGG. 2013. https://doi.org/10.1127/1860-1804/2013/0051.
Lepper J, Rambow D, Röhling H-G. Lithostratigraphy of the Buntsandstein in Germany. SDGG. 2014;69:69–149. https://doi.org/10.1127/sdgg/69/2014/69.
Les Landes AA, Guillon T, Peter-Borie M, Blaisonneau A, Rachez X, Gentier S. Locating geothermal resources: insights from 3D stress and flow models at the upper Rhine graben scale. Geofluids. 2019;2019:1–24. https://doi.org/10.1155/2019/8494539.
Leu W, Keller B, Matter A, Schärli U, Rybach L. Geothermische Eigenschaften Schweizer Molassebecken (Tiefenbereich 0–500m). Bern: Bundesamt für Energie; 1999.
Leydecker G. Erdbebenkatalog für Deutschland mit Randgebieten für die Jahre 800 bis 2008. Schweizerbart; 2011. ISBN 978-3-510-95989-1.
LGRB. Querschnitt durch den Oberrheingraben auf Höhe des Kaiserstuhls. 2022. https://lgrbwissen.lgrb-bw.de/geotourismus/aufschluesse/oberrhein-hochrheingebiet/vulkanite-am-kaiserstuhl. Accessed 3 Jun 2022.
Lippolt HJ, Todt WA, Horn P. Apparent potassium-argon ages of Lower Tertiary Rhine Graben volcanics. In: Illies JH, Fuchs K, editors. Approaches to Taphrogenesis. Stuttgart: Schweizerbart; 1974. p. 213–21.
Lippolt HJ, Kirsch H, Plein E. Karbonische und permische Vulkanite aus dem Untergrund des nördlichen Oberrheingrabens: Art, Altersbestimmung und Konsequenz. JBER_OBERRH. 1990;72:227–42. https://doi.org/10.1127/jmogv/72/1990/227.
Loeschke J, Güldenpfennig M, Hann HP, Sawatzki G. The Zone of Badenweiler-Lenzkirch (Black Forest): A Variscan suture zone. ZDGG_ALT. 1998;149(2):197–212. https://doi.org/10.1127/zdgg/149/1998/197.
Loges A, Wagner T, Kirnbauer T, Göb S, Bau M, Berner Z, Markl G. Source and origin of active and fossil thermal spring systems, northern Upper Rhine Graben, Germany. Appl Geochem. 2012;27(6):1153–69. https://doi.org/10.1016/j.apgeochem.2012.02.024.
Löschan G, Emmerich K, Reinhold C, Reinecker J. Clay mineralogy of Tertiary formations in the northern Upper Rhine Graben – New insights from geothermal and hydrocarbon exploration. ZDGG. 2017;168(2):233–44. https://doi.org/10.1127/zdgg/2017/0083.
Mack C. Geothermische Untersuchungen in Calw [Diplomathesis]: TU Darmstadt; 2007.

Madritsch H, Kounov A, Schmid SM, Fabbri O. Multiple fault reactivations within the intra-continental Rhine-Bresse Transfer Zone (La Serre Horst, eastern France). Tectonophysics. 2009;471(3–4):297–318. https://doi.org/10.1016/j.tecto.2009.02.044.
Maire R. Investigation of thermo-physical and mechanical parameters of crystalline geothermal reservoir rocks of the Upper Rhine Graben (Germany) [Masterthesis]: LaSalle Beauvais; TU Darmstadt; 2014.
Majer EL, Baria R, Stark M, Oates S, Bommer J, Smith B, Asanuma H. Induced seismicity associated with Enhanced Geothermal Systems. Geothermics. 2007;36(3):185–222. https://doi.org/10.1016/j.geothermics.2007.03.003.
Mann JC. Uncertainty in geology. Computers in geology—25 years of progress. Oxford: Oxford University Press; 1993. p. 241–54.
Manning CE, Ingebritsen SE. Permeability of the continental crust: implications of geothermal data and metamorphic systems. Rev Geophys. 1999;37(1):127–50. https://doi.org/10.1029/1998RG900002.
Marell D. Das Rotliegende zwischen Odenwald und Taunus. Hessisches Landesamt für Bodenforschung; 1989.
Martin U. The Early Palaeozoic Break-up of Northern Gondwana: Sedimentology, Physical Volcanology and Geochemistry of a Submarine Volcanic Complex in the Bavarian Facies Association, Saxothuringian Basin, Germany. Gondwana Res. 2003;6(4):839–58. https://doi.org/10.1016/S1342-937X(05)71029-7.
Massonne HJ. Metamorphic evolution. In: Dallmeyer RD, Franke W, Weber K, editors. Pre-Permian geology of Central and Eastern Europe. Berlin: Springer, Berlin Heidelberg; 1995. p. 132–7.
Matte P. The Variscan collage and orogeny (480–290 Ma) and the tectonic definition of the Armorica microplate: a review. Terra Nova. 2003;13(2):122–8. https://doi.org/10.1046/j.1365-3121.2001.00327.x.
McCann T, Skompski S, Poty E, Dusar M, Vozarova A, Schneider J, et al. Carboniferous. In: McCann T, editor., et al., The geology of central Europe: Volume 1: Precambrian and Palaeozoic. London: Geological Society of London; 2008. p. 410–530.
McCann T, editor. The Geology of Central Europe: Volume 1: Precambrian and Palaeozoic. London: Geological Society of London; 2008.
McKerrow WS, MacNiocaill C, Dewey JF. The Caledonian Orogeny redefined. J Geol Soc. 2000;157(6):1149–54.
McKie T. Paleogeographic evolution of latest Permian and Triassic salt basins in Northwest Europe. In: Soto JI, Flinch J, Tari G, editors. Permo-triassic salt provinces of Europe, North Africa and the atlantic margins: tectonics and hydrocarbon potential. Saint Louis: Elsevier Science; 2017. p. 159–73 (**10.1016/B978-0-12-809417-4.00008-2**).
Mégel T, Rybach L. Production Capacity and Systainability of Geothermal Doublets. In: World Geothermal Congress 2000; 28. May, 10. June; Kyushu - Tohoku, Japan; 2000.
Meghraoui M, Delouis B, Ferry M, Giardini D, Huggenberger P, Spottke I, Granet M. Active normal faulting in the upper Rhine graben and paleoseismic identification of the 1356 Basel earthquake. Science. 2001;293(5537):2070–3. https://doi.org/10.1126/science.1010618.
Meier L, Eisbacher GH. Crustal kinematics and deep structure of the northern Rhine Graben, Germany. Tectonics. 1991;10(3):621–30. https://doi.org/10.1029/91TC00142.
Meisel M. Petrographie, Fazies und Diagenese des Buntsandsteinreservoirs am Oberrhein [Diplomathesis]: Universität Jena; 2009.
Meisl S. III.C.3 Igneous Activity. In: Dallmeyer RD, Franke W, Weber K, editors. Pre-Permian geology of Central and Eastern Europe. Berlin: Springer, Berlin Heidelberg; 1995. p. 118–31.
Meixner J, Schill E, Gaucher E, Kohl T. Inferring the in situ stress regime in deep sediments: an example from the Bruchsal geothermal site. Geotherm Energy. 2014. https://doi.org/10.1186/s40517-014-0007-z.
Meixner J, Schill E, Grimmer JC, Gaucher E, Kohl T, Klingler P. Structural control of geothermal reservoirs in extensional tectonic settings: an example from the Upper Rhine Graben. J Struct Geol. 2016;82:1–15. https://doi.org/10.1016/j.jsg.2015.11.003.
Meller C, Ledésert B. Is there a link between mineralogy, petrophysics, and the hydraulic and seismic behaviors of the Soultz-sous-Forêts granite during stimulation? A review and reinterpretation of petro-hydromechanical data toward a better understanding of induced seismicity. J Geophys Res. 2017;122(12):9755–74. https://doi.org/10.1002/2017JB014648.
Meller C, Schill E, Bremer J, Kolditz O, Bleicher A, Benighaus C, et al. Acceptability of geothermal installations: a geoethical concept for GeoLaB. Geothermics. 2018;73:133–45. https://doi.org/10.1016/j.geothermics.2017.07.008.
Michon L, Merle O. Crustal structures of the Rhinegraben and the Massif Central grabens: an experimental approach. Tectonics. 2000;19(5):896–904. https://doi.org/10.1029/2000TC900015.
Moeck IS. Catalog of geothermal play types based on geologic controls. Renew Sustain Energy Rev. 2014;37:867–82. https://doi.org/10.1016/j.rser.2014.05.032.
Molenaar N, Felder M, Bär K, Götz AE. What classic greywacke (litharenite) can reveal about feldspar diagenesis: an example from Permian Rotliegend sandstone in Hessen, Germany. Sed Geol. 2015;326:79–93. https://doi.org/10.1016/j.sedgeo.2015.07.002.
Molzahn M, Anthes G, Reischmann T. Single zircon Pb/Pb age geochronology and isotope systematics of the Rhenohercynian basement. Terra Nostra. 1998;98(1):67–8.
Morris A, Ferrill DA, Brent HD. Slip-tendency analysis and fault reactivation. Geology. 1996;24(3):275. https://doi.org/10.1130/0091-7613(1996)024%3c0275:STAAFR%3e2.3.CO;2.
Morrow CA, Shi LQ, Byerlee JD. Permeability of fault gouge under confining pressure and shear stress. J Geophys Res. 1984;89(B5):3193–200. https://doi.org/10.1029/JB089iB05p03193.
Mouchot J, Genter A, Cuenot N, Scheiber J, Seibel O, Bosia C, Ravier G. First Year of Operation from EGS geothermal Plants in Alsace, France: Scaling Issues. In: Stanford University, ed. 43rd Workshop on Geothermal Reservoir Engineering; 12.-14. February; Stanford, California; 2018.
Müller H. Das Permokarbon im nördlichen Oberrheingraben: Paläogeographische und strukturelle Entwicklung des permokarbonen Saar-Nahe-Beckens im nördlichen Oberrheingraben. Wiesbaden: Hess. Landesamt für Bodenforschung; 1996.
Müller D. Investigation on the spatial variability of petrophysical parameters of sandstone (Buntsandstein) in the Spessart, Germany [Bachelorthesis]: TU Darmstadt; 2014.

Nance RD, Gutiérrez-Alonso G, Keppie JD, Linnemann U, Murphy JB, Quesada C, et al. Evolution of the Rheic Ocean. Gondwana Res. 2010;17(2–3):194–222. https://doi.org/10.1016/j.gr.2009.08.001.
Nehler M. Geothermische Untersuchungen des Zechsteins im Raum Sontra [Bachelorthesis]: TU Darmstadt; 2011.
Newman GA, Gasperikova E, Hoversten GM, Wannamaker PE. Three-dimensional magnetotelluric characterization of the Coso geothermal field. Geothermics. 2008;37(4):369–99. https://doi.org/10.1016/j.geothermics.2008.02.006.
Nickel E. Geologische Position und Petrogenese des kristallinen Odenwaldes. In: Amstutz GC, Meisl S, Nickel E, eds. Mineralien und Gesteine im Odenwald. Heidelberg; 1975. p. 1–25.
Okrusch M. Metamorphic evolution. In: Dallmeyer RD, Franke W, Weber K, editors. Pre-Permian geology of Central and Eastern Europe. Berlin: Springer, Berlin Heidelberg; 1995. p. 201–13.
Okrusch M, Schubert W, Nasir S. IV.D igneous activity (Pre- to Early Variscan Magmatism). In: Dallmeyer RD, Franke W, Weber K, editors. Pre-Permian geology of Central and Eastern Europe. Berlin: Springer, Berlin Heidelberg; 1995. p. 190–200.
Oncken O. III.B.2 Structure. In: Dallmeyer RD, Franke W, Weber K, editors. Pre-Permian geology of Central and Eastern Europe. Berlin: Springer, Berlin Heidelberg; 1995. p. 50–8.
Oncken O. Transformation of a magmatic arc and an orogenic root during oblique collision and it's consequences for the evolution of the European Variscides (Mid-German Crystalline Rise). Geol Rundsch. 1997;86(1):2–20. https://doi.org/10.1007/s005310050118.
Oncken O, Massonne HJ, Schwab M. III.B.4 metamorphic evolution. In: Dallmeyer RD, Franke W, Weber K, editors. Pre-Permian Geology of Central and Eastern Europe. Berlin: Springer, Berlin Heidelberg; 1995. p. 82–6.
Oncken O, von Winterfeld C, Dittmar U. Accretion of a rifted passive margin: the Late Paleozoic Rhenohercynian fold and thrust belt (Middle European Variscides). Tectonics. 1999;18(1):75–91. https://doi.org/10.1029/98TC02763.
Orendt R. Geothermisches Potenzial im Erlaubnisfeld Südtaunus [Diplomathesis]: TU Darmstadt; 2014.
Parkhurst DL, Appelo CA. User's guide to PHREEQC (Version 2): a computer program for speciation, batch-reaction, one-dimensional transport, and inverse geochemical calculations. WRIR. 1999;99(4259):312. https://doi.org/10.3133/wri994259.
Paschen H, Ortel D, Grünwald R. Möglichkeiten geothermischer Stromerzeugung in Deutschland: Sachstandsbericht: Büro für Technikfolgen-Abschätzung beim Deutschen Bundestag (TAB); 2003.
Paul J. Untere Buntsandstein des Germanischen Beckens. Int J Earth Sci. 1982;71(3):795–811. https://doi.org/10.1007/BF01821104.
Paul J, Wemmer K, Ahrendt H. Provenance of siliciclastic sediments (Permian to Jurassic) in the Central European Basin. ZDGG. 2008;159(4):641–50. https://doi.org/10.1127/1860-1804/2008/0159-0641.
Pauwels H, Fouillac C, Fouillac A-M. Chemistry and isotopes of deep geothermal saline fluids in the Upper Rhine Graben: Origin of compounds and water-rock interactions. Geochim Cosmochim Acta. 1993;57(12):2737–49. https://doi.org/10.1016/0016-7037(93)90387-C.
Pei L. Analysis of initiation and propagation of hydraulically induced fracture [Masterthesis]: TU Darmstadt; 2009.
Perner MJ. Evolution of Palaeoenvironment, Kerogen Composition and Thermal History in the Cenozoic of the Northern Upper Rhine Graben, SW-Germany [PhD thesis]: Universität Heidelberg; 2018.
Person M, Garven G. Hydrologie constraints on petroleum generation within continental rift basins: theory and application to the Rhine graben. Bulletin. 1992;76(4):468–88. https://doi.org/10.1306/BDFF883A-1718-11D7-8645000102C1865D.
Pflug R. Bau und Entwicklung des Oberrheingrabens. Darmstadt: Wissenschaftl; 1982.
Pienkowski G, Schudack ME, Bosak P, Enay R, Feldman-Olszewska A, Golonka J, et al. Jurassic. In: McCann T, editor., et al., The geology of central Europe: volume 2: Mesozoic and Cenozoic. London: Geological Society of London; 2008. p. 823–922.
Plenefisch T, Bonjer K-P. The stress field in the Rhine Graben area inferred from earthquake focal mechanisms and estimation of frictional parameters. Tectonophysics. 1997;275(1–3):71–97. https://doi.org/10.1016/S0040-1951(97)00016-4.
Portier S, Vuataz F-D, Nami P, Sanjuan B, Gérard A. Chemical stimulation techniques for geothermal wells: experiments on the three-well EGS system at Soultz-sous-Forêts. France. Geothermics. 2009;38(4):349–59. https://doi.org/10.1016/j.geothermics.2009.07.001.
Pribnow D, Schellschmidt R. Thermal tracking of upper crustal fluid flow in the Rhine graben. Geophys Res Lett. 2000;27(13):1957–60. https://doi.org/10.1029/2000GL008494.
Prodehl C, Mueller S, Haak V. The European Cenozoic rift system. In: Olsen KH, editor. Continental rifts: evolution, structure, tectonics. Amsterdam: Elsevier; 1995. p. 133–212 (**10.1016/S0419-0254(06)80012-1**).
Prodehl C, St. Mueller, Glahn A, Gutscher M, Haak V. Lithospheric cross sections of the European Cenozoic rift system. Tectonophysics. 1992;208(1–3):113–38. https://doi.org/10.1016/0040-1951(92)9033-8.
Rathnaweera TD, Wu W, Ji Y, Gamage RP. Understanding injection-induced seismicity in enhanced geothermal systems: From the coupled thermo-hydro-mechanical-chemical process to anthropogenic earthquake prediction. Earth Sci Rev. 2020;205: 103182. https://doi.org/10.1016/j.earscirev.2020.103182.
Reinecker J, Bauer JF, Bechstädt T, Drews T, Filomena M, Grobe R, et al. Verbundprojekt AuGE: Aufschlussanalogstudien und ihre Anwendbarkeit in der geothermischen Exploration—Entwicklung von Methoden zur Ermittlung von Permeabilitäten und Transmissivitäten aus Reservoir-Informationen des Oberrheingrabens. AUGE—Outcrop analogue studies in geothermal exploration: Schlussbericht Teilprojekt A; 2015.
Reinecker J, Hochschild T, Kraml M, Löschan G, Kreuter H. Experiences and challenges in geothermal exploration in the Upper Rhine Graben. In: European Geothermal Congress; 11.-14. June; Den Haag; 2019.
Reinhold C, Schwarz M, Bruss D, Heesbeen B, Perner M, Suana M. The Northern Upper Rhine Graben: re-dawn of a mature petroleum province? Swiss Bull Angew Geol. 2016;21(2):35–56. https://doi.org/10.5169/seals-658196.
Reischmann T, Anthes G. Geochronology of the mid-German crystalline rise west of the River Rhine. Geol Rundsch. 1996;85(4):761–74. https://doi.org/10.1007/BF02440109.
Reischmann T, Anthes G, Jaeckel P, Altenberger U. Age and origin of the Böllsteiner Odenwald. Mineral Petrol. 2001;72(1–3):29–44. https://doi.org/10.1007/s007100170025.

Reiter K, Heidbach O, Müller B, Reinecker J, Röckl T, Reiter K, et al. Stress Map Germany 2016 2016. https://doi.org/10.5880/WSM.Germany2016_en.
Reith S, Kölbel T, Schlagermann P, Pellizzone A, Allansdottir A. Public acceptance of geothermal electricity production: GEOELEC. EnBW Energie Baden-Württemberg AG, University of Milan & University of Sienna. 2013. http://www.geoelec.eu/wp-content/uploads/2014/03/D-4.4-GEOELEC-report-on-public-acceptance.pdf. Accessed 29 Aug 2022.
Rettenmaier D, Gaucher E, Ghergut J, Huttenloch P, Kohl T, Meixner J, et al. LOGRO—Langzeitbetrieb und Optimierung eines Geothermiekraftwerks in einem geklüftetporösen Reservoir im Oberrheingraben: Schlussbericht; 2013. https://www.tib.eu/de/suchen/id/TIBKAT:77165135X/Langzeitbetrieb-und-Optimierung-eines-Geothermiekraftwerks?cHash=9ba6621535f847902833cef0522ee635. Accessed 29 Aug 2022.
Ritter JRR, Wagner M, Bonjer K-P, Schmidt B. The 2005 Heidelberg and Speyer earthquakes and their relationship to active tectonics in the central Upper Rhine Graben. Int J Earth Sci. 2009;98(3):697–705. https://doi.org/10.1007/s00531-007-0284-x.
Robardet M. The Armorica 'microplate': fact or fiction? Critical review of the concept and contradictory palaeobiogeographical data. Palaeogeogr Palaeoclimatol Palaeoecol. 2003;195(1–2):125–48. https://doi.org/10.1016/S0031-0182(03)00305-5.
Röhling H-G, Lepper J, Diehl M, Dittrich D, Freudenberger W, Friedlein V, et al. Der Buntsandstein in der Stratigraphischen Tabelle von Deutschland 2016. ZDGG. 2018;169(2):151–80. https://doi.org/10.1127/zdgg/2018/0132.
Rosenbaum G, Lister GS, Duboz C. Relative motions of Africa, Iberia and Europe during Alpine orogeny. Tectonophysics. 2002;359(1–2):117–29. https://doi.org/10.1016/S0040-1951(02)00442-0.
Rothe JP, Sauer K. The Rhinegraben Progress Report 1967. Geologisches Landesamt Baden-Württemberg; 1967.
Rotstein Y, Edel JB, Gabriel G, Boulanger D, Schaming M, Munschy M. Insight into the structure of the Upper Rhine Graben and its basement from a new compilation of Bouguer Gravity. Tectonophysics. 2006;425(1–4):55–70. https://doi.org/10.1016/j.tecto.2006.07.002.
Rousse S, Duringer P, Stapf KRG. An exceptional rocky shore preserved during Oligocene (Late Rupelian) transgression in the Upper Rhine Graben (Mainz Basin, Germany). Geol J. 2012;47(4):388–408. https://doi.org/10.1002/gj.1349.
Rühaak W. 3-D interpolation of subsurface temperature data with measurement error using kriging. Environ Earth Sci. 2015;73(4):1893–900. https://doi.org/10.1007/s12665-014-3554-5.
Rühaak W, Bär K, Sass I. Combining numerical modeling with geostatistical interpolation for an improved reservoir exploration. Energy Proc. 2014;59:315–22. https://doi.org/10.1016/j.egypro.2014.10.383.
Rummel F, Baumgärtner J. Hydraulic fracturing stress measurements in the GPK1 borehole, Soultz sous Forêts. Geotherm Sci Technol. 1991;3(1–4):119–48.
Rupf I, Nitsch E. Das geologische Landesmodell von Baden-Württemberg: Datengrundlagen technische Umsetzung und erste geologische Ergebnisse. Landesamt für Geologie Rohstoffe und Bergbau Baden-Württemberg; 2008. https://produkte.lgrb-bw.de/docPool/c623_data.pdf. Accessed 29 Aug 2022.
Saevarsdottir G, Tao P, Stefansson H, Harvey W. Potential use of geothermal energy sources for the production of lithium-ion batteries. Renew Energy. 2014;61:17–22. https://doi.org/10.1016/j.renene.2012.04.028.
Sandkühler L. Untersuchung des Einflusses der Wassersättigung auf die thermophysikalischen Eigenschaften von Kernproben der Bohrungen Aura und Rosenthal [Bachelorthesis]: TU Darmstadt; 2015.
Sanjuan B, Millot R, Innocent C, Dezayes C, Scheiber J, Brach M. Major geochemical characteristics of geothermal brines from the Upper Rhine Graben granitic basement with constraints on temperature and circulation. Chem Geol. 2016;428:27–47. https://doi.org/10.1016/j.chemgeo.2016.02.021.
Sanjuan B, Négrel G, Le Lous M, Poulmarch E, Gal F, Damy PC. Main Geochemical Characteristics of the Deep Geothermal Brine at Vendenheim (Alsace, France) with Constraints on Temperature and Fluid Circulation. In: World Geothermal Congress 2020; April - October 2021; Reykjavik, Iceland; 2021.
Sass I, Hoppe A, Arndt D, Bär K. Forschungs-und Entwicklungsprojekt 3D Modell der Geothermischen Tiefenpotenziale von Hessen. Abschlussbericht: TU Darmstadt; 2011.
Sauer K, Munck F. Geothermische Synthese des Oberrheingrabens (Bestandsaufnahme): Geologisches Landesamt Baden-Württemberg; 1979.
Sauer K. Erdöl am Oberrhein. Ein Heidelberger Kolloquium. Abhandlungen des Geologischen Landesamtes Baden-Württemberg; 1962;4:1–136.
Sausse J, Genter A. Types of permeable fractures in granite. Geol Soc Spec Publ. 2005;240(1):1–14.
Sausse J, Dezayes C, Dorbath L, Genter A, Place J. 3D model of fracture zones at Soultz-sous-Forêts based on geological data, image logs, induced microseismicity and vertical seismic profiles. CR Geosci. 2010;342(7–8):531–45. https://doi.org/10.1016/j.crte.2010.01.011.
Schäfer A. Variscan molasse in the Saar-Nahe Basin (W-Germany), Upper Carboniferous and Lower Permian. Int J Earth Sci. 1989;78(2):499–524. https://doi.org/10.1007/BF01776188.
Schäfer A. Sedimentologisch-numerisch begrundeter stratigraphischer Standard fur das Permo-Karbon des Saar-Nahe-Beckens. Cour Forsch-Inst Senckenberg. 2005;254:369–94.
Schäfer A. Tectonics and sedimentation in the continental strike-slip Saar-Nahe Basin (Carboniferous-Permian, West Germany). ZDGG. 2011;162(2):127–55. https://doi.org/10.1127/1860-1804/2011/0162-0127.
Schäfer A, Korsch RJ. Formation and sediment fill of the Saar-Nahe Basin (Permo-Carboniferous, Germany). Zeitschrift Deutschen Geol Gesellschaft. 1998;149(2):233–69. https://doi.org/10.1127/zdgg/149/1998/233.
Schäffer R, Bär K, Sass I. Multimethod exploration of the hydrothermal reservoir in Bad Soden-Salmünster, Germany. ZDGG. 2018;169(3):311–33. https://doi.org/10.1127/zdgg/2018/0147.
Schälicke W. Die Otzberg-Zone. In: Amstutz GC, Meisl S, Nickel E, eds. Mineralien und Gesteine im Odenwald. Heidelberg; 1975. p. 47–59.
Schaltegger U. U–Pb geochronology of the Southern Black Forest Batholith (Central Variscan Belt): timing of exhumation and granite emplacement. Int J Earth Sci. 2000;88(4):814–28. https://doi.org/10.1007/s005310050308.
Schärli U, Kohl T. Archivierung und Kompilation geothermischer Daten der Schweiz und angrenzender Gebiete. Schweizerische Geophysikalische Kommission; 2002.

Scheck-Wenderoth M, Krzywiec P, Zühlke R, Maystrenko Y, Froitzheim N. Permian to Cretaceous tectonics of Central Europe. In: McCann T, editor. The geology of central Europe: volume 1: Precambrian and Palaeozoic. London: Geological Society of London; 2008. p. 999–1030.
Schellschmidt R, Clauser C. The thermal regime of the Upper Rhine Graben and the anomaly at Soultz. Z Angew Geol. 1996;42(1):40–4.
Schill E, Meixner J, Meller C, Grimm M, Grimmer JC, Stober I, Kohl T. Criteria and geological setting for the generic geothermal underground research laboratory, GEOLAB. Geotherm Energy. 2016. https://doi.org/10.1186/s40517-016-0049-5.
Schill E, Genter A, Cuenot N, Kohl T. Hydraulic performance history at the Soultz EGS reservoirs from stimulation and long-term circulation tests. Geothermics. 2017;70:110–24. https://doi.org/10.1016/j.geothermics.2017.06.003.
Schindler M, Baumgärtner J, Gandy T, Hauffe P, Hettkamp T, Menzel H, et al. Successful Hydraulic Stimulation Techniques for Electric Power Production in the Upper Rhine Graben, Central Europe. In: World Geothermal Congress 2010; 25–29 April; Bali, Indonesia; 2010.
Schintgen TV. The Geothermal Potential of Luxembourg: Geological and thermal exploration for deep geothermal reservoirs in Luxembourg and the surroundings [PhD thesis]: Universität Potsdam; 2016.
Schmidt RB, Bucher K, Drüppel K, Stober I. Experimental interaction of hydrothermal Na-Cl solution with fracture surfaces of geothermal reservoir sandstone of the Upper Rhine Graben. Appl Geochem. 2017;81:36–52. https://doi.org/10.1016/j.apgeochem.2017.03.010.
Schmidt RB, Bucher K, Stober I. Experiments on granite alteration under geothermal reservoir conditions and the initiation of fracture evolution. EJM. 2018;30(5):899–916. https://doi.org/10.1127/ejm/2018/0030-2771.
Schmidt RB, Göttlicher J, Stober I. Experiments on sandstone alteration under geothermal reservoir conditions and the formation of zeolites. EJM. 2019;31(5–6):929–44. https://doi.org/10.1127/ejm/2019/0031-2870.
Schmittbuhl J, Lambotte S, Lengliné O, Grunberg M, Jund H, Vergne J, et al. Induced and triggered seismicity below the city of Strasbourg, France from November 2019 to January 2021. Comptes Rendus Géosci. 2021;353(S1):1–24. https://doi.org/10.5802/crgeos.71.
Scholze F, Wang X, Kirscher U, Kraft J, Schneider JW, Götz AE, et al. A multistratigraphic approach to pinpoint the Permian-Triassic boundary in continental deposits: the Zechstein-Lower Buntsandstein transition in Germany. Global Planet Change. 2017;152:129–51. https://doi.org/10.1016/j.gloplacha.2017.03.004.
Schöpflin S. Determination of Rockmechanical Properties of the Palatinate Forest's Buntsandstein [Master thesis]: Albert-Ludwigs-Universität Freiburg; 2013.
Schröder B. Entwicklung des Sedimentbeckens und Stratigraphie der klassischen Germanischen Trias. Int J Earth Sci. 1982;71(3):783–94. https://doi.org/10.1007/BF01821103.
Schubert KO. Geothermische Untersuchungen des Buntsandsteins des Odenwaldes [Bachelorthesis]: TU Darmstadt; Goethe Universitaet Frankfurt am Main; 2011.
Schulz R, Schellschmidt R. Das Temperaturfeld im südlichen Oberrheingraben. Geol Jb E. 1991;48:153–65.
Schumacher ME. Upper Rhine Graben: role of preexisting structures during rift evolution. Tectonics. 2002. https://doi.org/10.1029/2001TC900022.
Schumann A. GIS basierte Erdwaermepotenzialkarte Spielberg und Wart [Diplomathesis]: TU Darmstadt; 2008.
Schwarz H-U, editor. Sedimentary structures and facies analysis of shallow marine carbonates. Stuttgart: Schweizerbart; 1975.
Schwarz M, Henk A. Evolution and structure of the Upper Rhine Graben: insights from three-dimensional thermomechanical modelling. Int J Earth Sci. 2005;94(4):732–50. https://doi.org/10.1007/s00531-004-0451-2.
Schwarz J, Abrahamczyk L, Amstein S, Kaufmann C, Langhammer T. Das Waldkirch-Erdbeben (Baden-Württemberg) vom 5. Dezember 2004. Bautechnik. 2006;83(3):202–8. https://doi.org/10.1002/bate.200610020.
Schwarz M. Evolution und Struktur des Oberrheingrabens - quantitative Einblicke mit Hilfe dreidimen-sionaler thermomechanischer Modellrechnungen [PhD thesis]. Freiburg i. Br.: University of Freiburg; 2006.
Scibek J. Multidisciplinary database of permeability of fault zones and surrounding protolith rocks at world-wide sites. Sci Data. 2020;7(1):95. https://doi.org/10.1038/s41597-020-0435-5.
Signorelli S, Kohl T. Technischer Bericht 08–03: Vorschlag geologischer Standortgebiete für das SMA- und das HAA-Lager: Nagra; 2008.
Sissingh W. Comparative Tertiary stratigraphy of the Rhine Graben, Bresse Graben and Molasse Basin: correlation of Alpine foreland events. Tectonophysics. 1998;300(1–4):249–84. https://doi.org/10.1016/S0040-1951(98)00243-1.
Skrzypek E, Schulmann K, Edel JB. Palaeozoic evolution of the Variscan Vosges Mountains. Geol Soc Spec Publ. 2014;405(1):45–75. https://doi.org/10.1144/SP405.8.
Smith DB. Rapid marine transgressions and regressions of the Upper Permian Zechstein Sea. J Geol Soc. 1979;136(2):155–6. https://doi.org/10.1144/gsjgs.136.2.0155.
Spottke I, Zechner E, Huggenberger P. The southeastern border of the Upper Rhine Graben: a 3D geological model and its importance for tectonics and groundwater flow. Int J Earth Sci. 2005;94(4):580–93. https://doi.org/10.1007/s00531-005-0501-4.
Stapf KRG. Einführung lithostratigraphischer Formationsnamen im Rotliegend des Saar-Nahe-Beckens (SW-Deutschland). Mitteilungen Der POLLICHIA. 1990;77:111–24.
Stein E. The geology of the Odenwald Crystalline Complex. Mineral Petrol. 2001;72(1–3):7–28. https://doi.org/10.1007/s007100170024.
Stets J, Schäfer A. The Lower Devonian Rhenohercynian Rift - 20 Ma of sedimentation and tectonics (Rhenish Massif, W-Germany). ZDGG. 2011;162(2):93–115. https://doi.org/10.1127/1860-1804/2011/0162-0093.
Stober I. Researchers study conductivity of crystalline rock in proposed radioactive waste site. Eos Trans AGU. 1996;77(10):93. https://doi.org/10.1029/96EO00062.
Stober I, Bucher K. Fluid sinks within the earth's crust. Geofluids. 2004;4(2):143–51. https://doi.org/10.1111/j.1468-8115.2004.00078.x.

Stober I, Bucher K. Hydraulic properties of the crystalline basement. Hydrogeol J. 2007;15(2):213–24. https://doi.org/10.1007/s10040-006-0094-4.
Stober I, Bucher K. Hydraulic and hydrochemical properties of deep sedimentary reservoirs of the Upper Rhine Graben, Europe. Geofluids. 2015;15(3):464–82. https://doi.org/10.1111/gfl.12122.
Stober I, Jodocy M. Characteristics of geothermal reservoirs in the Upper Rhine Graben of Baden-Württemberg and France. Grundwasser. 2009;14(2):127–37.
Stober I, Richter A, Brost E, Bucher K. The Ohlsbach plume—discharge of deep saline water from the crystalline basement of the Black Forest, Germany. Hydrogeol J. 1999;7(3):273–83. https://doi.org/10.1007/s100400050201.
Stober I, Ladner F, Hofer M, Bucher K. The deep Basel-1 geothermal well: an attempt assessing the predrilling hydraulic and hydrochemical conditions in the basement of the Upper Rhine Graben. Swiss J Geosci. 2022. https://doi.org/10.1186/s00015-021-00403-8.
Stollhofen H. Vulkaniklastika und Siliziklastika des basalen Oberrotliegend im Saar-Nahe-Becken (SW-Deutschland). Terminologie Ablagerungsprozesse Mainzer Geowissenschaftliche Mitteilungen. 1994;23:95–138.
Stollhofen H. Facies architecture variations and seismogenic structures in the Carboniferous-Permian Saar–Nahe Basin (SW Germany): evidence for extension-related transfer fault activity. Sed Geol. 1998;119(1–2):47–83. https://doi.org/10.1016/S0037-0738(98)00040-2.
Stollhofen H, Stanistreet IG. Interaction between bimodal volcanism, fluvial sedimentation and basin development in the Permo-Carboniferous Saar-Nahe Basin (south-west Germany). Basin Res. 1994;6(4):245–67. https://doi.org/10.1111/j.1365-2117.1994.tb00088.x.
Straub EW. Die Erdöl- und Erdgaslagerstätten in Hessen und Rheinhessen. Abh Geol Landesam Baden-Württem. 1962;4:123–36.
Stricker K, Grimmer JC, Egert R, Bremer J, Korzani MG, Schill E, Kohl T. The potential of depleted oil reservoirs for high-temperature storage systems. Energies. 2020;13(24):6510. https://doi.org/10.3390/en13246510.
Suess FE. Intrusion-und Wandertektonik im variszischen Grundgebirge. Berlin: Gebr. Bornträger; 1926.
Surma F, Geraud Y. Porosity and Thermal Conductivity of the Soultz-sous-Forêts Granite. In: Kümpel H-J, editor. Thermo-hydro-mechanical coupling in fractured rock. Basel: Birkhäuser; 2003. p. 1125–36.
Surma F. Determination de la porosite des zones endommagees autour des failles et rle de l'etat du materiau sur les proprietes d'echange fluides-roches: mineralogie, structures de porosite, caracteristiques mecaniques [PhD thesis]. Strasbourg, France: Universite Louis Pasteu; 2003.
Szulc J. Middle Triassic evolution of the northern Peri-Tethys area as influenced by early opening of the Tethys Ocean. Ann Soc Geol Pol. 2000;70(1):1–48.
Teichmüller M. Zur geothermischen Geschichte des Oberrhein-Grabens. Zusammenfassung und Auswertung eines Symposiums. 1979.
Teza D, Menzel H, Baumgärtner J. Multihorizontansatz zur Erschließung ökonomisch relevanter Fließraten am Beispiel des Geothermieprojektes Landau: Schlussbericht; 2008.
Tischendorf G, Förster H-J, Frischbutter A, Kramer W, Schmidt W, Werner CD. Igneous activity. In: Dallmeyer RD, Franke W, Weber K, editors. Pre-Permian geology of central and eastern Europe. Berlin: Springer, Berlin Heidelberg; 1995. p. 249–59.
Tóth J. Gravity-induced cross-formational flow of formation fluids, red earth region, Alberta, Canada: Analysis, patterns, and evolution. Water Resour Res. 1978;14(5):805–43. https://doi.org/10.1029/WR014i005p00805.
United Nations, editor. Paris Agreement; 2015.
Valeton I. Petrographie des süddeutschen Hauptbuntsandsteins. Heidelberger Beitr Mineral Petrogr. 1953;3(5):335–79.
Valley B, Evans KF. Stress orientation to 5 km depth in the basement below Basel (Switzerland) from borehole failure analysis. Swiss J Geosci. 2009. https://doi.org/10.1007/s00015-009-1335-z.
Valley B, Evans KF. Stress magnitudes in the Basel enhanced geothermal system. Int J Rock Mech Min Sci. 2019;118:1–20. https://doi.org/10.1016/j.ijrmms.2019.03.008.
Valley BC. The relation between natural fracturing and stress heterogeneities in deep-seated crystalline rocks at Soultz-sous-Forêts (France) [PhD Thesis]: ETH Zurich; 2007.
van der Vaart J, Bär K, Frey M, Reinecker J, Sass I. Quantifying model uncertainty of a geothermal 3D model of the Cenozoic deposits in the northern Upper Rhine Graben, Germany. ZDGG. 2021. https://doi.org/10.1127/zdgg/2021/0286.
van Horn A, Amaya A, Higgins B, Muir J, Scherer J, Pilko R, Ross M. New opportunities and applications for closed-loop geothermal energy systems. GRC Transact. 2020;44:1123–43.
Vecsei A, Duringer P. Sequence stratigraphy of Middle Triassic carbonates and terrigenous deposits (Muschelkalk and Lower Keuper) in the SW Germanic Basin: maximum flooding versus maximum depth in intracratonic basins. Sed Geol. 2003;160(1–3):81–105. https://doi.org/10.1016/S0037-0738(02)00337-8.
Vecsei A, Rauscher R, Hohage K. Palynology of the marine Middle Triassic in the SW Germanic Basin (Upper Muschelkalk, Luxembourg): evidence for an important latest Anisian-early Ladinian sea-level lowstand. Paläontol Z. 2003;77(1):195–202. https://doi.org/10.1007/BF03004568.
Vidal J, Genter A. Overview of naturally permeable fractured reservoirs in the central and southern Upper Rhine Graben: Insights from geothermal wells. Geothermics. 2018;74:57–73. https://doi.org/10.1016/j.geothermics.2018.02.003.
Vidal J, Genter A, Chopin F. Permeable fracture zones in the hard rocks of the geothermal reservoir at Rittershoffen. France J Geophys Res. 2017;122(7):4864–87. https://doi.org/10.1002/2017JB014331.
Vidal J, Patrier P, Genter A, Beaufort D, Dezayes C, Glaas C, et al. Clay minerals related to the circulation of geothermal fluids in boreholes at Rittershoffen (Alsace, France). J Volcanol Geoth Res. 2018;349:192–204. https://doi.org/10.1016/j.jvolgeores.2017.10.019.

Vilà M, Fernández M, Jiménez-Munt I. Radiogenic heat production variability of some common lithological groups and its significance to lithospheric thermal modeling. Tectonophysics. 2010;490(3–4):152–64. https://doi.org/10.1016/j.tecto.2010.05.003.
Villemin T, Alvarez F, Angelier J. The Rhinegraben: extension, subsidence and shoulder uplift. Tectonophysics. 1986;128(1–2):47–59. https://doi.org/10.1016/0040-1951(86)90307-0.
Villemin T, Coletta B. Subsidence in the Rhine Graben: a new compilation of borehole data. In: ICL-WG-3. Symp.; 1990.
Vogel BC. Petrophysikalische und felsmechanische Untersuchung kristalliner Gesteine des Weschnitz-Plutons [Bachelorthesis]: TU Darmstadt; 2016.
Volpi G, Manzella A, Fiordelisi A. Investigation of geothermal structures by magnetotellurics (MT): an example from the Mt Amiata area, Italy. Geothermics. 2003;32(2):131–45. https://doi.org/10.1016/S0375-6505(03)00016-6.
von Seckendorff V. Der Magmatismus in und zwischen den spätvariscischen permokarbonen Sedimentbecken in Deutschland. SDGG. 2012;61:743–860. https://doi.org/10.1127/sdgg/61/2012/743.
von Seckendorff V, Arz C, Lorenz V. Magmatism of the late Variscan intermontane Saar-Nahe Basin (Germany): a review. Geol Soc Spec Publ. 2004;223(1):361–91. https://doi.org/10.1144/GSL.SP.2004.223.01.16.
Wächter J, Lehné R, Prein A, Hoselmann C, Schüth C. Zusammenführung von Bohrschichtinformationen zur bundesländerübergreifenden 3D-Modellierung im nördlichen Oberrheingraben. Grundwasser. 2018;23(4):337–46. https://doi.org/10.1007/s00767-018-0400-9.
Wagner GA. Fission track dating on apatite and sphene from the subvolcanics of the Kaiserstuhl (Germany). Neues Jahrbuch fuer Geologie und Palaeontologie: Monatshefte; 1976. p. 389–93.
Walenta K. Die Mineralien des Schwarzwaldes und ihre Fundstellen. München: Weise; 1992.
Wangen M. The blanketing effect in sedimentary basins. Basin Res. 1995;7(4):283–98. https://doi.org/10.1111/j.1365-2117.1995.tb00118.x.
Weber K. IV.C.1 The spessart crystalline complex. In: Dallmeyer RD, Franke W, Weber K, editors. Pre-Permian geology of Central and Eastern Europe. Berlin: Springer, Berlin Heidelberg; 1995a. p. 167–73.
Weber K. IV.C.3 The Saar-Nahe Basin. In: Dallmeyer RD, Franke W, Weber K, editors. Pre-Permian geology of Central and Eastern Europe. Berlin: Springer; 1995b. p. 182–5.
Weber JN. Geothermische Aufschlussanalyse des Steinbruches Mainzer Berg, oestlich von Darmstadt [Bachelorthesis]: TU Darmstadt; 2014.
Weinert S, Bär K, Sass I. Database of petrophysical properties of the Mid-German Crystalline Rise. Earth Syst Sci Data. 2021;13(3):1441–59. https://doi.org/10.5194/essd-13-1441-2021.
Weinert S, Bär K, Sass I. Petrophysical properties of the mid-german crystalline high: a database for Bavarian, Hessian, Rhineland-Palatinate and Thuringian Outcrops; 2020. doi:https://doi.org/10.25534/tudatalib-278.
Weisenberger T. Zeolites in fissures of crystalline basement rocks [PhD Thesis]: Albert-Ludwigs-Universität Freiburg im Breisgau; 2009.
Welsch B. Geothermische Untersuchungen an ausgewählten Standorten der Schwäbischen Alb [Bachelorthesis]: TU Darmstadt; 2011.
Wenk H-R, Wenk E. Physical constants of Alpine rocks: density, porosity, specific heat, thermal diffusivity and conductivity. Kümmerly und Frey: Leemann; 1969.
Wicke H. Faziesabhängigkeit geothermischer Kennwerte am Beispiel des Oberen Muschelkalk (Crailsheim, Baden-Württemberg) [Diplomathesis]: TU Darmstadt; 2009.
Wickert F, Altherr R, Deutsch M. Polyphase Variscan tectonics and metamorphism along a segment of the Saxothuringian-Moldanubian boundary: the Baden-Baden Zone, northern Schwarzwald (FRG). Geol Rundsch. 1990;79(3):627–47. https://doi.org/10.1007/BF01879206.
Wiedemann T. Autoklav und Thermotriaxialversuche zur Untersuchung des Einflusses von Fluid Gesteins Wechselwirkungen auf die Permeabilität [Master thesis]: Technical University Of Darmstadt; 2021.
Wiesner P. Modellierung einer mitteltiefen Erdwaermesonde zur Heiz-Grundlastabdeckung des Taunusgymnasiums Koenigstein [Masterthesis]: TU Darmstadt; 2014.
Will TM, Lee S-H, Schmädicke E, Frimmel HE, Okrusch M. Variscan terrane boundaries in the Odenwald-Spessart basement, Mid-German Crystalline Zone: new evidence from ocean ridge, intraplate and arc-derived metabasaltic rocks. Lithos. 2015;220–223:23–42. https://doi.org/10.1016/j.lithos.2015.01.018.
Witter JB, Trainor-Guitton WJ, Siler DL. Uncertainty and risk evaluation during the exploration stage of geothermal development: a review. Geothermics. 2019;78:233–42. https://doi.org/10.1016/j.geothermics.2018.12.011.
Zangerl C, Loew S, Eberhardt E. Structure, geometry and formation of brittle discontinuities in anisotropic crystalline rocks of the Central Gotthard Massif. Switzerland Eclogae Geol Helv. 2006;99(2):271–90. https://doi.org/10.1007/s00015-006-1190-0.
Zeh A, Gerdes A. Baltica- and Gondwana-derived sediments in the mid-german crystalline rise (Central Europe): implications for the closure of the Rheic ocean. Gondwana Res. 2010;17(2–3):254–63. https://doi.org/10.1016/j.gr.2009.08.004.
Zhang YK. The thermal blanketing effect of sediments on the rate and amount of subsidence in sedimentary basins formed by extension. Tectonophysics. 1993;218(4):297–308. https://doi.org/10.1016/0040-1951(93)90320-J.
Ziabakhsh-Ganji Z, Nick HM, Donselaar ME, Bruhn DF. Synergy potential for oil and geothermal energy exploitation. Appl Energy. 2018;212:1433–47. https://doi.org/10.1016/j.apenergy.2017.12.113.
Ziegler PA. Geological atlas of western and central Europe 1990. 2nd ed. The Hague: Shell Internationale Petroleum Maatschappij BV; 1990.
Ziegler PA. European Cenozoic rift system. Tectonophysics. 1992;208(1–3):91–111. https://doi.org/10.1016/0040-1951(92)90338-7.
Ziegler PA. Cenozoic rift system of Western and Central-Europe-an overview. Geol Mijnbouw. 1994;73(2–4):99–127.
Ziegler PA, Dèzes P. Evolution of the lithosphere in the area of the Rhine Rift system. Int J Earth Sci. 2005;94(4):594–614. https://doi.org/10.1007/s00531-005-0474-3.

Ziegler PA, Cloetingh S, van Wees J-D. Dynamics of intra-plate compressional deformation: the Alpine foreland and other examples. Tectonophysics. 1995;252(1–4):7–59. https://doi.org/10.1016/0040-1951(95)00102-6.
Zimmermann G, Zang A, Stephansson O, Klee G, Semiková H. Permeability enhancement and fracture development of hydraulic in situ experiments in the Äspö hard rock laboratory, Sweden. Rock Mech Rock Eng. 2019;52(2):495–515. https://doi.org/10.1007/s00603-018-1499-9.
Zoback MD, Barton CA, Brudy M, Castillo DA, Finkbeiner T, Grollimund BR, et al. Determination of stress orientation and magnitude in deep wells. Int J Rock Mech Min Sci. 2003;40(7–8):1049–76. https://doi.org/10.1016/j.ijrmms.2003.07.001.

Publisher's Note